Identification of genes related to peritoneal metastasis using a three dimensional in vitro model of peritoneum

Thesis submitted in accordance with the requirements of the University of Liverpool for the degree of Doctor in Medicine by Enrique Manuel Riera-Portell

March 2010

Statement and acknowledgements

The studies described in this thesis were performed at the Clinical Sciences Centre, University Hospital Aintree and the University of Liverpool. The project commenced in 2003 and was completed in 2006. My first supervisor, Mr P McCulloch moved on from the University of Liverpool in 2004. Dr Thomas Jagoe, Dr Laszlo Pazmany and Dr Joe Slupsky were appointed as replacement supervisors.

I performed all experimental work, including patient consent, tissue collection, 3D peritoneal model preparation, laser capture microdissection, RNA isolation and amplification, microarray hybridisation and PCR experiments. Dr Jagoe helped with the analysis of microarray data and validation studies.

I would like to thank the following for their invaluable help: Mr Miguel Aguirreburualde, chief technician at the Neuropathology Department, the Walton Centre for Neurology and Neurosurgery, who allowed me to use the equipment at the laboratory for immunocytochemistry studies and closely supervised my work there. Dr C Walker, Senior Lecturer in Pathology at the JK Douglas laboratory, Clatterbridge Hospital, who granted access to the laser dissection microscope, and taught me how to obtain cells of interest from the peritoneal models; and Mrs S McMillan, Department of Surgery, Royal Liverpool University Hospital, who provided all the cancer cell lines.

I would also like to thank Mr D Kerrigan, Mr P Skaife and Mr C Mackie, Consultant General Surgeons, who agreed to the collection of tissues from their patients, Mr R Ward who appointed me as Research Associate at University Hospital Aintree, and Prof D W Chadwick and Dr D Gray who helped with other aspects of my welfare during this period of research. My colleague and friend, Dr S Wong, who shared many hours of experiments, and the associated highs and lows, whilst working on his own studies in the same lab, contributed much through his hard work and optimism, and was crucial in my progress. Also Mrs Jenny Austin, Laboratory Technician at the Clinical Sciences Centre, Aintree, was always very supportive and helpful in my learning of many laboratory techniques.

This project was part-funded by Aintree Research on Cancer Charity.

TABLE OF CONTENTS

1 TABLE OF ABBREVIATIONS

aaUTP	Aminoallyl-UTP
APAF	Apoptotic protein activating factor
BAT3	HLA-B associated transcript 3
BTG1	B cell translocation gene 1
CASP8	Caspase 8
CO2	Carbon dioxide
CTSK_1	Cathepsin K
Cy	Cyanine
DAB	Diaminobenzidine
DEPC	Diethylpyrocarbonate
DMEM	Dulbecco's Modified Eagle's Medium
DMSO	Dimethyl Sulfoxide
EB	Elution Buffer
ECM	Extracellular matrix
EDTA	Ethylenediaminetetraacetic acid
EtOH	Ethanol
FCS	Foetal calf serum
FGF	Fibroblast growth factor
GAPDH	Glyceraldehyde-3-phosphate
dehydrogenase	
H2O	Water
HGF	Hepatocyte growth factor
HMGB-1	High-mobility group non-histone chromosomal protein 1
HPMC	Human peritoneal mesothelial cells
ICAM	Intercellular adhesion molecules
IER3	Immediate early response 3 gene
IGBP5	Insulin growth factor receptor binding protein 5
IGF	Insulin growth factor

IL	Interleukin
IVT	In vitro transcription
LCM	Laser capture microdissection
LFA	Leukocyte function antigen
M	Molar
ML-1 protein	Myeloid leukaemia cell gene encoded
MMPs	Matrix metalloproteinases
mRNA	Messenger RNA
NaOH	Sodium Hydroxide
ng	Nanogram
PARP1	Poly (ADP-ribose) polymerase family
PBS	Phosphate buffered saline
PCR	Polymerase chain reaction
RT	Reverse Transcription
SDS	Sodium Dodecyl Sulphate
SMART	Switching mechanism at the 5' end of the RNA transcript
SNR	Signal to noise Ratio
SSC	Sodium Chloride and Sodium Cytrate
Taq	Thermus aquaticus
TBP	TATA box binding protein
TGF	Tumour growth factor
TIMP	Tissue inhibitor of MMP
Tm4sf7	Transmembrane 4 superfamily member 7
TNF	Tumour necrosis factor
Topors	Tumour protein p53-binding protein
TP53BPL	Tumour protein p53-binding protein
TRIS	Hydroxymethylaminomethane
VEGF	Vascular endothelial growth factor
µl	Microlitre

2 ABSTRACT

Patients who develop peritoneal metastases are usually regarded as entering a terminal stage of cancer disease progression, have poor prognosis and rarely benefit from surgery. Unfortunately little is known about the molecular mechanisms underlying peritoneal metastasis, but it seems likely that such mechanisms may be distinct from those of haematogenous metastatic spread. It was hypothesised that by correlating the patterns of gene expression of different malignant cells invading the peritoneum with their differing microscopic behaviour, it might be possible to define genes of particular mechanistic importance in the development of peritoneal metastasis.

A three-dimensional model of peritoneum was constructed from human mesothelial cells, fibroblasts and rat-tail collagen. Highly metastatic gastric cancer cells (TMK I, KATO III) or colonic cancer cells with low metastatic potential (SW480, HT 29) were seeded onto this 3-D model. After seven days invasion was assessed by light microscopy and immunocytochemistry. Cancer and neighbouring mesothelial cells were removed from the models by laser capture microdissection. Messenger RNA was extracted from both cancer cells and mesothelial cells, and amplified, labelled and hybridised on microarrays spotted with oligonucleotides representing 1853 cancer-associated genes. Genes for which mRNA levels correlated with the degree of invasion were selected, to identify those from both tumour and 'host' mesothelial cells that were most likely to be involved in common pathophysiological pathways of peritoneal metastasis and invasion. Using this approach five cancer cell genes were identified in which expression levels was associated with degree of invasion (four progressively up-regulated and one down-regulated). Eighteen mesothelial cell genes (Fifteen up-regulated and three down-regulated) were similarly related to degree of invasion by the cancer cells. Functional annotation of the candidate genes identified revealed that they span a variety of relevant biological functions including apoptosis, calcium metabolism, tumour suppression, cell cycle and adhesion. The results suggest further similar studies are likely to be highly informative, particularly in relation to the modification of the host cell response in the peritoneum.

3 INTRODUCTION

3.1 CHARACTERISTICS OF THE NORMAL PERITONEUM

The peritoneum is a serous membrane which lines the abdominal cavity. Its name is derived from the Greek word "peritonaion" meaning to stretch around. The peritoneal cavity is the potential space between the parietal peritoneum (which lines the abdominal cavity) and the visceral peritoneum (the inner layer which closely covers the organs and includes the mesenteries). Its surface is covered by a single layer of mesothelial cells, the mesothelium. This type of epithelium is mesodermal in origin. Like all epithelia the mesothelium is separated from underlying tissues by a basement membrane that provides structural support as well as binding the mesothelium to the underlying supporting tissue. The mesothelial basement membrane is also involved in the control of mesothelial growth and differentiation and forms an impenetrable barrier to mesothelial cell growth into the deeper connective tissue layer. The peritoneum functions as a gliding, non-adhesive surface for the internal organs and as a selective barrier, regulating transport of fluid and solutes between the circulation and the body cavity (R.M.H.McMinn, 1994).

Characteristic features of the mesothelial cells include: broad cytoplasmic extensions with numerous microvilli, micropinocytotic vesicles concentrated at the surface of the cells and around the Golgi apparatus, intracellular storage organelles called lamellar bodies, cytoplasm containing many free ribosomes, abundant rough endoplasmic reticulum, numerous mitochondria and a well developed Golgi apparatus. Mesothelial cells have a high synthetic and secretory capacity. They are a major source of prostaglandins, cytokines and phospholipids in the peritoneal cavity, synthesize and secrete various pro and anti inflammatory cytokines, and locally contribute to the fibrinolytic cascade (Stylianou, Jenner et al., 1990).

3.2 DEFINITION OF PERITONEAL METASTASIS

The term peritoneal metastasis was first described by Sampson in 1931 to describe the intra-abdominal spread of ovarian carcinoma. Peritoneal metastases take place when tumours seed cells in the peritoneal cavity, leading to the formation of ascitic fluid or metastatic deposits. Although ovarian tumours are a common source of peritoneal metastasis, neoplasms of the gastrointestinal tract (oesophagus, stomach, liver, pancreas, small intestine and colon) may also invade the peritoneum (Jayne, 2003).

While some patients have marked symptoms from peritoneal metastases such as abdominal pain and ascites, others may be asymptomatic at the time of diagnosis. Regardless, the presence of peritoneal metastasis denotes a late stage of disease progression, and numerous reports confirm that such patients have poorer prognosis and generally do not benefit from surgery (Yoshikawa, Kanari et al., 2003a).

3.3 EPIDEMIOLOGY, TUMOUR CLASSIFICATION AND PROGNOSIS

Most tumours able to metastasise to the peritoneum are common in the western world, particularly in the UK. Those patients developing peritoneal metastasis will ultimately die of the disease (Yoshikawa, Kanari et al., 2003b). Although incidence and mortality figures for individual tumours are available in national databases, the true overall incidence of peritoneal metastasis is unknown. However individual figures published by some authorities reflect the high mortality of this disease. Some neoplasms are more likely to metastasise in the peritoneum, such as oesophagus and pancreas, which carry very high mortality rates. However, other common cancers, such as bowel, may metastasise directly to the liver instead. At present, reliable factors which predict peritoneal metastasis have not been identified. The following tables show the incidence of peritoneal metastasis from primary and recurrent gastrointestinal tumours and their mortality

ORIGIN	PRIMARY	RECURRENCE	SOURCE
Stomach	40%	60%	(Kobayashi, Tsuburaya et al., 2006)
Colon	5-10%	20-50%	(Culliford, Brooks et al., 2001)
Pancreas	40-60%	N/A	(Nakao, Fujii et al., 2006)
Oesophagus	17%	N/A	(Chau, Norman et al., 2004)

Table 1 Incidence of peritoneal metastasis from gastrointestinal tumours. (Primary) indicates initial diagnosis. In the presence of recurrent disease peritoneal metastases are more likely and they may be the mode of presentation. (N/A) No available figures were found for recurrent disease for oesophageal and pancreatic cancers, both of which have overall mortality of over 90% at 12 months from the moment of diagnosis.

ORIGIN	MEDIAN SURVIVAL IN MONTHS	SOURCE
Stomach	8.9	(Shiraishi, Sato et al., 2007)
Colon	Less than 12	(Assersohn, Norman et al., 1999;Mahteme, Hansson et al., 2004)
Pancreas	2.7	(Yonemori, Okusaka et al., 2007)

Table 2 Although overall mortality figures for peritoneal metastasis are not available some studies report survival in months, with disease progression and survival of less than 12 months for colorectal cancer, 8.9 for gastric cancer and as little as 2.7 months for pancreatic cancer. No figures were available for oesophageal cancer.

As mentioned already a number of primary tumours, affecting various organs in the abdomen, can spread into the peritoneal cavity and cause metastatic lesions.

Bowel cancer is second most common cancer in females (11%), and the third most common in males (14%) (Source: www.statistics.gov.uk). In North America and Western Europe this remains the second commonest cause of cancer death. Surgery still remains the only curative treatment (Dorudi, Steele et al., 2002).

The incidence of gastric cancer increases from the fifth decade of life reaching its peak at the seventh. Its incidence is low in Western Europe. Overall mortality rates are high and relatively unchanged over the past 30 years (Dicken, Bigam et al., 2005). In the United Kingdom, gastric cancer is the fifth most common cancer in males and ninth in females (Source: www.statistics.gov.uk).

The incidence of oesophageal cancer has rapidly increased in the UK. Adenocarcinoma is now more frequent than squamous cell carcinoma. Being the sixth most common malignancy in males and thirteenth in females, the five year mortality is over 80% (Source: www.statistics.gov.uk). Patients suffering with Barrett's oesophagus are particularly at risk (Fitzgerald, 2004). 50% of newly diagnosed patients will present with metastatic disease and a vast majority of the remaining 50% will develop it (Ilson, 2003).

Pancreatic cancer is the eleventh most commonly diagnosed cancer in the UK, seventh most common in females, and less than 3% of males (Source: www.statistics.gov.uk). However, it is the sixth most common type of cancer death. The late presentation with advanced disease is responsible for the overall median survival of less than six months (Alexakis, Halloran et al., 2004).

Ovarian cancer is the fourth most common cancer diagnosed in females in UK (Source: www.statistics.gov.uk). Incidence is increasing in some Eastern and Southern European countries (Bray, Loos et al., 2005). Family history of ovarian or breast cancer and mutations in the BRCA-1 and BRCA-2 genes are correlated to the disease (Bertone-Johnson, 2005). The risk is reduced by high parity and use of oral contraceptives (Parkin, Bray et al., 2005). The 5 year survival rates for advanced disease are approximately 20-25% (Ozols, 2005).

Other far less common tumours, which may metastasise into the peritoneum, include primary liver cell carcinoma, small intestinal tumours and carcinoma of the gallbladder (Source: www.statistics.gov.uk).

3.4 CURRENT VIEWS IN THE MANAGEMENT OF PERITONEAL METASTASIS

The management of peritoneal metastatic disease from gastrointestinal cancer has been discussed in a number of studies. Numerous drugs and antibodies have been tested, and only a few patients have obtained a marginal survival benefit. No studies have conclusively shown long term survival benefits. Most of the available research up to date has been on advanced gastric cancer and the most successful treatments are described below.

The agent that has shown the most potential is an oral fluoropyrimidine which acts as inhibitor of DNA synthesis, called S-1. Sasaki published a systematic review of various studies, where S-1 was used alone or in combination therapy with 5-fluorouracil (antimetabolite drug) for advanced gastric cancer and peritoneal metastasis. The study showed that this drug could be a key in the treatment of the disease (Sasaki, 2003). Kitamura et al published a small pilot study with 31 patients with gastric cancer and peritoneal metastasis. They were treated with S-1 until disease progression or withdrawal from the regime. Median survivals of up to 12 months were reported (Kitamura, Hayashi et al., 2003). The literature also contains a few promising case studies. Tamura et al reported one case of recurrent gastric cancer with peritoneal metastasis treated with a combination of paclitaxel (pro-apoptotic and anti-angiogenic factor from the taxane group) and S-1. The patient had survived nearly two years up to the time of publication (Tamura, Miki et al., 2006). Kobayashi et al reported a patient with advanced gastric cancer and peritoneal metastasis who survived more than two years after treatment with S-1 (Kobayashi, Konishi et al., 2002) In a study conducted by Ishizone et al, sixteen patients with peritoneal metastases from gastric cancer where treated with S-1. They showed significantly longer median survival times (median=550) days than the 25 patient control group (median=215 days) (Ishizone, Maruta et al., 2006). Saikawa et al conducted a

phase II trial including 13 patients with unresectable gastric cancer, 3 of them with peritoneal metastases, using S-1 with cisplatin and radiotherapy. Peritoneal dissemination disappeared in all 3 patients (Saikawa, Kubota et al., 2008).

Other chemotherapy regimes have been attempted for the management of peritoneal metastases. Fukasawa and Yokoyama reported a patient with peritoneal carcinomatosis treated with paclitaxel in combination with fluorouracil; she was still alive after 25 months (Fukasawa, Shoji et al., 2006;Yokoyama, Tazawa et al., 2005). A multicenter study, phase II, published by Takiuchi et al (Takiuchi, Goto et al., 2008) used paclitaxel in combination with doxifluridine (intermediate metabolite of capecitabine) and fluorouracil for the treatment of patients with advanced and recurrent gastric cancer who had previously been treated with S-1 for 4 or more weeks. 8 out of the 35 patients involved in the study had peritoneal metastases. Unfortunately this regime did not provide any added benefit in terms of survival rates.

Intraperitoneal hyperthermic therapy is another avenue previously tried, but unfortunately unsuccessful. In one study with 103 patients this technique was combined with intraperitoneal Mitomycin C (cytotoxic antibiotic). Although significant survival rates were observed in patients with gastric cancer stage III (serosal invasion, peritoneal seeding) no significant difference was observed in stage IV disease (peritoneal and distant metastasis). All patients eventually developed recurrence (Kim & Bae, 2001). Sugarbaker et al combined peritonectomy and intraperitoneal hyperthermic therapy in patients with gastric cancer and peritoneal metastasis (Yonemura, Kawamura et al., 2004). The median survival was 16 months and 87% of patients died of disease progression at 46 months.

Some of the above results are encouraging, and they show some short term benefits in term of survival even though long term figures remain unchanged. However it is difficult to assess how strong is the effect of different chemotherapy regimes on patients with peritoneal metastasis. This is because most studies compare treatment regimes for the management of advanced cancer, where patients included may have metastases to lymph nodes, peritoneum and distant metastases. Stratification of these patients is complex. Often they present with disease in more than one location, such as the liver, lung and peritoneum. Subsequently it is difficult to assess what effect, in terms of survival, would the

treatment have in those patients if they had peritoneal disease only. Furthermore, it is difficult to assess whether patients with widespread metastatic and peritoneal disease could have better survival rates if peritoneal metastasis was not present. More robust answers to the management of peritoneal metastasis could be drawn from multi-centre randomised controlled trials where the treatment arm included patients with primary tumour and peritoneal metastasis only and the control group included patients with primary tumour only.

At present it may be concluded that there is not enough evidence for the management of peritoneal metastasis and effects on patient survival. More research is required into the underlying molecular mechanisms of peritoneal disease in these advanced cancers, in the hope that new rational and effective treatments can be developed.

3.5 MOLECULAR BIOLOGY OF PERITONEAL METASTASIS

3.5.1 GENERAL STEPS IN THE METASTATIC CASCADE

The process of metastasis is thought to involve a series of linked sequential steps involving multiple tumour-host interactions (Meyer & Hart, 1998). Having disengaged from its primary site the metastatic tumour must pass through the surrounding stroma and enter the vasculature or lymphatic system, or seed in a body cavity. The tumour cell must be able to survive these different environments and when settled at a distant site it can then extravasate or invade into the target organ interstitium and parenchyma. The numerous interconnections between the lymphatic and vascular compartments may allow disseminating tumour cells to transit between these two systems. After establishing an adequate blood supply, the metastatic cell may proliferate and develop into a secondary mass (Ahmad & Hart, 1997). All these steps are summarised in the following diagram (Fig 1):

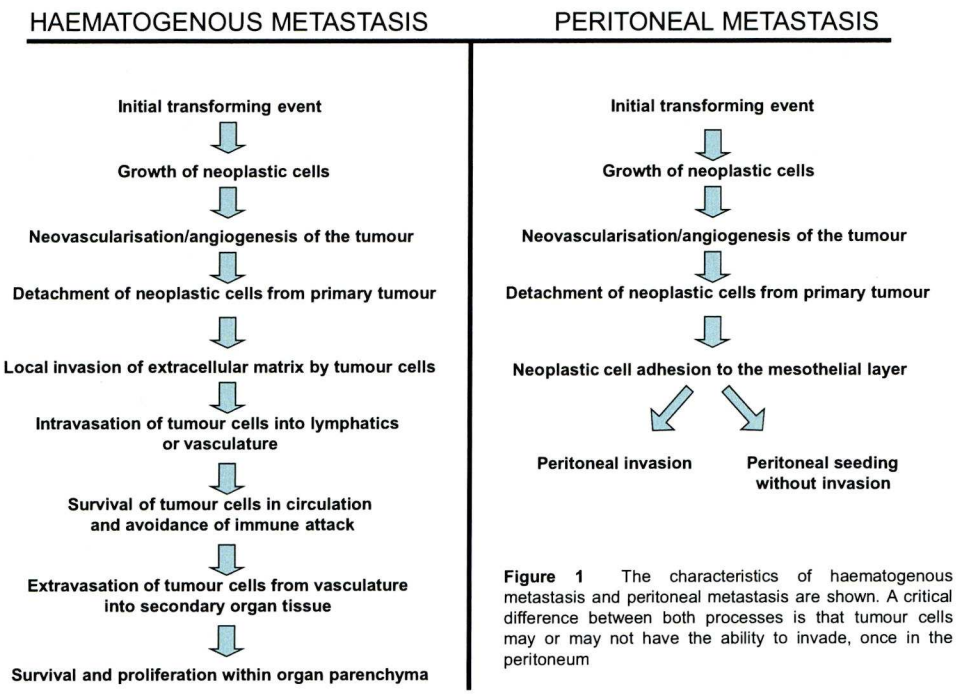

Figure 1 The characteristics of haematogenous metastasis and peritoneal metastasis are shown. A critical difference between both processes is that tumour cells may or may not have the ability to invade, once in the peritoneum

3.5.2 SPECIAL FEATURES OF PERITONEAL METASTASIS

As mentioned above, neoplasms can invade natural body cavities such as the pleura or the peritoneum by direct seeding, thus by-passing the circulation and it seems likely that the mechanisms for metastatic spread via this route are somewhat different from the better characterised process of haematogenous metastasis. Once the tumour cells separate from a primary abdominal tumour, they can disseminate throughout the abdominal cavity and adhere to the mesothelial layer. They may then invade the mesothelium and its basement membrane thus gaining access to the underlying stroma. Tumour cells can then proliferate and induce angiogenesis in order to survive. Interestingly, intra-peritoneal tumour spread may take the form of simply glazing all peritoneal surfaces without invasion of the underlying parenchyma of the abdominal organs. This raises the idea of "seed and soil", which considers the ability to reimplant and the capacity to invade as different patterns of cell behaviour. This concept was first defined by the experiments of Souter et al (Souter, Wells et al.,

1985), who reported that the placement of peritoneal venous shunts to control symptoms in women with ascites due to ovarian cancer did not result in metastases in other organs. This was in spite of the presence of millions of tumour cells from the peritoneal cavity being introduced into the circulation via the shunt. Thus, ovarian cancer cells were unable to "seed". They were not competent to invade distant organs and establish metastases from the blood. Furthermore these cells were metastatic in the peritoneum but not in the circulation confirming that the mechanisms involved in the two processes have some key differences. However, other neoplasms such as gastrointestinal carcinomas can penetrate the wall of the viscus, reimplant and invade at distant sites in the peritoneal cavity. A similar sequence occurs with lung cancers in the pleural cavities.

Clinically, tumours originating in the same organ and from the same histopathological type behave remarkably similarly, especially for the distribution of haematogenous metastasis. The distribution of metastases follows a reproducible pattern, which can often be explained by the anatomical location of a neoplasm e.g. Colon tumours invade locally and metastasise primarily to draining lymph nodes and then liver. However anatomical drainage may not be the only reason for the location of metastases in specific organs. Metastases derived from breast carcinomas that appear in bone must do so by bypassing the lung as do prostate metastases to the skull or colon metastases to brain (Frost & Levin, 1992). These are known as skip metastases and represent a convincing illustration of the importance of the host factors in determining where and how easily metastases can develop.

An as yet poorly understood issue in the development of peritoneal metastases is the role played by the peritoneum, in preventing or protecting against metastasis formation. It is unclear whether the mesothelium or basal membrane or both can, to a certain extent, protect the underlying tissues against invading cells. A number of publications have reported correlation between peritoneal disruption caused by surgical trauma and increased incidence of loco-regional cancer recurrences (van den Tol, van Rossen et al., 1998;van den, ten et al., 2005). These results suggest that the peritoneum may, in some way, act as a physical barrier against invasion. However, there are unanswered questions about whether the mesothelial cells themselves have a particular role in limiting cancer

spread e.g. through direct cellular interactions with cancer cells, or indirectly via locally produced cytokines.

Although it is generally understood that neoplasms with worse histological grade, i.e. poorly differentiated, are more likely to metastasise, there are no studies, clearly correlating histological grade and peritoneal metastasis. Some histological types of a given tumour are more likely to invade peritoneum e.g. oesophageal and gastric carcinoma overall more invasive than colorectal neoplasms; but while histology may provide information about cell behaviour (abundance of mitotic counts and nuclear pleomorphism) and tissue architecture, it does not provide specific information about the potential for peritoneal metastasis.

3.6 CELLULAR PROCESSES IN PERITONEAL METASTASIS

Close anatomic interaction over time between cancer cells and host cells, via numerous molecules is essential for the metastatic process to occur. Adhesion, extracellular matrix (ECM) degradation or proteolysis, angiogenesis, cell signalling, tumour suppression, cell cycle control, apoptosis and other functions have been described in blood-borne metastasis. The role of these mechanisms is far less well understood in peritoneal metastasis. A review of molecules and their functions is provided below.

3.6.1 EXTRACELLULAR MATRIX PROTEOLYSIS

Collagens, laminins, fibronectins and elastins are components of the extracellular matrix (ECM) which can be degraded by a number of proteases. Metalloproteinases are one group of these extracellular proteases which have a role in cancer metastasis, as well as many other cellular processes. At least 20 human MMPs have been identified. These enzymes have both a descriptive name and an MMP number. Common features in all MMPs include a pre- domain which is a signal peptide for secretion, a pro- domain, important for maintaining latency, a catalytic domain with a highly conserved Zinc binding site and a haemopexin like domain. Most MMPs are secreted in the latent form. However a

few of them have a transmembrane domain and remain attached to the membrane.

The role of MMPs in neoplasia was first described by Liotta et al in the early 80s when ECM proteolysis was identified as one of the basic steps in invasion (Liotta, Tryggvason et al., 1980). Further *in vitro* studies have shown that the MMPs are capable of degrading a wide range of connective tissue proteins, indicating that these enzymes may play a role in connective tissue destruction and remodelling associated with cancer invasion and metastasis (Ye, 2000). Murray et al studied the metalloproteinases and their tissue inhibitors in a series of 74 gastric cancers, most of which were advanced gastric cancers. MMP2 was consistently found in tumour cells, but not in adjacent gastric epithelium. However no such association was seen with MMP1 (Curran & Murray, 2000). Otani et al found that the MMP1 gene was over-expressed in stromal cells around cancer nests, particularly at the margins of invasion, but there was no definite pattern of expression among cancer cells (Otani, Okazaki et al., 1994). These findings indicate that raised levels of MMP1 associated with tumour invasion and metastasis. Moreover Inoue et al studied the relationship between gastric cancer cells, MMP1 expression and peritoneal metastasis (Inoue, Yashiro et al., 1999). They found significant association between MMP1 expression and peritoneal metastasis. It was suggested that MMP1 could have a role as prognostic factor MMP2 is well known as a decomposing enzyme of type IV collagen, laminin and fibronectin, which are all components of the basement membrane, and its relationship to the degree of cell differentiation and the potential for invasion and metastasis has been reported. Mizutani et al used an artificial model of peritoneum (matrigel) to study MMP1 and MMP2 expression when in contact with gastric cancer cells, and whether such expressions would result in enhanced cancer invasion. MMP1 derived from peritoneal cells was found to be involved in local invasion and peritoneal dissemination of gastric cancer. (Mizutani, Kofuji et al., 2000a). Yoshikawa et al (Yoshikawa, Tsuburaya et al., 2000) found significantly higher levels of circulating tissue inhibitor of metalloproteinase (TIMP) 1 in patients with peritoneal disease. In their studies they found that although less sensitive than laparoscopy and cytology, plasma TIMP 1 levels were better to predict peritoneal dissemination than other markers.

Yonemura et al suggested that MMP-7 may play an important role in peritoneal dissemination as they managed to stop MKN-45 P cells from proliferating in a peritoneal model after introducing Antisense oligonucleotides complementary to exon 3 of the MMP-7 mRNA (Yonemura, Endo et al., 2001).

Some novel approaches in the management of metastatic disease with inhibitors of metalloproteinases have been developed (Hoekstra, Eskens et al., 2001). Aparicio et al have successfully prevented the development of peritoneal metastasis in rat models by treating them with Batimastat, a synthetic MMP inhibitor (Aparicio, Kermorgant et al., 1999). Similar results were reported by Giavazzi et al who reported positive results by the administration of Batimastat combined to cisplatin (Giavazzi, Garofalo et al., 1998). Aslam et al commenced a trial of Batimastat for the management of malignant ascites. After intraperitoneal injection of the drug, less accumulation of ascitic fluid was reported; overall tolerance was good and overall survival was up to 112 days. At the time of publication the cohort was not large enough, nevertheless the results were encouraging (Aslam & Marino, 2001).

3.6.2 ADHESION

Cells detect their extracellular milieu through interactions employing a variety of cell adhesion molecules. They interact with extracellular matrix components via integrins and syndecan molecules, and with adjacent cells via members of the cadherin, selectin and ICAM families.

3.6.2.1 ICAM

Intercellular adhesion molecules are cell surface glycoproteins that are important in cell to cell and cell to extracellular matrix interactions (Tempia-Caliera, Horvath et al., 2002). There are five intercellular adhesion molecules (ICAM) known in humans. They all have two to nine extracellular immunoglobulin-like domains thus making them members of the immunoglobulin superfamily (Ihanus, Uotila et al., 2003). ICAM-1, also known as CD54 has 5 extracellular immunoglobulin like domains and serves a role in promoting adhesion in inflammatory and immune reactions is also a ligand for

leukocyte function antigen (LFA-1, CD11a, CD18) , which is an αβ complex, member of the integrin family of cell-cell and cell-matrix receptors mediating various cell to cell interactions involved in immunity. ICAM-2 has two extracellular domains, one of which is also a ligand for LFA-1 (Kaihara, Iwagaki et al., 1998).

ICAM-1 has been reported to be secreted by tumour cells in order to promote the invasion of organs such as liver, thyroid, ovary, stomach, colon, bladder and pancreas. Tempia-Caliera et al demonstrated high expression levels of ICAM-1 and VCAM-1 in pancreatic cancer cells by immunohistochemistry (Tempia-Caliera, Horvath et al., 2002). Alexiou et al found increased serum levels of these adhesion molecules in patients with colonic cancer. There was correlation between serum levels, cancer stage and the presence of lymph nodes and distant metastases (Alexiou, Karayiannakis et al., 2001). Yasuda et al demonstrated in their study that ICAM-1 was down-regulated by a signalling mechanism involving β1 integrin, thus inhibiting adhesion of lung cancer cells to T cells and preventing their recognition and elimination (Yasuda, Tanaka et al., 2001).

3.6.2.2 CADHERINS AND CATENINS

Cadherins are transmembrane glycoproteins with an extracellular region composed of four repeat domains, a transmembrane domain and a short cytoplasmic domain, which is the most highly conserved region. The cytoplasmic tails of functional cadherins associate with accessory cytoplasmic proteins (catenins) that mediate binding to the actin cytoskeleton. The catenin complex consists of α-catenin, β-catenin and γ-catenin. The extracellular N-terminal end is essential to the process of homophylic calcium dependent cell-cell adhesion. Deletion of the cytoplasmic tail or modification of the catenin will abrogate cadherin function. Thus cadherins and catenins have a major role in regulating adhesive activity and alteration of their function or expression is a crucial step in the process of metastasis formation (Meyer & Hart, 1998).

The cadherin family contains several members, including E-cadherin which is involved in epithelial cell-cell adhesion. Levels of E-cadherin are often

down-regulated in malignant cells, and re-expression of E-cadherin in such cells has a tumour suppressor effect.

Oka et al (Oka, Shiozaki et al., 1992) studied 103 gastric tumours using immunohistochemistry. There were 11 cases of peritoneal metastasis, and 9 of them showed significantly reduced expression of E-cadherin, compared to non-metastatic tumours, thus suggesting that reduced expression of E-cadherin may be relevant to invasion and metastasis.

Yonemura et al (Yonemura, Endou et al., 2000) analysed E-cadherin mRNA and protein expression in clinical specimens of primary gastric cancers and gastric cancer cell lines. They found that 88% of differentiated adenocarcinomas and 50 % of poorly differentiated adenocarcinomas expressed E-cadherin ($p=0.0015$). However no significant differences were found in those with or without liver, lymph node or peritoneal metastasis. Hedge et al (Hegde, Qi et al., 2001) used microarray technology to identify genes relevant to metastasis in colorectal cancer. They found no significant changes in the pattern of expression of homotypic cell adhesion molecules. However, gross abnormalities were found in expression of genes involved in the formation of cytoskeletal architecture and the extracellular matrix. Toyoda et al (Toyoda, Doi et al., 2005) compared the expression of cadherins and catenins of seven human pancreatic cancer cell lines. Increased expression of E-cadherin and catenins was found in all but one cell line. Two cell lines with increased expression were metastatic.

The above studies were performed in different centres with different sources and materials and the results are conflicting. Almost every author reported changes in expression but correlation between adhesion molecule expression across studies is almost nonexistent.

3.6.2.3 INTEGRINS

Integrins comprise a diverse family of receptors that mediate adhesion between the cell membrane and the extracellular matrix or other cell adhesion molecules, ICAMs. They are composed of two non-covalently associated α and β subunits and the combination of 8 β subunits with 14 α subunits generates an

heterogeneous family of over 20 heterodimers (Hynes, 1992). The majority of integrins mediate cell-matrix interactions during cell migration, by binding to components of the basement membrane and interstitial stroma, including fibronectin, laminin, thombospondin, vitronectin and collagens so that many cell types expressing several different integrins can bind to several of these extracellular proteins. However, some integrins which are expressed on lymphocytes and leukocytes mediate heterophilic cell-cell adhesion. This process, so important for the extravasation of leukocytes at sites of inflammation, is mimicked by certain tumour types in the analogous process of metastatic extravasation (Ahmad & Hart, 1997;Meyer & Hart, 1998).

Interactions between tumour cells and the ECM occur during the initial invasive action of metastatic cells. Changes in adhesive properties of malignant cells, in co-operation with increased proteolytic activity around tumour cells are extremely important events in mediating some of the changes involved in metastatic progression.

Ura et al (Ura, Denno et al., 1998) examined the correlation between the expression of $\alpha 2\beta 1$ and $\alpha 3\beta 1$ integrins and the clinicopathological features of gastric cancer, focusing particular attention on the different types of metastases. 18 out of 110 patients had peritoneal metastases. Specimens were tested by immunohistochemistry using anti-integrin monoclonal antibodies. They concluded that the expression of $\alpha 3$ subunit was directly related to the presence of peritoneal metastasis ($p<0.0005$)

In a different study, with sections from 121 malignant effusions and 30 corresponding primary and metastatic lesions from ovarian tumours protein expression of αv and $\beta 1$ integrin subunits was studied using immunohistochemistry, immunoblotting and flow cytometry. Although expression of the $\beta 1$ subunit was rare in mesothelial cells, this was present in 54% of peritoneal effusions and 27% of pleural effusions. αv expression in peritoneal effusions was 61%. Based on these results, a role was suggested for the $\alpha v\beta 1$-integrin fibronectin receptor in mediating carcinoma-mesothelium binding (Davidson, Goldberg et al., 2003). Ishii et al demonstrated in their study with murine invasion models and human gastric cancer samples a role for integrin $\alpha 6\beta 4$ as a biological marker for both the prediction of recurrence of peritoneal dissemination and the outcome of patients with gastric cancer. Integrin

α6β4 suppressed peritoneal dissemination by inducing apoptosis in metastatic models. The loss of integrin α6β4 expression in gastric cancer accelerated peritoneal dissemination (Ishii, Ochiai et al., 2000).

3.6.2.4 CD44

CD44 comprises a family of heterogeneous integral membrane proteoglycans derived from a single gene. This gene is composed of 20 exons, 10 of which are variably expressed due to alternative splicing. CD44 functions primarily in the immune system. CD44 and integrins are thought to be involved in the peritoneal dissemination of cancer cells and in the adhesion of cancer cells to extracellular matrix components such as collagen, laminin, fibronectin and hyaluronic acid. Nakashio et al (Nakashio, Narita et al., 1997a) studied the role of adhesion molecules using monolayer models of mesothelial cells and gastric cancer cell lines. They found that strong expression of CD44H and β1 and weak expression of α5 integrin in cancer cells are necessary for an early development of peritoneal metastasis. The same authors also found that the binding activity and invasion of NUGC-4 gastric cancer cells into mesothelial cells appeared increased by pre-incubating mesothelial cells with TGF-β1.

3.6.3 CYTOKINES AND CHEMOKINES

Cytokines are polypeptide products of many cell types that are able to modulate the action of other cell types. Chemokines are a group of heparin-binding cytokines that act as powerful chemo-attractants for leukocytes, and are well known for their role in acute and chronic inflammatory reaction (Yoshie, Imai et al., 2001). In recent years there has been a growing interest in the role of these molecules in neoplasia and metastasis. There is increasing evidence that certain aspects of tumour growth are related to persistent and unresolving inflammation (Szlosarek, Charles et al., 2006). Particularly chronic inflammation, with the persistence of an inflammatory trigger provided by pro-inflammatory cytokines is partly responsible for the process of carcinogenesis.

An example is the process of chronic gastric infection with Helicobacter pylori, where there is strong association with the presence of Interleukin 1ß, and polymorphisms in the gene expressing this cytokine are associated with gastric cancer (Dinarello, 2006). Likewise, TNF-α which is upregulated at an early stage after infection and polymorphic variants of IL-10, an anti-inflammatory cytokine that inhibits cell mediated immune responses, have been associated with an increased risk of gastric cancer (El-Omar, Rabkin et al., 2003) . Several cytokines of the growth factor family have been identified in gastric cancer according to histopathological type. For instance epidermal growth factor, tumour growth factor α and basic fibroblast growth factor are usually overexpressed in the intestinal type, whereas tumour growth factor ß and basic fibroblast growth factor are overexpressed in the diffuse type (Tahara, 2004).

Although the precise involvement of cytokines and chemokines in peritoneal metastasis is still poorly understood, a few publications have provided some insight. It is of particular interest that many of these molecules seem to inhibit on cell-cell adhesion leading into increased invasion in the peritoneum.

Interleukin 2, a mediator for activation of immune cells, has been reported to have antitumour effect, presumably by T cell activation, described in some tumour models (Cayeux, Richter et al., 1997). Interleukin 6, which triggers antibody secretion and maturation of B lymphocytes, stimulates tumour cell growth in most cases, such as gastric carcinoma (Schneider, Hoeflich et al., 2000). Ikeguchi et al. studied the expression of a number of cytokines in peritoneal washing from patients with gastric cancer. They found lower levels of Interleukin 2 (IL-2) and higher levels of Interleukin 6 (IL-6) in patients with peritoneal seeding, while levels of Interleukin 12 (IL-12) and Tumour Growth Factor ß did not differ from those seen in controls (Ikeguchi, Matsumoto et al., 2004).

IL-12 has also been linked to carcinogenesis, although its role is less understood. During inflammation, antigen presenting cells, such as macrophages secrete IL-12, which activates natural killer cells and T cells to produce of interferon γ and increasing NK and T cell cytotoxicity and proliferation (Gately, Renzetti et al., 1998). Murakami et al studied IL-12 levels in human gastric cancer (127 patients and 35 controls). They concluded that whilst IL-12 levels were higher in gastric cancer patients compared to controls, patients with

advanced disease and indeed peritoneal seeding had lower IL-12 serum levels and IL-2 receptor levels than patients with early gastric cancer. The same author already reported 10 years earlier that IL-2 receptor levels were higher overall in gastric cancer, but not significantly different in the presence of liver or peritoneal metastasis. However the reasons for this difference were unclear (Murakami, Okubo et al., 2004;Murakami, Satomi et al., 1994)

Yasumoto et al reported that the chemokine receptor CXCR4 was very highly expressed in metastatic gastric cancer cell lines compared to primary gastric cancer cells. They were able to demonstrate suppression of peritoneal metastasis in a peritoneal model using a CXCR4 receptor antagonist (Yasumoto, Koizumi et al., 2006).

Alkhamesi et al reported that the expression of ICAM-1 in mesothelial cells was increased in the presence of the pro-inflammatory cytokine Tumour Necrosis Factor Alpha (TNF-α). Increasing evidence suggests that chronic TNF-α production regulates many processes such as angiogenesis, cell replication, apoptosis and tumour progression at cellular level (Szlosarek, Charles et al., 2006). In the peritoneum, this change in ICAM-1 concentration enhanced the ability of tumour cells to adhere and invade peritoneum in mice(Alkhamesi, Ziprin et al., 2005). Mochizuki et al also reported similar findings regarding the role of TNF-α. Mesothelial cells suffered morphological changes, including decrease in actin stress fibre levels and intercellular gap formation. Loss of HPMC cell-cell adhesion led to increased tumour-mesothelial cell adhesion (Mochizuki, Nakanishi et al., 2004). Different results had previously been published by Van Rosen et al (van Rossen, Hofland et al., 2001) who performed similar experiments with a colonic cancer cell line in mesothelial rat cells. They found that Interferon-gamma (IFN-gamma), TNF-α, IL-6, and insulin-like growth factor (IGF-I) pre-incubation of a monolayer of mesothelial cells had no effect on tumour cell adhesion. These differences may illustrate important sources of variability including possible differences in response of different tumours (gastric versus colonic), organism (human versus rat) and experimental model systems (mice *in vivo* versus mesothelial cell *in vitro* monolayer).

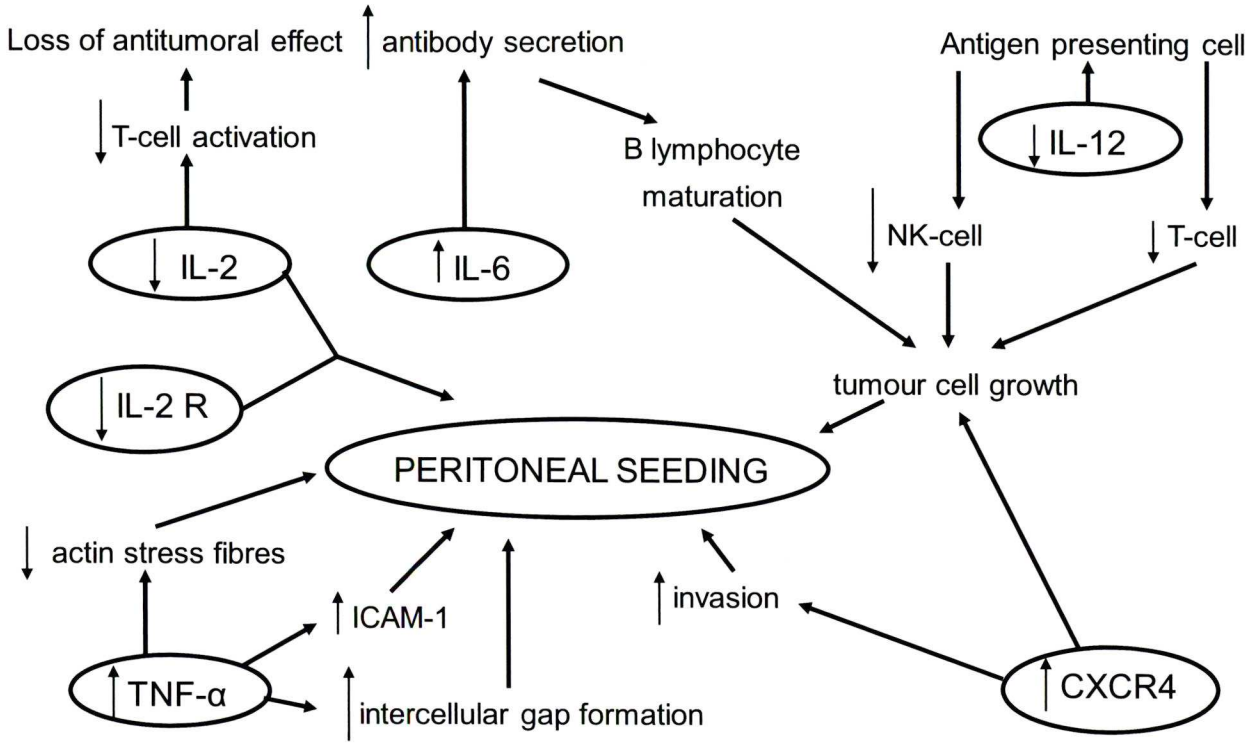

FIG 2 The above diagram illustrates the role of those cytokines reported to be involved in the process of peritoneal carcinomatosis. Levels of IL-2 and its receptor, and which have a protective effect are reduced in peritoneal metastasis. IL-12 levels are decreased in peritoneal carcinomatosis. Increased Levels of IL-6, and CXCR4 receptor promote tumour growth and peritoneal metastasis. Despite TNF-α being protective by regulating apoptosis, it may also promote peritoneal carcinomatosis by various mechanisms. By increasing ICAM-1 levels, cancer cells may use to seed onto the mesothelial cells; increase in intercellular gap formation also facilitates invasion.

3.6.4 ANGIOGENESIS AND GROWTH FACTORS

The role of growth factors in the development of peritoneal metastasis has been reported in numerous publications. However, the specific role of angiogenesis in peritoneal metastasis is a poorly understood area. While neovascularisation may be necessary for the survival of newly formed peritoneal deposits, further research is needed to understand all the factors involved in the process.

The most well known angiogenic factor to date is vascular endothelial growth factor (VEGF). VEGF, also called vascular permeability factor, is a potent mediator of normal vessel permeability and has an endothelial cell mitotic potential (Glass, Harper et al., 2006). Physiologically, VEGF expression is regulated by exogenous stimuli, such as tissue hypoxia (Sooriakumaran & Kaba, 2005). VEGF may be expressed in tumour cells; expression may also be induced by oncogene products. VEGF inhibition causes immature blood vessels to regress, without disturbing normal mature blood vessels (Fang, Zhou et al., 2007). High levels of VEGF increases vascular permeability leading to high interstitial pressure and uneven delivery of nutrients, oxygen and even therapeutic drugs into the tissue (Rasila, Burger et al., 2005). The important role of angiogenesis in the development of peritoneal metastasis from gastric cancer has been further studied by Aoyagi et al (Aoyagi, Kouhuji et al., 2005). They found that not only a higher number of cells would show higher levels of VEGF by immunohistochemistry when the tumour had reached the serosal layer and invaded the peritoneum but also the intensity was higher. Having established a scoring system for all samples, they concluded that higher immuno-staining scores positively correlated with peritoneal recurrence thus suggesting that VEGF scores were a good marker of peritoneal metastasis in patients with gastric cancer. Sako et al reported that VEGF may be produced by HPMC in large amounts when stimulated by fibroblast growth factor 2 (FGF-2), and due to the increased vascular permeability at local level this may provide an ideal environment for disseminated cancer cells to grow on the peritoneum (Sako, Kitayama et al., 2003). Gerber et al reported that angiogenesis could be promoted in areas of the peritoneum where hypoxia was more marked, thus stimulating

mesothelial cells to secrete VEGF promoting angiogenesis and subsequent metastatic survival (Gerber, Rybalko et al., 2006). Garcia Gomez et al demonstrated that HPMC cells incubated in the peritoneal cavity of rats, they proliferated and formed neo-vessels, and synthesised basic fibroblast growth factor and VEGF (Garcia-Gomez, Goldsmith et al., 2005).

Tumour growth factor ß1, TGF-ß1, has also been linked to peritoneal metastasis. This factor was reported to stimulate the production of ECM components associated with morphological changes in mesothelial cells (Ignotz & Massague, 1986). Nakashio et al pre-incubated the gastric cancer cell line NUGC-4 and HMPC with TGF-ß1 and observed a marked increment of binding activity of cancer cells to HMPC thus concluding that the growth factor promotes peritoneal metastasis (Nakashio, Narita et al., 1997b).

Hepatocyte growth factor (HGF) a growth factor mainly produced by fibroblasts, has also been related to peritoneal metastasis. HGF greatly enhances cell motility and breakdown of extracellular matrix in a variety of cancer cells leading to tumour cell spread. c-Met, the HGF receptor, which is a membrane-spanning tyrosine kinase, is over-expressed in many kinds of cancer cells (Zarnegar & Michalopoulos, 1995). In fact, HGF acts on cancer cells via this receptor to promote their proliferation and on stromal cells to promote neovascularisation. Furthermore it has been shown that inhibition of HGF with HGF-antagonist NK4 in a murine model effectively suppressed peritoneal metastasis (Tanaka, Shimura et al., 2004;Ueda, Iwahashi et al., 2004).

3.6.5 MICROARRAY STUDIES TO DATE

Hybridization based quantitation of mRNA abundance has extensively been used in molecular biology for decades. However, Northern blots, slot blots and other related approaches could only detect one or - with the use of stripping and rehybridization- a few genes of interest. However, the development of microarray technology permits the simultaneous study of the expression of a large number of genes in a given total RNA or mRNA sample. When the samples tested are paired, for example treated versus untreated cells or affected versus non-affected tissue samples changes associated with the treatment or the disease

process can theoretically identified. One of the most extensive utilization of DNA arrays is in cancer research, where it allows the comparison of gene expression in primary tumours, lymph nodes and distant metastases, thereby identifying genes that are specifically over or under-expressed at different levels during the development of metastatic lesions.

The principle of printed DNA microarrays was first developed in the nineties at Stanford University, where short DNA fragments complementary to hundreds of genes were printed on glass slides using robotic technology (Schena, Shalon et al., 1995). The RNA extracted from tissues or cells of interest was labelled with a fluorescent dye and hybridised to the arrays. A laser scanner read the intensity of fluorescence at each spot present on the platform. With the aid of computer software spot intensities were translated into a numerical value that was proportional to the abundance of the mRNA hybridized to each particular spot. Subsequently, changes were made to the printing process, including the use of single stranded gene-specific oligonucleotides, and the isolation and amplification of mRNA from tissues of interest. This technology is used in numerous areas of medicine and biology and particularly in cancer research.

Since 1999, there has been an increasing use of microarrays in cancer studies. These early investigations contributed to the discovery of new subtypes of cancers and have shown the diagnostic and prognostic potential of this approach. Studies on a number of solid tumours included prostate cancer (Bull, Ellison et al., 2001;Dhanasekaran, Barrette et al., 2001), breast cancer (Hedenfalk, Duggan et al., 2001), oesophageal cancer (Fukuda, Sakakura et al., 2004), ovarian cancer (Yoshida, Furukawa et al., 2009), colon cancer (Witkowska, Gumprecht et al., 2010), lung cancer (Yang & Sun, 2010) and gastric malignancies (Mimori, Fukagawa et al., 2008;Wang, Zhu et al., 2006).

Subsequently it has been possible to print thousands of gene fragments on one slide which allows the simultaneous study of many gene expression levels on each slide. Isolated mRNA from a tissue of interest is amplified, labelled and hybridised to the DNA fragments on the platform. A laser scanner reads the intensity as fluorescence of each spot in the platform. With the aid of computer software it is possible to collect those images containing spot intensities and translate them into numerical data that can be further analysed. Hence it is possible to learn expression levels of thousands of genes from each sample and

establish comparisons amongst numerous samples which will lead to meaningful conclusions. Microarray technology has dramatically changed the approach to molecular biology research.

However, despite the extent of the literature on this topic, to date few studies have specifically researched into the formation of peritoneal metastases.

The largest study on this topic is that of Galamb et al (Galamb, Sipos et al., 2005), a comprehensive review of 12 publications in gastric cancer including nearly 400 patients and a further 17 publications including 272 patients with colorectal cancer. While the emphasis is on primary tumour gene expression, the genes identified provide sound understanding into the mechanisms of growth and invasion. Despite differences in gene expression in gastric and colonic cancers, some cellular processes were affected similarly. Upregulated genes related to tumour suppression, oncogenes and apoptotic genes included v-raf 1, CAS and semaphorin 5 for gastric cancer; v-myc and bcl-2 for colorectal cancer. Both tumours showed upregulated GRO-1, an oncogene activated by RAS, dependent on p53, which is vital for cancer cell survival. Similarly, caspases 8 and 9 were dowregulated in gastric cancer and caspase 10 in colorectal cancer, which contribute to loss of apoptotic control, potentially leading to uncontrolled cell growth. DNA topoisomerase 2α, involved in cell cycle control, was upregulated in gastric cancer and downregulated in colorectal cancer. Cytokine genes such as IGF-2, which stimulates insulin action and cell growth, and TGF-ß3, which controls cell proliferation and differentiation, were upregulated in gastric cancer; TGF-gene ß3, and IFN induced protein were upregulated in colorectal cancer. No cytokines were downregulated in gastric cancer and only HGF in colorectal cancer. Several cadherins, catenins, integrins and other cell adhesion related genes were upregulated in both gastric and colonic cancer. Proteases involved in ECM digestion and remodelling were upregulated mostly in gastric cancer, whereas only TIMP-3 was upregulated in colonic cancer. Although the gene signatures for both cancers are different, it becomes apparent that both cancers use similar mechanisms to invade. Oncogene activation, tumour suppression gene suppression, loss of apoptotic control, necessary for controlled cell growth, breakdown of ECM and loss of adhesion, are pathways to facilitate uncontrolled cell growth and invasion in this study.

When comparing primary tumour with metastatic deposits, Wang et al (Wang, Zhu et al., 2006) found a small group of genes that were differentially expressed, not only between normal mucosa and primary tumour, but also in metastatic lymph nodes. These experiments were performed on human cDNA arrays, and confirmed by RT-PCR and immunohistochemistry. OPCML, previously reported as a tumour suppressor gene in ovarian cancer, had highest level of expression in normal mucosa, lower in primary tumour and lowest in metastatic lymph node. YES 1, a homolog virus oncogene associated with oesophageal cancer followed a similar pattern of expression. ACK-1, involved in tyrosine phosphorylation and transduction, was downregulated, and reported to act as pro-oncogene, thus facilitating tumour progression. Although other genes, involved in adhesion, ECM breakdown and cell cycle were identified in the primary tumour, these were not present in the metastatic lymph nodes.

Chen, Lin et al studied a number of cell cycle and apoptosis related genes in human colonic cancer in 85 samples. (Chen, Lin et al., 2007). Combining tissue microarrays and immunohistochemistry they found that p53, p21 (responsible for cell cycle arrest in G1 phase), cyclin D, Blc-2 and Bax (both apoptotic genes) over-expression, all showing correlation with histopathological grade. Additionally, p53 expression levels correlated with clinical staging (Dukes classification) and the presence of lymph node metastasis. Bcl-2 correlated with histological grade and liver metastases. The authors proposed that loss of cell cycle and apoptotic control played a crucial role in colonic cancer progression and altered Bcl-2 altered expression may be involved in development of distant metastasis.

Sakakura et al (Sakakura, Hagiwara et al., 2002a) conducted a study of various gastric cancer and peritoneal metastasis cell lines. They hypothesised that gene expression in peritoneal metastasis was different to primary tumours thus indicating that differences existed in the mechanisms of both processes. They identified a possible metastatic signature involving up and down regulated genes from gastric cancer related malignant ascites, compared to primary tumours. Two apoptosis related genes Leukocyte elastase inhibitor and TGFb-induced antiapoptotic factor were up-regulated in malignant ascites and peritoneal metastasis. Nine genes were up-regulated which play a pivotal role in adhesion. These included integrin α3, S100 (a ligand of annexin II) and CD44 (a ligand for

integrins; over-expression of the latter was previously reported to be linked to peritoneal metastasis by Nakashio et al (Nakashio, Narita et al., 1997a). Keratins 7,8,14 were also over-expressed. However the adhesion related gene integrin ß4 was down-regulated. Only two apoptotic genes were downregulated: H2A histone family member L and Death associated protein. RAD 51 homolog C, a gene responsible for chromosomal stability, was also downregulated. Finally, other genes linked to various signalling pathways (examples: Histone deacetylase 3, Acyl-Coenzyme A dehydrogenase and Chaperonin containing TCP1) were also downregulated.

Fukui et al (Fukui, Nishimori et al., 2005), in a similar study, also identified a series of genes differentially expressed in peritoneal metastasis. Peritoneal metastatic cancer cell lines were established from a previous gastric cancer cell line (AZ521) grown in the abdominal cavities of nude mice. Gene expression patterns were then compared between the peritoneal metastatic versus primary tumour cell lines. A number of up-regulated genes were identified which were involved in regulation of cell cycle, cell growth, DNA transcription. These included Mitogen induced nuclear orphan receptor, which is involved in regulation of transcription, protein tyrosine phosphatase, involved in cell cycle and EGR alpha, a transcription factor. Downregulated genes included IGFBP 7 (cell growth), PISSLRE (oncogenesis, cell cycle), human chorionic gonadotrophin (ß-HCG) ß subunit (apoptosis, signal transduction) and RNA polymerase II homolog (transcription) The cell adhesion receptor Integrin alpha E precursor was also down-regulated.

Yanagihara et al (Yanagihara, Takigahira et al., 2005) conducted similar experiments, injecting peritoneal metastatic cell lines into the peritoneal cavities of mice. Once ascites and peritoneal deposits developed, mice were sacrificed and gene expression patterns in the recovered tissue were analysed further. Up-regulated genes included MMP1, apoptotic genes galectin-1 and BCL-2; cathepsin-L, all of which are well associated with invasive tumours, and plasma protein activated by p53 gene, which controls cell cycle. MMP1 plays a pivotal role in ECM proteolysis and its association with invasion and metastasis has been previously documented (Inoue, Yashiro et al., 1999). Cathepsin L is a cystein protease of the papain family and its role in ECM proteolysis has been documented, particularly in melanoma (Yang & Cox, 2007). Down-regulated

genes included Thrombospondins 1 and 4, CD 44 (cell adhesion, signal transduction, calcium ion binding) and cyclin (cell cycle). In normal tissues, thrombospondins are implicated in cell to cell adhesion, cytoskeleton organisation and cell motility (Ioachim, Michael et al., 2006). CD44, a cell membrane proteoglycan, known to be involved in cell adhesion of invading cancer cells, was also reported to be relevant to the development of peritoneal metastasis (Nakashio, Narita et al., 1997a).

Mimori et al studied MT1-MMP (membrane type matrix metalloproteinase, previously recognised as a key molecule in primary tumour invasion) in metastatic gastric cancer using microarray technology. Tissue samples from six cases of recurrent gastric cancer after surgery were compared to 3 non recurrent gastric cancer controls. They also studied blood and bone marrow samples of 810 patients with gastric cancer (629 undifferentiated and 181 differentiated tumours, using blood samples taken in the anaesthetic room before surgery. 26 of these patients had peritoneal metastasis. They found higher levels of circulating blood and bone marrow MT1-MMP in patients with peritoneal metastasis, compared to controls. Particularly, significant correlation was found between high levels of MT1-MMP-1 in both circulating blood and bone marrow and the presence of peritoneal metastases. When multivariate analysis was performed using a logistic regression model, they found that blood levels of MT1-MMP were associated with a higher potential for peritoneal metastasis. Likewise when levels were higher in bone marrow, these correlated with higher potential for haematogenous metastasis. (Mimori, Fukagawa et al., 2008).

Varghese et al carried out gene expression profile of metastasis to the liver and peritoneum from patients with lower gastrointestinal malignancy. Although peritoneal dissemination is less common than liver metastasis, its presence has a detrimental effect on the management and prognosis of these patients. The study was performed on 20 patients with colorectal cancer, 6 of who had peritoneal metastasis with no hepatic involvement. Genes that were differentially upregulated in the presence of peritoneal metastasis, included CD14, V-CAM, IGF-1 and Thrombospondin 1, all of which are angiogenic factors. Also upregulated were TIMP-1 (a tissue metalloproteinase inhibitor with well recognised role in metastasis formation) and TGF-ß and EGR-1 (early

growth response factor) both of which are involved in cell cycle control. This is the first publication that has also identified angiogenesis related genes which appeared to be overexpressed in peritoneal metastasis from colorectal cancer. Finally adhesion molecules such as chondroitin sulphate proteoglycan 2, TGF- ß and various cadherins and integrins were also involved. These findings corroborate that functions already described above play a very important role in the development of peritoneal metastasis (Varghese, Burness et al., 2007).

All the above studies aimed to explain the possible molecular pathways involved in cancer cell growth metastasis formation (Figure 3). However, this quick overview highlights the deficiencies of these investigations. Some of the studies were conducted directly on tissue samples obtained during surgery; other used established cell lines while alternatives included the study of the process of peritoneal metastasis formation in very artificial animal models. In addition, the use of the range of different array platforms and non-standardised sample handling protocols make the comparisons between these studies difficult. Nonetheless, when gene functions are compared amongst the studies, it may be concluded that certain molecular pathways share some similarities across the studies. Changes in oncogene activation, mutated tumour suppressor genes, increased proteolysis, loss of cell to cell adhesion, abnormal cell cycle control, inability to repair DNA damage and loss of apoptotic control were pathways seen in multiple studies. At the same time, it is also noticeable that microarray studies so far failed to identify the role of certain biological pathways, such as angiogenesis in the process of peritoneal metastasis. Furthermore, comparison between the studies published to date fails to identify a core set of genes that appear to be essential for the formation of peritoneal metastases.

A major drawback in microarray technology is that it is not possible to stratify steps within molecular pathway into those particular to peritoneal metastasis and separable from those relevant to primary tumour formation. Further research into this field is required, ideally with larger numbers of subjects and enough peritoneal metastatic tissue available.

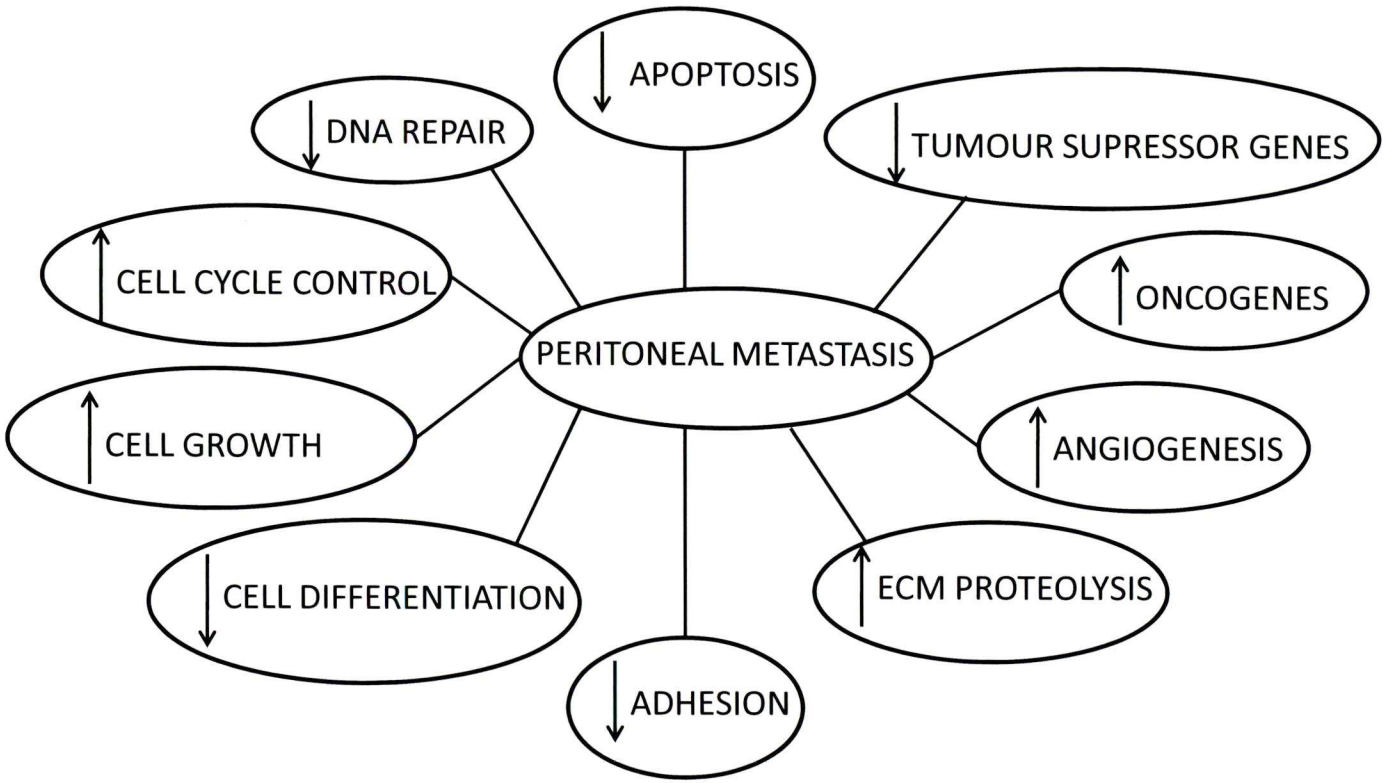

Figure 3 Numerous pathways are involved in maintaining normal cellular architecture. Over or under expression of individual genes or groups of genes may lead to loss of function thus encouraging uncontrolled growth, invasion and development of peritoneal metastasis.

3.7 IMPORTANCE OF A SUITABLE MODEL

One major hurdle in the study of peritoneal metastasis in humans is the nature of the clinical context. As most of the patients with peritoneal metastases are debilitated and have very limited life expectancy, large scale or prolonged clinical studies are usually impossible. Thus a suitable model of peritoneal metastasis is needed, which resembles, as closely as possible the human peritoneum, to allow further experiments on mechanisms of metastases. To date most of the knowledge about peritoneal metastasis has been gained from work on mesothelial monolayer cultures and animal models but both of these have their limitations. Mesothelial monolayer studies typically consist of mesothelial cells laid in a tissue culture plate; onto which cancer cells are applied. Using this system it is possible to observe growth along the surface of the mesothelial layer, but the depth of invasion cannot be assessed. Thus these studies are restricted and provide information on the initial stages of the metastatic process only. In contrast animal models usually involve injected cancer cells from either commercially available cell lines or modifications thereof into the peritoneal cavity. Metastatic behaviour may be observed by sacrificing the animals after a period of days or weeks (Nishimori, Yasoshima et al., 2000). However to observe multiple time points requires many animals, and can prove costly.

To overcome these problems a more representative experimental model has been developed which offers a reliable means of pre-animal experimental study. The three-dimensional peritoneal model described by Jayne et al (Jayne, O'Leary et al., 1999a) is fabricated from human peritoneal mesothelial cells, fibroblasts and rat tail collagen, and is a much closer representation of the human peritoneum than the simple mesothelial monolayer.

The source of human peritoneal mesothelial cells (HPMC) for such models can also be problematic. HPMC have also been isolated from human serous effusions, like peritoneal ascitic fluid or pleural collections. However this method is not popular because they may also contain other cells, and such effusions are often a sign of underlying disease (Allen, Porter et al., 1987;Jap, Mungyer et al., 1984;Sakakura, Hagiwara et al., 2002b;Zhang, Pettengell et al., 1999) which may

be a confounding factor. To avoid these concerns HPMC can also be harvested from peritoneum during surgery for benign disease.

However the in vitro peritoneal model of peritoneum also has some limitations. While valuable information may be gained about the early stages of invasion of the in vitro models, these are removed from culture after a given number of days. If models could survive weeks or months, a more thorough study of peritoneal metastasis during later stages of the disease could be possible. Moreover, only three cell types are present in the model: cancer cells, fibroblasts and HPMC. There are no vessels nor blood supply, no immune system, which translates into a lack of ability to generate a systemic response to invasion, as it would take place in humans. Therefore, some functions which take place at the very local level, such as disruption of HPMC adhesion and proteolysis of the extracellular matrix may be reproduced in an in vitro model, whereas the understanding of those functions provided by a host response such as immunity, angiogenesis, cell repair or apoptosis may be limited.

4 AIMS AND METHODOLOGY

The studies described centred on the use of an in-vitro model system to study the mechanisms of human peritoneal metastases, and to define molecular features which distinguish tumours with high propensity for peritoneal invasion. The main hypothesis was that gene expression by invading cancer cells and host mesothelial cells in a 3D model of peritoneum would correlate with observed microscopic invasion. The experimental aims are outlined below:

1. To establish the 3-D model of human peritoneum as described by Jayne et al (Jayne, O'Leary et al., 1999b)
2. To characterise the behaviour of the cancer cell lines with different metastatic potential on this model using immunocytochemistry
3. To extract mRNA from cancer cells and associated mesothelial cells using laser capture microdissection
4. To study patterns of gene expression using amplified RNA and cancer microarrays
5. To define gene expression changes which may be particularly important in the process of peritoneal invasion

5 MATERIALS AND METHODS

5.1 TUMOUR CELL LINES

All cell lines were kindly provided by S McMillan, Department of Surgery, the Royal Liverpool Hospital NHS Trust and the University of Liverpool. Details of each cell line are specified in table 7.

	HT 29	SW480	TMK	KATO
Species	Human	Human	Human	Human
Origin	Colon	Colon	Stomach	Metastatic, Pleural
Histology	well differentiated adenocarcinoma	grade III-IV adenocarcinoma	Undifferentiated, diffuse type (scirrhous)	Signet ring carcinoma of the stomach
Metastatic Potential	Low	Low-medium	High	High
Characteristics	Fast growth, adherent cells	Fast growth, adherent cells	Fast growth	Slow growth
Culture requirements	RPMI 10% FCS, penicillin-streptomycin and glutamine	RPMI 10% FCS, penicillin-streptomycin and glutamine	RPMI 10% FCS, penicillin-streptomycin and glutamine	RPMI 20% FCS, penicillin-streptomycin and glutamine

Table 3 Four cancer cell lines were used for invasion of the 3D model. HT29 and SW480 were colonic cancers and TMK and KATO were primary and metastatic gastric cancers respectively.

5.1.1 CELL CULTURE

Handling of tissue culture flasks was always performed in a laminar airflow safety cabinet, in the tissue culture room. Medium was changed every two to three days, according to cell requirements. Cells were checked for confluence under a phase contrast microscope (Leica, Leica Geosystems AG Heerbrugg, Switzerland, www.leica.com). When they reached 80% confluence they were subcultured using 0.05% Trypsin EDTA (Gibco, Gibco®, Invitrogen, Paisley, UK, www.invitrogen.com) and resuspended in fresh medium.

5.1.2 MYCOPLASMA DETECTION

All cell lines, HT29, TMK I, Kato III and SW480 were routinely tested for mycoplasma before every new batch of invasive peritoneal models was made (Appendix 8.1.1). If mycoplasma infection was detected, cells were excluded from any further experiments.

The PCR Mycoplasma Detection Set (Takara Bio Inc.) was used. This primer set allowed the detection of the following mycoplasma species (M fermentans, M hiorhinis, M arginini, M orale, M salivarium, M hominis, M pulmonis, M arthritidis, M neurolyticum, M hyopneumoniae, M capricolum) and Ureaplasma urealyticum.

The supernatant from cells cultured for 4 days after subculture without antibiotic was used as a sample. The following reaction mixture was prepared for the first PCR:

H2O	70µ
10x PCR Buffer	10µl
dNTP mixture	8µl
MCGp F1 primer	1µl
MCGp R1 primer	1µl
Takara Taq	0.5µl

10µl of sample were added to the above reaction mixture to make 100µl of total volume. 10µl of water were added to the negative control and 10µl of Control Template (1ng/µl) to the positive control. All microtubes were placed in

a gradient cycler (Eppendorf UK ltd, Histon, Cambridge, www.eppendorf.com). The following parameters were set and PCR was performed:

94°C	30 seconds	1 cycle
94°C	30 seconds	35 cycles
55°C	2 minutes	
72°C	1 minute	

Another reaction mixture was then prepared for a second PCR by combining the reagents as shown below:

H2O	78.5µl
10x PCR Buffer	10µl
dNTP mixture	8µl
MCGp F2 primer	1µl
MCGp R2 primer	1µl
Takara Taq	0.5µl

1µl of each first PCR product was added to the above reaction mixture to obtain a final volume of 100µl. Care was taken to avoid cross contamination. All microtubes were again placed in the gradient cycler and a second PCR was performed. On this occasion 30 cycles rather than 35 were performed. The amplified products were analysed by gel electrophoresis (2% agarose). The presence and size of any DNA fragments present as bands was compared to those of 12 species provided by Takara Bio Inc.

Species	Pairs of Primer	
	F1 and R1 (bp)	F2 and R2 (bp)
M hyopneumoniae	681	237
M neurolyticum	501	196
M fermentans	491	195
M pulmonis	477	189
M hiorhinis	448	211
M orale	423	179
M capricolum	415	179
M arthritidis	408	157
M salivarium	403	151
M hominis	370, 369	147, 148
M arginini	369	145
U urealyticum	482, 481	154

In order to confirm that a sample did not include any inhibition substance, a positive control band was present in both PCR. A band of 810 bp appeared with F1 and R1 primers, and a band of 590 bp with F2 and R2 primers.

The same protocol was used to assess the success of antibiotic treatment of infected cells.

5.2 THE THREE DIMENSIONAL PERITONEAL MODEL

5.2.1 MESOTHELIAL CELL ISOLATION AND CULTURE

Human peritoneal mesothelial cells (HPMC) and fibroblasts were isolated from human omental tissue obtained from consenting patients undergoing elective abdominal surgery. Ethical approval was granted by South Sefton Research Ethics Committee. Samples of omental tissue were washed in cold PBS and incubated in either 0.05% or 0.25% Trypsin-EDTA (Gibco, Gibco®, Invitrogen, Paisley, UK, www.invitrogen.com) at 37°C for 10 or 20 minutes, depending on protocol. Three different methods of HPMC isolation were used, then assessed for HPMC growth and presence of fibroblast contamination. Method A (n=11): incubation in 0.05% trypsin solution for 20 minutes, method B (n=15): incubation in 0.25% trypsin for 10 minutes, method C (n=14): incubation in 0.25% trypsin for 20 minutes. After incubation, cells released by trypsin were collected by centrifugation of the trypsin solution for five minutes at 460 g. The cell pellet obtained was re-suspended in 5ml of complete medium which was prepared as follows:

500ml Dulbecco's Modified Eagle's Medium Ham's F-12 (Sigma, Sigma-Aldrich Ltd, Dorset, UK, www.sigmaaldrich.com); 10% FCS (Sigma, Sigma-Aldrich Ltd, Dorset, UK, www.sigmaaldrich.com); 5ml Penicillin-Streptomycin (10,000 U/ml of penicillin base and 10,000 µg/ml of streptomycin base utilising penicillin G (sodium salt) and streptomycin sulfate in 0.85% saline, Gibco, Gibco®, Invitrogen, Paisley, UK, www.invitrogen.com) and 5ml 200mM L-glutamine (Gibco, Gibco®, Invitrogen, Paisley, UK, www.invitrogen.com); 5ml Insulin-Transferrin (50µg Insulin + 50µg transferrin in 100ml of unprepared medium in water bath and stirred until dissolved). Insulin was prepared from Human Actrapid (Insulin concentration: 3.5mg/ml, Novo Nordisk A/S, Bagsvaerd, Denmark, www.novonordisk.com). Transferrin was available from Gibco, (Transferrin concentration: 10mg/ml, Gibco®, Invitrogen, Paisley, UK, www.invitrogen.com); 50 µl of hydrocortisone (100mg hydrocortisone in 0.5ml Ethanol 100% and 0.5ml of water, Solu-Cortef®, Pharmacia Corporation Kalamazoo, Michigan 49001, USA).

After centrifugation at 460 g for five minutes and re-suspension in fresh complete medium, cells were transferred into a 0.2% gelatine (10 mg gelatine in 5ml PBS, BDH Chemicals Ltd, Dorset, UK) coated T25 tissue culture flask (Greiner, Greiner Bio-One Ltd, Stonehouse, UK www.greinerbioone.com). Every 48 hours the medium was changed. As soon as the mesothelial cells achieved full confluence, they were split using 0.05% Trypsin-EDTA and transferred into a 0.2% gelatine coated T75 flask.

5.2.2 FIBROBLAST ISOLATION AND CULTURE

Cell suspensions were prepared from operative samples as above. However incubation lasted 45 minutes at 60rpm in a rotating incubator and 37°C. Medium used for fibroblast culture consisted of Dulbecco's F-12 Ham medium (Sigma, Sigma-Aldrich Ltd, Dorset, UK, www.sigmaaldrich.com) containing 10% FCS (Sigma, Sigma-Aldrich Ltd, Dorset, UK, www.sigmaaldrich.com), 5ml penicillin-streptomycin and 5ml of glutamine (Gibco, Gibco®, Invitrogen, Paisley, UK, www.invitrogen.com). Routine use of gelatine was not necessary for fibroblast culture. Medium was changed every 2 to 3 days. 0.05% Trypsin (Gibco, Gibco®, Invitrogen, Paisley, UK, www.invitrogen.com) was used to split confluent cells as above.

5.2.3 COLLAGEN PREPARATION

Freshly removed rat tails were washed in 70% Ethanol at room temperature for two hours. An incision was made through the length of tail with a sterile scalpel and its skin was stripped, thus exposing four tendons. These were also stripped, thoroughly minced in a Petri dish and transferred into a Falcon tube (BD Biosciences, Oxford, UK, www.bdbeurope.com) containing 50ml of 17mM acetic acid (Fisher Chemicals Ltd. UK, www.fisherchemicals.co.uk). They were stirred mechanically for 48 hours at 4°C using a R100 Rotatest shaker (Luckham Ltd UK). Undissolved tendon was removed by centrifugation at 30000g and 4°C for 60 minutes (Beckman Ultraclear™ Centrifuge tubes, Beckman Coulter™ Allegra 64 Centrifuge, Beckman-Coulter, High Wycombe,

UK, www.beckmancoulter.com). Soluble collagen was precipitated by adding 0.1M NaOH (Sigma, Sigma-Aldrich Ltd, Dorset, UK, www.sigmaaldrich.com), until pH 7. The solution was stirred for further 90 minutes at 4°C. Precipitated collagen was collected by centrifugation (10000g 20min 4°). Type I collagen pellets were redissolved in sterile 17mM acetic acid by stirring at 4°C for 48 hours. The total protein content of the collagen solution was assessed at the Department of Biochemistry, University Hospital Aintree and adjusted to be within the range 3.5-5mg/ml.

5.2.4 FABRICATION OF THE 3D MODEL

The 3-D model was constructed as originally described by Jayne et al (Jayne, O'Leary et al., 1999b). Peritoneal fibroblasts were suspended in Hams's F-12 (Sigma, Sigma-Aldrich Ltd, Dorset, UK, www.sigmaaldrich.com), at $5x10^5$ cells/ml and one part mixed with three parts of 2xDMEM (Sigma, Sigma-Aldrich Ltd, Dorset, UK, www.sigmaaldrich.com), one part 0.1M NaOH, one part FCS (Sigma, Sigma-Aldrich Ltd, Dorset, UK, www.sigmaaldrich.com), and three parts rat-tail type I collagen. 1.2ml of the above mixture was pipetted into individual wells of a 12-well tissue culture plate and incubated at 37°C for 30 min to facilitate gel formation.

2.5ml of complete medium was pipetted into each well. The gels were incubated for 24 hours. Thereafter they were detached from their culture wells using a sterile 12-gauge hypodermic needle. The floating gels were cultured for another six days to allow contraction to dense collagen matrices. The upper surfaces of the matrices were seeded with mesothelial cells ($5x10^4$ cells in 20µl Ham's, concentration $2.5x10^6$ cells/ml) and allowed to attach by incubation at 37°C and 5% CO_2 for 30 minutes. Complete medium was added. The matrices were cultured for a further five days to allow mesothelial cells to attain confluence. At this point, complete medium was substituted for Hams's F-12 1% FCS (Sigma, Sigma-Aldrich Ltd, Dorset, UK, www.sigmaaldrich.com), and the models were incubated for a further 48 hours to encourage mesothelial cell quiescence and stimulate the resting state of the in vivo peritoneum prior to further studies.

5.2.5 PERITONEAL MODEL INVASION

HT29, SW480, TMK and KATO III cells were used in invasion assays. All cancer cells were removed from their tissue culture flasks with 0.05% Trypsin (Gibco, Gibco®, Invitrogen, Paisley, UK, www.invitrogen.com) and re-suspended in RPMI medium. 20µl of RPMI (Gibco, Gibco®, Invitrogen, Paisley, UK, www.invitrogen.com) containing cancer cells at different concentrations, measured in a haemocytometer, were gently placed on the peritoneal surface after removing complete medium from their wells. Tissue culture plates were immediately incubated at 37°C and 5% CO_2 for 30 minutes. 2.5ml of complete medium was pipetted into each well thereafter. Medium was replaced every 48 hours. Pellets were snap frozen in liquid nitrogen after seven days incubation period.

Because the original intention was to study the effects of seeding with three different concentrations of cancer cells (10^4, 10^5, 10^6 cells/ml) with four different cell lines, a total of 50 individual models of were created. Two models were made for each concentration and cell type. The 24 models were made in duplicate. Furthermore two models of normal, un-invaded peritoneum were made.

5.3 LIGHT MICROSCOPY CHARACTERISATION

5.3.1 HAEMATOXYLIN AND EOSIN

Paraffin sections were de-waxed twice for five minutes in xylene, dehydrated in absolute alcohol (740P) for one minute and washed in water. They were stained in Gill's haematoxylin for four minutes, rinsed in water and differentiated in 1% acid alcohol until the background became clear and nuclei remained intense blue. Slides were placed in warm water and then stained in 1% eosin for four minutes. These were rinsed very briefly in water, dehydrated in alcohol (740P) and cleared in xylene. Finally all slides were mounted in DPX mountant medium (All reagents and materials were provided by the Neuropathology Laboratory, The Walton Hospital for Neurology and Neurosurgery, NHS Trust).

5.3.2 IMMUNOCYTOCHEMISTRY

The following antibodies were kindly provided by the Department of Neuropathology as above: Cytokeratins 5, 8, 18 (Cam complex), Vimentin, Factor VIII, CEA, CAM 5.2, EMA and CK20. Epithelial antibody Ber EP4, ICAM, VCAM, PECAM, fibronectin and laminin were purchased from Dako (Dako UK Ltd, Ely, www.dako.co.uk) collagens III and IV from Chemicon (Chemicon Europe Ltd, Hampshire, UK, www.chemicon.com). Characteristics of the antibodies are summarised in the table below.

Positive control tests were performed on appendix, bowel and uterus for epithelial antibodies and adhesion molecules. Muscle was used to test collagens, fibronectin and laminin. All controls satisfactorily confirmed staining efficiency. A negative control using distilled water instead of antibody did not stain at all.

Paraffin sections were de-waxed and dehydrated as above. Endogenous peroxidase activity was blocked by placing the slides in 10% hydrogen peroxide in absolute alcohol 740P for 15 minutes. They were then rinsed in running water and placed in TRIS buffer (pH 7.4). The slides were placed in a solution of 1200ml of water, 120ml of 0.1M citrate buffer (pH 6) and boiled for ten minutes, cooled immediately in cold water and washed in water thereafter. This process was performed when heat antigen retrieval was required, thus facilitating antigen to antibody binding. 80µl of the primary antibody (dilution according to manufacturer's recommendations) were placed on the slides and incubation followed for 30 minutes at 37°C. After washing in TRIS buffer, 80µl of the secondary antibody were placed and incubation continued for another 30 minutes at 37°C. Again the slides were washed in TRIS buffer. 80µl of the ABC (Avidin-Biotin) complex (Vector laboratories, Peterborough, www.vectorlabs.com) was added on the slides. While these were incubated for 30 minutes at 37°C, liquid DAB (Diaminobenzidine) was prepared: briefly two drops of buffer stock (Vector laboratories, Peterborough, www.vectorlabs.com) were added to 5 ml of distilled water and mixed well. Four drops of DAB stock solution (Vector laboratories, Peterborough, www.vectorlabs.com) and 2 drops of hydrogen peroxide were added and mixed thoroughly. The solution was used immediately. 80µl were placed on the slides and left for 10 minutes. After washing off excess reagent slides were counterstained with Gills Haematoxylin for 1 minute.

Characteristics of each antibody, including, type, target cell concentration, optimal dilution and sample preparation required are summarised in the table below.

ANTIBODY	TARGET	TYPE	CONCENTRATION	DILUTION	APPLICATION
I-CAM	Epithelia, leucocytes, endothelia	Monoclonal	0.05 mol/l	1:100	Frozen
V-CAM	Endothelia	Monoclonal	0.05 mol/l	1:25	Paraffin
PECAM	Endothelia, leucocytes	Monoclonal	0.05 mol/l	1:20	Paraffin
Ber-EP4	Normal and neoplastic epithelia of ectodermal origin	Monoclonal	0.02 mol/l	1:200	Paraffin or frozen
CAM 5.2	Normal and neoplastic epithelia	Monoclonal	0.02 mol/l	1:100	Paraffin
EMA	Normal and neoplastic epithelia	Monoclonal	0.05 mol/l	1:50	Paraffin
CYTOKERATINS 5,8,18	Normal and neoplastic epithelia	Monoclonal	0.05 mol/l	1:25	Paraffin
VIMENTIN	Cytosketelon	Monoclonal	0.05 mol/l	1:100	Paraffin
COLLAGEN III	Human Collagen	Polyclonal	0.15 mol/l	1:500	Frozen
COLLAGEN IV	Human Collagen	Monoclonal	0.1 mol/l	1:200	Paraffin or frozen
LAMININ	Human laminin	Monoclonal	0.05 mol/l	1:20	Paraffin
FIBRONECTIN	Human fibronectin	Polyclonal	0.1 mol/l	1:400	Paraffin

Table 4 Characteristics of antibodies used for immunocytochemistry, including target cells, type, antibody concentration, dilution and sample preparation

5.4 LASER CAPTURE MICRODISSECTION

5.4.1 PREPARATION OF THE MODELS

Peritoneal models were removed from their 12 well tissue culture plates and immediately frozen in liquid nitrogen to avoid RNA degradation. Frozen samples were brought from liquid nitrogen to the cryostat (Jung CM3000 Leica) at a temperature of -20°C. Tissue was embedded in Cryoblock TBS Tissue embedded Matrix for cryotomy. 5μm tissue sections were cut with the cryotome. Sections were stained with Haematoxylin/eosin and viewed in a phase contrast microscope. If satisfactory peritoneal invasion by cancer cells was visualised then further sections were cut. These were placed on slides pre-treated at 200°C for 4 hours to destroy RNases. Each slide was placed in a Falcon tube and frozen at -80°C.

5.4.2 HAEMATOXYLIN AND EOSIN STAIN OF LCM SAMPLES

All staining dishes were thoroughly cleaned, rinsed in DEPC water, autoclaved and dried in a hot drying cabinet before use. Frozen slides were kept for 2 minutes in a Coplin jar containing 95% Ethanol at -20°C. They were washed in DEPC water for 30 seconds, stained in filtered Harris's Haematoxylin for one second, rinsed in DEPC water for one second, and placed in Scott's DEPC water (1g Sodium Bicarbonate and 40g Magnesium Sulphate in 500ml of water). The tissue was then dehydrated in 70% ethanol for 30 seconds followed by 95% ethanol for 30 seconds. Thereafter it was stained with eosin (1% eosin in 95% ethanol) for five seconds. Finally the tissue was washed twice in 95% ethanol for 30 seconds and dehydrated twice in 100% ethanol for 30 seconds and twice in xylene for five minutes. The slides were then air dried for five minutes or until xylene evaporated completely and then placed in the oven at 37°C to keep tissues dry.

5.4.3 LASER CAPTURE PROCEDURE

The laser capture microscope (Pixcell, Arcturus, Molecular Devices Ltd, Berkshire, www.arctur.com) was set as follows: sample thickness 5μm, laser spot size 7.5μm, pulse power 69μW, pulse width 1ms and threshold voltage 220 mV. A cap (Capsure, LCM Caps Arcturus, Molecular Devices Ltd, Berkshire, www.arctur.com) was placed on the slide and vacuum was applied. The laser beam was selectively aimed at those cells of interest. The cap was released from the slide and rubbed against a cap pad (LCM Caps Arcturus, Molecular Devices Ltd, Berkshire, www.arctur.com) to remove unwanted tissue.

5.4.4 CELL LYSIS

Caps containing the tissue of interest were tightly placed on a 0.5ml microtube containing 50μl of lysis buffer XB (Picopure RNA extraction Kit, Arcturus, Molecular Devices Ltd, Berkshire, www.arctur.com). The microtubes were incubated upside down at 42°C for 30 minutes, thus allowing the buffer in contact with the cap surface. Thereafter the microtubes were centrifuged at 6000 g for one minute and kept at -80°C. The product was ready for RNA extraction.

5.4.5 RNA EXTRACTION AND ISOLATION

RNA was extracted from the LCM caps using the Picopure RNA isolation kit (Picopure™ RNA Isolation Kit, Arcturus, Molecular Devices Ltd, Berkshire, www.arctur.com). 50μl of Extraction Buffer (XB) were pipetted into a 0.5ml microcentrifuge tube. A Capsure Macro LCM cap was inserted onto the microcentrifuge tube which was then inverted, hence allowing all Extraction Buffer to cover the Capsure Macro LCM Cap. Gentle tapping helped the process. The assembly was incubated for 30 minutes at 42° and centrifuged at 800g for 2 minutes. After centrifugation, the microcentrifuge tube contained the cell extract, necessary to complete the protocol. The Capsure Macro LCM Cap was removed. At this stage we could proceed with the RNA isolation protocol or freeze the cell extract at -80°C.

RNA Purification columns were pre-conditioned as follows: 250µl of Conditioning Buffer were pipetted onto the purification column filter membrane. The column was incubated for five minutes at room temperature and then centrifuged at 16000xg for one minute.

50µl of 70% Ethanol (EtOH) were pipetted into the cell extract above and mixed well. The mixture was pipetted into the preconditioned purification column. The combined volume was approximately 100µl. Centrifugation for two minutes at 100g followed by 30 seconds at 16000g to remove flow-through followed. This process binds the RNA to the column. 100µl of Wash Buffer (W1) were pipetted into the purification column and this was centrifuged for one minute at 8000g. A second wash and centrifugation was performed using Wash Buffer (W2). A third wash was performed by pipetting 100µl of W2 into the purification column followed by centrifugation at 16000xg. If any residual W2 was left a further cycle at 16000xg for one minute followed. Finally the purification column was transferred to a new 0.5ml microcentrifuge tube. 30µl of Elution Buffer was pipetted directly onto the membrane of the purification column. The purification column was incubated for one minute at room temperature and centrifuged for one minute at 1000xg to distribute EB in the column and then one minute at 16000g to elute RNA. The RNA was now ready for SMART/T7 amplification. Alternatively it could be stored at minus 80°C.

5.5 LCM RNA AMPLIFICATION

Two rounds of amplification were necessary to obtain sufficient representative amounts of mRNA. At the time of these experiments, the recommended minimum amount by the slide manufacturers, MWG, was 5µg per reaction. The rational for two rounds of amplification was that insufficient amounts of starting total RNA from laser captured cells would not yield enough amplified RNA from one round only. LCM samples are well known to produce small quantities of total RNA, and different methods of amplification have successfully obtained sufficient amplified RNA (Luzzi, Mahadevappa et al., 2003). In fact successful amplification from as little as one cell has been reported (Kamme, Zhu et al., 2004).

The first round (Fig 4a) was based on a single-stranded linear amplification protocol developed and validated by D Stirewalt et al (Stirewalt, Pogosova-Agadjanyan et al., 2004). This switch primer protocol was a modified version of BD SMART™ PCR cDNA (BD Biosciences, Oxford, UK, www.bdbeurope.com). BD SMART™ technology is based on template switching technique (switching mechanism at the 5' end of the RNA transcript) thus resulting in a full length single-strand cDNA containing the complete 5' end of the mRNA. The usual SMART PCR protocol simultaneously amplifies transcripts from both ends; however this technique amplifies only from the 5' end producing large amounts of first strand cDNA. Therefore this protocol combines the reproducibility of single-stranded linear amplification and the amplification robustness of the PCR.

The second round (Fig 4) was performed following the protocol from Eberwine et al. available as Amino Allyl MessageAmp™ II aRNA kit from Ambion (Applied Biosystems, Warrington, UK, www.ambion.com).

During the first round, as shown in figure 5, total RNA, BD SMART oligonucleotide and oligo T7 (dt) primer, (Invitrogen, Paisley, UK, www.invitrogen.com) were used to initiate first strand cDNA synthesis. Oligo T7 (dt) annealed to the mRNA poly A tail. When the BD Powerscript Reverse Transcriptase reached the end of the mRNA, the enzyme's terminal transferase activity added a few nucleotides, primarily deoxycytidine to the 3' end of the cDNA. The BD SMART oligonucleotide, containing an oligo (G) sequence at its

3' end, base-paired with the deoxycytidine stretch, thus creating an extended template. The reverse transcriptase then switched templates and continued replicating to the end of the SMART oligonucleotide. The resulting full length single stranded cDNA contained 5' end sequences that were complementary to the BD SMART oligonucleotide. 5' PCR primer II A annealed to this complementary sequence and 50x Advantage DNA polymerase enzyme synthesised sense strand cDNA. DET7F primer filled in the above sense strands with the complementary antisense strands in a separate reaction, thus creating double stranded cDNA.

RNA was created by in vitro transcription, using the T7 amplification protocol (MEGAscript™, Ambion, (Applied Biosystems, Warrington, UK, www.ambion.com). The cDNA contained the T7 recognition sequence that was used as the Oligo T7 (dt) RNA polymerase promoter site for in vitro transcription (minimal sequence requirements TAATACCGACTCACTATA**G**GGAGA). The first base incorporated during transcription was G (in bold, sequence above). The resulting transcription from this promoter would result in antisense RNA.

The second round of amplification, shown in figure 4b, was similar to the first but the reagents and enzymes were different and switching template technique was not used in this step; however the principle of single linear amplification still applied. Instead random primers would anneal to the initial aRNA in a reverse transcription reaction. The resulting first strand cDNA was primed to oligo T7 (dt) primer and DNA polymerase would synthesise double stranded cDNA. Finally T7 amplification was performed as above, but with the addition of aminoallyl dUTP for incorporation into the final amplified RNA product to the master mix in order to obtain coupled RNA for enhanced hybridisation.

Finally, RNAse free water was used as a negative control. Where amplification was unsuccessful whether in quantity or quality, samples were discarded and the procedure was repeated.

FIRST ROUND

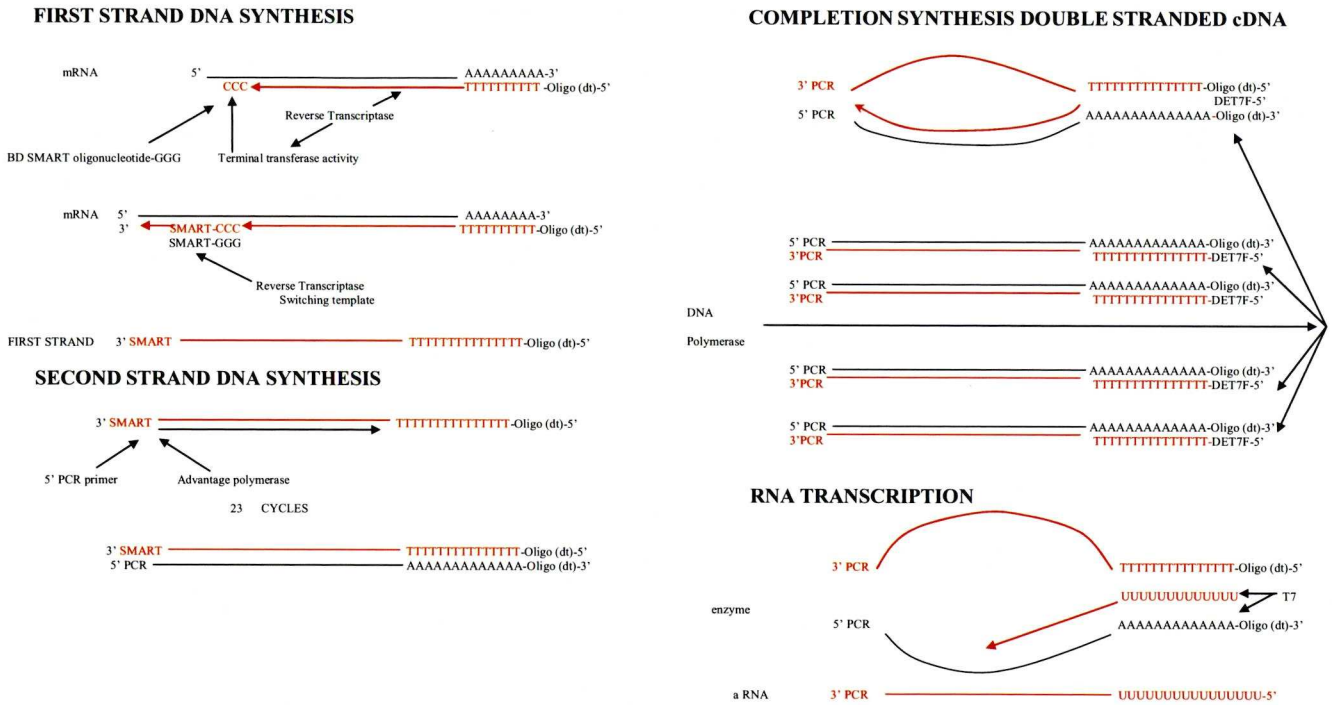

Figure 4a Graphic representation of the first round of amplification as described by Stirewalt et al. Sense strands are represented in black. Antisense strands in red. Oligo sequences are as follows:

SMART: 5'-AAGCAGTGGTATCAACGCAGAGTACGCGGG-3'

5 PCR PRIMER: 5'-AAGCAGTGGTATCAACGCAGAGT-3'

DET7F: 5'-GGCCAGTGAATTGTAATACGACTCA-3'

OLIGO (dt): 5'-GGCCAGTGAATTGTAATACGACTCACTATAGGGAGGCGGTTTTTTTTTTTTTTTTTTTTTTT-3'

SECOND ROUND

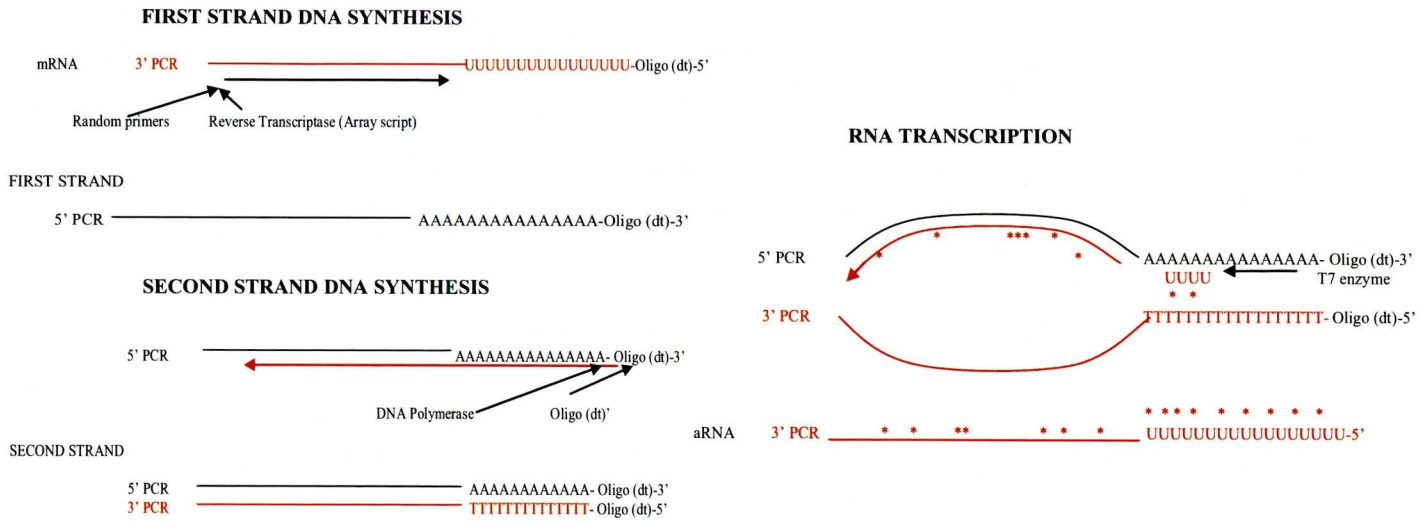

Figure 4b The above diagram illustrates the second round of amplification as described by Eberwine et al and commercially available by Ambion. Sense strands are represented in black, antisense strands in red. (*) represents the aminoallyl molecule incorporated into the nucleotide UTP. The oligonucleotide sequences are as follows:

SMART: 5'-AAGCAGTGGTATCAACGCAGAGTACGCGGG-3'

5 PCR PRIMER: 5'-AAGCAGTGGTATCAACGCAGAGT-3'

DET7F: 5'-GGCCAGTGAATTGTAATACGACTCA-3'

OLIGO (dt): 5'GGCCAGTGAATTGTAATACGACTCACTATA*G*GGAGGCGGTTTTTTTTTTTTTTTTTTTTTTT-3'

5.5.1 FIRST ROUND OF AMPLIFICATION

5.5.1.1 FIRST STRAND cDNA SYNTHESIS

Precipitation of RNA from 30µl to a final volume of 3.5µl was performed in a speed vac (Univapo 150 ECH).

The first round of amplification was prepared as shown:

RNA mixture	RNA (max 1µg)	3.5µl
	Smart oligo	1µl
	T7 oligo dT (100ng/µl)	0.5µl
Master mix	5x first strand buffer	2µl
	DDT (Dithiothreitol 20mM)	1µl
	dNTP mix 10mM	1µl
	Powerscript Reverse Transcriptase	1µl

The RNA mixture was incubated at 70°C for two minutes, placed on ice for one minute and incubated a further two minutes at 42°C to allow priming of the oligo dt. 5µl of the master mix were added and the final solution was incubated at 42°C for one hour, followed by seven minutes at 72°C.

5.5.1.2 cDNA PURIFICATION

Purification was performed following the Quiaquick protocol (Qiagen, Crawley, West Sussex, UK, www.qiagen.com). Finally samples were eluted in 50µl of RNAse free H_2O.

Briefly, to 10µl of RT mix, 35µl of H2O, 5µl of sodium acetate (pH 5.5) and 250µl of binding buffer (five volumes) were added. The final solution was added in the column. This was centrifuged at 10000g for one minute. After discarding the flow-through the column was washed with 750µl of PE buffer containing ethanol for one to two minutes and centrifuged at 10000g for one minute. Further centrifugation was performed at full speed to dry the column. The column was transferred to a collection tube. 50µl of RNAse free H2O were added to the column, left at room temperature for one minute and centrifuged at

10000g for one minute. The process was repeated with 30µl of RNAse free H2O, thus obtaining a final volume of approximately 80µl.

5.5.1.3 SECOND STRAND cDNA SYNTHESIS

H2O was added to the above product to a final volume of 84µl. 16µl of the master mix below were added to the product:

10x Advantage PCR Buffer	10µl
dNTP mix 10mM	2µl
5' PCR primer	2µl
50x Advantage polymerase mix	2µl

The 100µl would undergo 10 cycles of SMART amplification (one minute at 95°C followed by 10 cycles of 15 seconds at 95°C, 30 seconds at 65°C and six minutes at 68°C).

5.5.1.4 CDNA PURIFICATION

The PCR purification Quiaquick protocol, (Qiagen, Crawley, West Sussex, UK, www.qiagen.com) was used as above.

5.5.1.5 COMPLETION OF SYNTHESIS OF DOUBLE STRANDED CDNA

H_2O was added to the above product to a final volume of 84µl. 16µl of the master mix below were added to the product:

10x Advantage PCR Buffer	10µl
dNTP mix 10mM	2µl
DET7F primer	2µl
50x Advantage polymerase mix	2µl

The amplified cDNA was denatured at 95°C for 75 seconds , followed by primer annealing at 60°C for 15 seconds and elongation at 68°C for ten minutes. Upon completion the double stranded cDNA was purified again with the Quiaquick protocol. As the product contained 100µl, 500µl of PE binding buffer (5 volumes) and 10µl of Sodium Acetate (pH 5.5) were added instead at the initial

stage. The procedure would then continue as above. The resulting final volume was reduced (vacuumed) to 8µl.

5.5.1.6 T7 AMPLIFICATION

This process involved the synthesis (transcription) of RNA from the DNA above with the enzyme T7 RNA polymerase. I used the above protocol from Ambion (Applied Biosystems, Warrington, UK, www.ambion.com). 26µl of the above were mixed with the cDNA. The solution was left at 37°C for 14 hours. Thereafter samples were purified and eluted in 100 µl of pre-heated nuclease free water. aRNA integrity was measured by UV absorbance against 50µl of nuclease free water. Quality was checked by 2% electrophoresis gel.

The protocol provided in the MegaScript kit from Ambion (Applied Biosystems, Warrington, UK, www.ambion.com) was used. Once all reagents were defrosted they were all put on ice except the buffer. The following mixture was prepared at room temperature.

ATP 75mM	2µl
CTP 75mM	2µl
GTP 75mM	2µl
UTP 75mM	2µl
Buffer	2µl
Enzyme mix	2µl

12µl of the mixture were added to 8µl of cDNA. The solution was left at 37°C for 16 hours.

5.5.1.7 aRNA PURIFICATION

The clean-up protocol from RNeasy (Qiagen, Crawley, West Sussex, UK, www.qiagen.com) was used. To the above cRNA mixture, 80µl of H2O and

350µl of lysis buffer (RLT+βmercaptoethanol) were added, and thoroughly mixed. 250µl of 100% ethanol were added. The total solution was added to the column, which was centrifuged at 8000 g for 20 seconds. The column was placed in a new collection tube. 500µl of RPE buffer were added and centrifuged again for 20 seconds at 8000 g. After discarding the flow-through, 500µl of RPE buffer were added and centrifuged for 2 minutes at 8000g. Effluent was discarded and the column was centrifuged dry at 20000g for one minute. The column was placed in a new collection tube, 80µl of H2O were added. The column was left at room temperature for one minute and centrifuged at 8000g for another minute. The total cRNA was measured in the spectrophotometer against 50µl of water.

5.5.2 SECOND ROUND OF AMPLIFICATION

5.5.2.1 FIRST STRAND cDNA SYNTHESIS

The Amino Allyl MessageAmp™ II (Ambion, Applied Biosystems, Warrington, UK, www.ambion.com) was used. The first round of amplification was prepared as shown:

RNA mixture	RNA (max 2µg)	10µl
	Second Round primers	2µl
Master mix	10x first strand buffer	2µl
	RNase inhibitor	1µl
	dNTP mix	4µl
	Reverse trancriptase	1µl

The RNA mixture was incubated at 70°C for 10 minutes and placed on ice briefly before commencing reverse transcription. 8µl of the master mix were added. The final solution was incubated at 42°C for two hours.1µl of RNAse H was added to degrade the RNA, thus leaving DNA only for second strand synthesis. Incubation was performed at 70°C for 30 minutes.

5.5.2.2 SECOND STRAND cDNA SYNTHESIS

5µl of oligo (dt) primer was added to the above mixture. The master mix was prepared as follows:

10x Advantage PCR Buffer	10µl
dNTP mix	4µl
RNAse free water	58µl
DNA polymerase mix	2µl

74µl of master mix was added to the sample. The resulting mixture was placed on ice at 16°C for two hours.

5.5.3 cDNA PURIFICATION

250µl of Binding Buffer were added to the sample and mixed thoroughly. The mixture was passed through a cDNA filter cartridge and centrifuged for one minute at 10000g. Flow-through and the columns were washed with 500µl of Wash Buffer for one minute at 10000g. Finally cDNA was eluted with 2x9µl of nuclease free water.

5.5.4 T7 AMPLIFICATION

The following mixture was prepared at room temperature. Aminoallyl UTP was incorporated at this stage.

A, C, GTP 25mM	12µl	
UTP 50mM	3µl	
aaUTP50mM	3µl	(aminoallyl-UTP)
10X Buffer	4µl	
Enzyme mix	4µl	

26μl of the above were mixed with the cDNA. The solution was left at 37°C for 14 hours.

5.5.5 aRNA PURIFICATION

Nuclease free water was added to each sample to bring the final volume to 100μl. 350μl of aRNA binding buffer and 250μl of ACS grade 100% ethanol were added to the samples and these were loaded into aRNA filter cartridges. Centrifugation for one minute at 10000g followed. Flow through was discarded and 650μl of wash buffer were applied to the cartridges. These were centrifuged twice for one minute in order to remove traces of ethanol. Finally the aRNA was eluted in 100μl of pre-heated nuclease free water. aRNA integrity was measured by UV absorbance against 50μl of nuclease free water. Quality was checked by 2% electrophoresis gel.

5.6 RNA LABELLING

A number of techniques are available which allow comparison of two or more RNA samples and identification of differences in the abundance of specific transcripts. Microarrays are one such technique, which enables relative amounts of many hundreds of genes to be measured in different RNA samples simultaneously. To do this the RNA from each sample is differentially labelled, usually with a fluorescent dye, prior to hybridisation to the microarray.

Fluorescent cyanine dyes Cy3 and Cy5 were chosen to label previously amplified RNA which contained aminoallyl-UTP for enhanced labelling efficiency ('t Hoen, de et al., 2003). Both cyanine dyes can be excited and detected in the same slide. They also produce bright signals and have a wide dynamic range of detection (Fig 5).

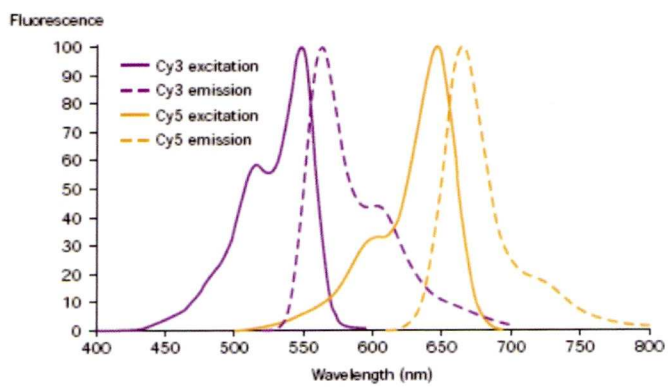

Figure 5 Excitation and emission wavelengths for cyanine dyes Cy3 and Cy5. Source: MWG, Milton Keynes, UK

Following synthesis of the antisense copy of the original mRNA (aRNA) incorporating a proportion of aminoallyl-UTP residues, fluorescent labels can be covalently attached to the aminoallyl groups on the aRNA using N-hydroxyl succinimidyl-ester derivative of each cyanine dye. NHS-esters react with amine groups to form a covalent bond between cyanine dye and the amine group of the

mRNA while the NHS-ester group is released along with fluorescence emission (Fig 6).

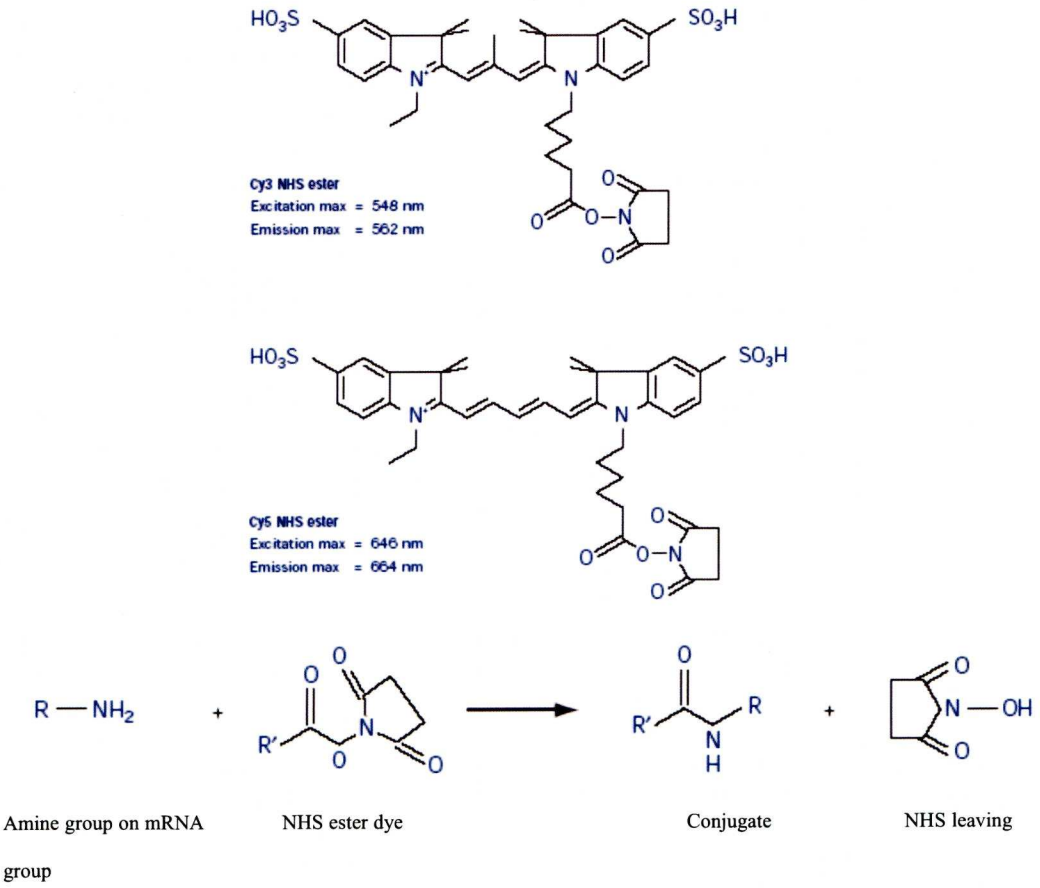

Figure 6 Chemical structure of cyanine dyes and labelling reaction. The above diagram represents the chemical structure of both Cy3 and Cy5 cyanines. When mRNA covalently binds to the Cy NHS ester, NHS ester is released along with emission of fluorescence. Source MWG, Milton Keynes, UK

5.6.1 PROCEDURE

The labelling protocol of choice was Amino Allyl MessageAmp™ (Ambion, Applied Biosystems, Warrington, UK, www.ambion.com). Dyes were purchased from Amersham Pharmacia Biotech (Amersham PLC, Buckinghamshire, UK, www.amersham.com) and were compatible with the above protocol. Briefly, 20μg of Amino Allyl aRNA were placed in a nuclease free microtube and vacuumed dry. Cy3 and Cy5 monofunctional dyes were suspended in 92μl of DMSO to make the labelling reaction more efficient, and kept in the dark for up to one hour before use. This would allow coupling of eight samples, thus avoiding storage and potential dye degradation. 9μl of coupling buffer and 11μl of NHS ester dye were added to our dry samples. Incubation in the dark for 30 minutes allowed coupling to occur. All reactions were then quenched with 4.5μl of 4M Hydroxylamine and incubated at room temperature for 15 minutes hence removing any unreacted dye molecules. Dye labelled aRNA was purified as follows: Nuclease free water was added to each sample to bring the final volume to 100μl. 350μl of aRNA binding buffer and 250μl of ACS grade 100% ethanol were added to the samples and these were loaded into aRNA filter cartridges. Centrifugation for one minute at 10000g followed. Flow through was discarded and 650μl of wash buffer were applied to the cartridges. These were centrifuged twice for one minute in order to remove traces of ethanol. Finally the aRNA was eluted in 100μl of pre-heated nuclease free water. aRNA integrity and coupling efficiency were measured by UV absorbance against TE buffer.

Dye incorporation was calculated using this formula from Ambion, available at http://www.ambion.com/techlib/misc/aama_dye_calc.html:

Figure 7 Calculation of dye incorporation

$$\frac{\#\text{ dye molecules}}{1000\text{ nt}} = \frac{A_{dye}}{A_{260}} \times \frac{9010\ M^{-1}\ cm^{-1}}{\text{dye extinction coefficient}} \times 1000$$

Dye extinction coefficients:

Cy3 = 150000

Cy5 = 250000

All data recorded from spectrophotometric readings are available in the appendix section (Tables 19, 20). In order to continue the experiments, every sample and its reference counterpart had to fulfil these criteria:

- Minimum aRNA yield of 8µg
- A260/A280 ratio between 1.8 and 2.2
- Dye incorporation between 20-50 molecules per 1000 nucleotides

Sample volumes containing equal amounts in µg of sample versus reference labelled RNA were mixed together. The total volume was reduced (vacuumed) to 9µl. RNA mixture data is available in the appendix section (Tables 19, 20).

5.6.2 FRAGMENTATION

This procedure allowed aRNA to fragment into sizes between 60-200 nucleotides. This is a recommended step prior to hybridisation on oligonucleotide printed microarrays. Hybridisation kinetics and overall signal produced will be enhanced. Reagents and protocol were available from Ambion. To achieve this, equal amounts of sample versus reference set were vacuumed to 4.5µl and combined together. The resulting 9µl were mixed with 1µl of fragmentation buffer and incubated for 15 minutes at 70°C. 1µl of stop solution was added and the samples were then incubated on ice for 2 minutes.

5.7 MICROARRAY HYBRIDISATION AND DATA ANALYSIS

5.7.1 OVERVIEW

MWG Human Cancer Array slides were used. These contained oligonucleotides representing 1,853 human genes associated with cancer development and progression selected from the following public databases: OMIM, (Online Mendelian Inheritance in Man, McKusick et al (McKusick, 2007)), NCBI, (National Institute for Biotechnology Information, www.ncbi.nlm.nih.gov), SAGE (Serial Analysis of Gene Expression; John Hopkins Oncology Center, Baltimore, USA) . The genes included carcinoma (colon, breast, prostate, lung, bladder, kidney, liver, pancreas and thyroid), melanoma, neuroblastoma, leukemia, lymphoma and sarcoma-related genes. Thus, this selection of genes was thought to cover a wide range of potentially relevant biological pathways: including cell cycle control, cell adhesion, angio-genesis, signaling and immunity (Source MWG, Milton Keynes, UK).

Table 5 Characteristics of MWG Cancer Array slides are summarised as follows. Source: MWG, Milton Keynes, UK

Minimal number of genes:	1,853 cancer associated human genes
Information sources:	NCBI (Release 123) - 1,660 genes were referenced by NCBI's Online Inheritance in Man (OMIN) as cancer related. - 167 were also identified as differentially ex-pressed in cancer from Serial Analysis of Gene Expression (SAGE).
Strand analyzed:	Sense strand
Number of slides:	1
Length of probes:	50 mer
Number of oligonucleotides per gene:	1
Total number of spots:	1,920
Replicated spots:	40
Arabidopsis control oligos:	27
Spot area:	1.8 x 1.8 cm

A decision to use commercial pre-printed microarrays was taken late in the project as attempts at in-house manufacture of spotted microarray slides proved unsuccessful. At the time of this project the MWG slides provided a good selection of relevant probes which could be analysed using the equipment e.g. Affymetrix 428 Scanner, available in the laboratory. However the use of commercial pre-printed slides cost considerably more than anticipated in the original budget and limited the number of possible hybridisations.

5.7.2 PROCEDURE

To improve hybridisation reactions, labelled aRNA samples were fragmented into smaller nucleotides (60-200), as described above. MWG salt based hybridisation buffer was pre-heated at 42°C for 10 minutes. 120µl of heated hybridisation buffer was added to 11 µl of sample and mixed well, then incubated for three minutes at 95°C and 3 minutes on ice. Then samples were pipetted onto the MWG-Biotech Human Cancer Array (MWG, Milton Keynes, UK) slides and incubated overnight at 42°C in a humid Genetix (Genetix, Hampshire, UK) hybridisation chamber, with gentle agitation. Adhesive MWG Gene Frames® were applied to the slides to seal the reaction within the slide. The use of coverslips prevented problems such as bubbles on the platform, and insufficient humidity or dust.

In addition, control oligonucleotides for non-human (Arabidopsis) genes were provided by MWG. These allowed checking the quality of the hybridisation reaction and 2µl were added to the hybridisation solution along with the buffer. However because of the small number of available slides, the control nucleotides were finally not used.

Thereafter incubation slides were washed with the following buffers prepared in DEPC water and warmed at 30°C, as follows:

Wash 1: 2x SSC, 0.1% SDS
Wash 2: 1x SSC
Wash 3: 0.5x SSC

Slides were washed for five minutes in each wash buffer at room temperature with gentle agitation on an orbital shaker. Finally the slides were dried by centrifugation at room temperature for two minutes at 500g. The slides were then read using an Affymetrix 428 scanner, and fluorescence was measured at two wavelengths: 532 and 635nm corresponding to the emission frequencies of the Cy3 and Cy5 dyes respectively. Setting adjustments were performed using the software available, as per manufacturers' instructions (Jaguar 2.0):

1. **Scan Area (ROI)** This was the actual spotted area in the slide, cropped and separated from the edges of the array.
2. **Dye channels** Cy™5, Cy™3, according to wavelength
3. **Resolution** 10 μm
4. **Gain** 20-35 dB
5. **Line average** 2 (Note: This setting resolves low-expressed probes above threshold)

All the above settings except gain were constant throughout the readings. Gain was individually adjusted for each slide to provide the best possible image with minimum background and photo bleaching, (white spot), effect.

5.7.3 EXPERIMENTAL DESIGN

A reference design was adopted (Dobbin & Simon, 2002a) for these studies. With a reference design, level of expression of any gene in a sample can be related to the expression of that gene in the common reference, as measured on that slide. Subsequently, expression levels of a gene on different slides may be compared using the common reference to control for sources of variability, amongst spots that affect both channels similarly (Dobbin & Simon, 2002b). The reference design is a practical and popular choice for microarray studies using two colour platforms (Kerr, Serikawa et al., 2007). Regarding the choice of reference RNA, no consensus has been reached so far, but commercial reference RNA is frequently used (Park, Cao et al., 2004). In this project total universal reference RNA containing total RNA from 10 different human cell lines

(Stratagene Universal Human Reference RNA, La Jolla, CA, US www.stratagene.com) was used.

The reference design approach seemed most appropriate for my studies, given the multiple pair-wise comparisons of interest between models with different cell types and at different seeding concentrations and incubations. Furthermore, at least for the cancer cell studies, there was no clear candidate for a control sample. The original intention was to study the effects of seeding with three different concentrations of cancer cells (10^4, 10^5, 10^6 cells/ml) with four different cell lines. Therefore, a total of 50 individual models of were created, including 2 un-invaded models. As mentioned above, funding considerations markedly limited the number of slides and hybridisations that were possible, and thus the final microarray studies completed were only a proportion of those originally intended. Thus, hybridisations (sample versus reference) were finally performed using RNA extracted from 3-D models seeded with the same cell concentration (10^6 cells/ml).

Samples were made up of aRNA from each of the four cancer cell lines and from mesothelial cells from the same model, as well as samples of two uninvaded models. Biological replicates contained RNA from different models, from the same cancer cell line. Technical replicates contained RNA from the same model. Replicates for each hybridisation were performed as summarised below in tables 6, 7.

CANCER CELLS	HT 29	SW 480	TMK	KATO
Biological replicates	2	2	2	2
Technical replicates	2;3	3;3	3;3	3;3
Total number of samples	5	6	6	6

MESOTHELIAL CELLS	HMPC	HT 29	SW 480	TMK	KATO
Biological replicates	2	2	2	2	2
Technical replicates	2;3	1;3	2;3	2;3	2;3
Total number of samples	5	4	5	5	5

Table 6-7 Replicate classification. For each sample there were two biological replicates and these would provide one, two or three technical replicates. Technical replicates are shown as number of replicates per biological sample, separated by (;).

5.7.4 Analysis

Scanned images were analysed with Genepix Pro 6.0 software, Molecular Devices Corporation, California, www.moleculardevices.com/logos). Using a compatible gene identification file supplied by MWG Biotech, London, automatic spot or feature detection was used, and data from both channels was linked to the appropriate gene annotation information. The feature detection options in Genepix were selected as follows:

- Find irregular features
- Fill irregular features
- Resize features during alignment (Min diameter 25%-Max diameter 200%)

Microarray spot quality control was performed following the parameters below, as per manufacturers' instructions. Poor quality spots were flagged for elimination from further analysis.

1. [SNR 635] > 3 and [SNR 532] > 3

   Signal to noise ratio (SNR) on both channels must be higher than 3, to exclude spots with signal close to background, which would eventually result in a high number of false positive results arising from noise rather than true signal (Seo, Bakay et al., 2004).

2. [Circularity] > 80

   Defective spots are excluded. While there are deviations from a perfect uniform circle, by defining spot circularity, very abnormal spots, pieces, or scratches can be excluded from analysis (Jain, Tokuyasu et al., 2002).

3. [Rgn R2 (532/635)] > 0.6

   Regression ratio for both wavelengths is higher than 0.6. Slope of the line of best fit (chi-square or minimum-of-squares method) through the set of pixels in a circle of diameter twice that of the feature-indicator of the current feature).This value measures pixel uniformity across the feature (spot) and excludes spots with highly non-uniform pixel intensities.

Further analysis was carried out with BRB-Array tools (version 3.3.0) described by Simon et al (Simon, Lam et al., 2007). This is a free software package from the Biometric Research Branch, Division of Cancer Treatment and Diagnosis, National Cancer Institute, Rockville, Maryland, USA. It is free and available online to download as application to be used with Microsoft Excel. Once each array file had been processed by Genepix as above, including flagging, but not normalised, these were loaded onto BRB as text files, which contained information on gene ID, median and standard deviations for signal intensity of each spot and its background. In addition the programme required a Microsoft Excel experimental descriptor file. This contained the names of the samples to which the files would subsequently be linked. The files were then loaded into BRB-Array tools in class comparison mode. Data normalisation was performed before the analysis. A submenu named "filter and subset the data" provided the normalisation options. The programme offered two options: to

normalise using the median over house-keeping genes or to normalise over the entire array, using median array as reference. In this project, normalisation was performed over the entire array. Median centring, as previously described by Eisen et al (Eisen, Spellman et al., 1998), allowed removal of any systematic bias in expression between different cell-type models and facilitated comparison across columns.

Once the data was flagged and normalised, the analysis was performed using the class comparison approach. This allowed identification of differentially expressed genes among samples, both biological and technical replicates. Each biological sample was defined as named class, and within each class technical replicates were included for analysis. Gene expression of different technical replicates was averaged for each class. Then differences amongst classes were analysed as mean log-ratios between the classes, relative to the variation expected in the mean differences. The variation was computed assuming that all the samples were independent. The class comparison between groups of arrays was calculated with the F test (a generalisation of the t-test which allowed comparisons amongst groups) separately for each gene using normalised log ratios from the arrays. The random variance version of the F-test was used, because the number of samples per class was small. Random variance tests take into account information among genes of the within-class variance in log-ratios. Subsequently the class comparison tool computed the number of genes that were differentially expressed among the classes at the statistical significance level selected in the F-test menu, in this project set at $p<0.001$, and finally generated a list of differentially expressed genes.

Moreover BRB array tools also provided univariate permutation tests for the significance of individual genes. This test looked into which genes belonged to what classes. For each random permutation, random variance F-test was re-computed for each gene. This provided the proportion of random permutations that would result in as many genes significant at the level selected by the user as were found in comparing the true class labels. In summary this approach allowed to compare gene expression patterns within each class, which is easier than to calculate exactly what genes are different amongst the classes.

The false discovery rate was also calculated as an estimate of the proportion of the genes with univariate p values less than or equal to the one in

that row that represent false positives. The method of Benjamini and Hochberg was used for this estimation (Hochberg & Benjamini, 1990).

The analysis strategy for this project, aimed to maximise the sensitivity of the study and minimise the rate of false discoveries by setting the p-value at $p<0.001$ with a maximum false discovery rate set at 10 genes or 10% of the total of the genes identified as differentially regulated.

5.8 REAL TIME PCR VALIDATION STUDIES

5.8.1 INTRODUCTION

Real-time PCR was used to corroborate some of the findings of the microarray studies. Three different genes were selected: cathepsin k, caspase 8 and vimentin. They represent different pathways (ECM proteolysis, apoptosis and cytoskeletal disruption) that could be relevant to the process of peritoneal metastasis. Cathepsin K gene encodes for a lysosomal cystein protease, usually found in osteoclasts (Li, Yasuda et al., 2004). The role of this collagenase in neoplasia is well recognised, particularly in breast, lung, prostate cancer and bone metastasis although less understood in gastrointestinal malignancy (Brubaker, Vessella et al., 2003;Rapa, Volante et al., 2006;Rose & Siegel, 2010).

Caspase 8 is a protein involved in the extrinsic pathway of caspase activation, necessary to trigger cell apoptosis. Disruption of apoptosis may lead to the development of cancer (Hajra & Liu, 2004) Regarding caspase 8 expression in mesothelial cells, there is one study based on peritonitis. Mesothelial cells were activated by TNF-α and entered apoptosis via the Fas/Fas (CD95, TNF, caspase 8 and nerve growth factor receptor family) ligand pathway. Chen et al concluded that mesothelial cell apoptosis during peritonitis may be related to the resolution of peritoneal inflammation(Chen, Chi et al., 2003).

Vimentin is an important component of the cytoskeleton along with microfilaments (actins) and microtubules (tubulins) (Source: Entrez Gene, www.ncbi.nlm.nih.gov). This gene was selected to assess whether destruction of the cytoskeleton architecture in host mesothelial cells was a relevant step during the process of invasion. The role of vimentin in peritoneal disease has been reported in ovarian cancer and pseudomixoma peritonei, but is poorly understood

in peritoneal metastasis (Bibi, Pranesh et al., 2006;Zhang, Pettengell et al., 1999).

Genes were selected from validated probes available from Qiagen (www.qiagen.com, Qiagen Ltd, West Sussex, UK): Vimentin (Hs_VIM_1_FAM QuantiTect Gene Expression Assay (100), locus link 7431, Catalog: 241356), Caspase 8 (Hs_CASP8_1_FAM QuantiTect Gene Expression Assay (100) Catalog: 841241136) and Cathepsin K (Hs_CTSK_1_FAM QuantiTect Gene Expression Assay (100), locus link 1513, Catalog 241681).

The PCR assays used (QuantiTect Multiplex PCR, www.qiagen.com, Qiagen Ltd, West Sussex, UK) included primers and probes for the gene of interest and a normalising gene (GAPDH). As the probes for both target and GAPDH genes were differentially-labelled with fluorescent dyes (FAM and JOE respectively) both could be measured simultaneously in the same multiplex PCR reaction. Standard curves constructed using serial dilutions of reference RNA were used to determine the efficiency of amplification for GAPDH and target gene for each combined PCR reaction. Relative quantification of gene expression was then determined in each sample, using normalisation to GAPDH levels, and the Pfaffl method (Pfaffl, 2001) with the least invasive cell type (HT29) as the calibrator or baseline with which other samples were compared.

5.8.2 REVERSE TRANSCRIPTION

Amplified RNA from all samples and the reference set was reverse transcribed using the kit from Promega (IMPROM II, Cat A#3800, www.promega.com Promega UK ltd, Southampton, UK). Templates were prepared as shown:

Experimental RNA (up to 1µg/reaction)(1)	1µl
Random Primer, 0.5µg/µl (0.5µg/reaction)	1µl
Nuclease-Free Water	3µl

The above mixture was denatured by incubation at 70°C for five minutes, followed by five minutes on ice. A positive control Template (1.2kb Kanamycin Positive Control RNA) and a negative control (RNAse free water) were included. The master mix was prepared as follows:

Nuclease-Free Water	6.1µl
ImProm-II™ 5X Reaction Buffer	4.0µl
MgCl2, 25mM	2.4µl
dNTP Mix, 10mM, each dNTP (final concentration 0.5mM)	1.0µl
Recombinant RNasin® Ribonuclease Inhibitor	0.5µl
ImProm-II™ Reverse Transcriptase	1.0µl
Final Volume	15.0µl

15µl of the master mix were added to the above samples. Reverse transcription was performed:

Annealing	25°C	5 minutes
RT	42°C	1 hour
RT inactivation	70°C	15 minutes

Samples from the reference set previously used in microarray experiments were serially diluted, 10 fold, to perform calibration curves. At this point samples were frozen at -20°C or used in the next step. Spectrophotometry was not performed at this stage due to the small amounts of DNA per sample.

5.8.3 REAL TIME PCR

The protocol used was from QuantiTect Multiplex PCR (www.qiagen.com, Qiagen Ltd, West Sussex, UK), which had a specifically pre-mixed and pre-optimized Mastermix, containing HotStar Taq DNA polymerase, dNTPs, fluorescent dye and RNAse free water. DNase I treatment prior to reverse transcription was not used. This prevents DNA contamination of the samples; however I was not familiar with its use at the time of the experiments.
The mixture was prepared as follows:

Primer, (gene specific)	1µl
Probe, (antisense sequence)	1µl
GAPDH (primer and probe)	2µl
RNAse free water	5µl
Mastermix	10µl

To the above 19 µl we add 1 µl of sample (cDNA). Hence these are 20µl reactions. During every experiment a negative control containing no DNA was included.

All reactions were performed in a Rotor-gene™, (Machine serial number 110159, www.corbettlifescience.com, Corbett Life Science, Sydney, Australia) using a 72 well rotor. PCR settings were as follows:

Hold 15min at 95°C (Hot Taq activation)
Followed by 50 cycles of:
45 seconds at 94°C, (Denaturation)
45 seconds at 56°C, (Annealing)
45 seconds at 76°C, (Extension)

Channel settings were set as follows:

Channel	Source	Detector	Gain
FAM	470	510	7
JOE	530	555	9

Table 8 Channel settings for both FAM and JOE channels

Rotor-gene version 6 software, (www.corbettlifescience.com, Corbett Life Science, Sydney, Australia), was used for analysis.

RESULTS

6 DEVELOPMENT OF A 3D MODEL OF PERITONEUM

The in-vitro 3D model of peritoneum was the platform used to perform invasion with various gastrointestinal cancer cell lines. The interaction between invading cancer cells and host mesothelial cells was studied to understand the mechanisms of human peritoneal metastases, and to identify those molecular features which may distinguish tumours with different propensity for peritoneal invasion. The main hypothesis was that gene expression by invading cancer cells and host mesothelial cells in a 3D model of peritoneum would be associated with observed microscopic invasion.

The choice of a human in vitro model of peritoneum was based on the difficulties encountered when studies are to be performed in patients. Most patients with peritoneal metastases have very limited life expectancy, thus preventing large scale or prolonged clinical studies. Therefore, the 3D model of peritoneum would represent the closest match to human peritoneum. It was aimed in this project to demonstrate for the first time that such model could be useful to research into the molecular biology of metastases.

However the in vitro peritoneal model of peritoneum also had some limitations. Its design was technically challenging, particularly regarding the isolation and growth of HMPC. While valuable information could be gained about the early stages of invasion of the in vitro models, these were removed from culture after a given number of days. The lifespan of the models was limited. If they could survive weeks or months, a more thorough study of peritoneal metastasis during later stages of the disease would be possible. Moreover, only three cell types were present in the model: cancer cells, fibroblasts and HPMC. There are no vessels nor blood supply, no immune system, which translates into a lack of ability to generate a systemic response to invasion, as it would take place in humans. Therefore, those functions which take place at the very local level, such as disruption of HPMC adhesion and proteolysis of the extracellular matrix may be reproduced in an in vitro model.

Since little is known about the molecular biology of peritoneal metastasis, this initial approach to the steps that take place at local level may in fact be benefitial because of its potential simplicity compared to a model with a systemic reponse. However the understanding of those functions provided by a host response such as immunity, angiogenesis, cell repair or apoptosis in the 3D model of peritoneum may be limited or non-existent.

6.1 HPMC ISOLATION AND GROWTH

In the process of collecting omental samples from patients undergoing laparotomy, three different methods of HPMC isolation were compared, to establish which was superior in terms of HPMC growth success and absence of fibroblast contamination. Figure 8A-D demonstrated successful isolation and growth to full confluence without fibroblast contamination. Table 9 below showed the isolation results. No HPMC were recovered using method A (0.05% trypsin for 20 minutes), whereas 71% of samples using method C (0.25% trypsin for 20 minutes), and 26% of samples using method B (0.25% trypsin for 10 minutes) yielded HPMC. Furthermore the proportion of samples yielding HPMC was significantly higher for method C compared to method B (C versus B, Fisher's exact test $p=0.02$). The presence of fibroblast contamination was also more common for method B (53%) than method C (21%) although this difference was not statistically significant (Fisher's exact test $p=0.128$). HPMC were usually discarded either after 3 passages or in the presence of fibroblast contamination.

After optimizing the trypsin digestion conditions of the omentum samples, HMPC and fibroblasts were isolated and cultured. The 3D model was established from these cells and collagen. As confirmed by both light microscopy and immunocytochemistry the models consisted of a distinct fibroblast and collagen cove coated by HPMCs, which formed a monolayer without showing any signs of invasive behavior. The availability of these 3D peritoneal models made the next stage of the planned work possible. The invasion of these structures by various cancer cells will be discussed in the following chapter.

HPMC CELL ISOLATION FROM HUMAN OMENTUM			
	0.05% Trypsin 20 minutes	0.25% Trypsin 10 minutes	0.25% Trypsin 20 minutes
Number (Total=40)	11	15	14
Satisfactory growth	0	4 (26%)	10 (71%)
Absent growth	11 (100%)	3 (21%)	1 (8%)
Fibroblast contamination	0	8 (53%)	3 (21%)

Table 9 HMPC isolation. Optimal results were achieved with 0.25 trypsin digestion for 20 minutes. Neither experiment improved fibroblast contamination.

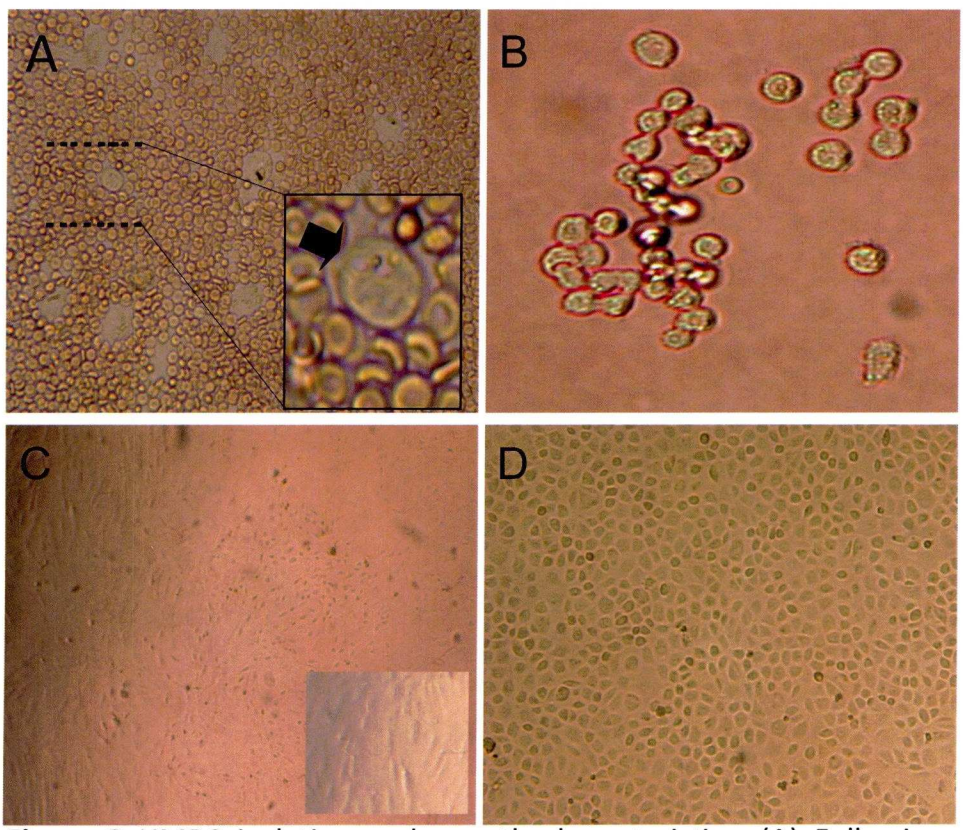

Figure 8 HMPC isolation and growth characteristics. (A) Following peritoneal digestion with trypsin, HPCM cells appeared as large nucleated cells (solid arrow in magnified x100 inset) surrounded by red blood cells. (B) Culture morphology after RBC removal. (C) HPCM cultures heavily contaminated with fibroblasts (inset magnified x100). (D) Confluent HPMC cultures without fibroblast contamination forming a typical mosaic pattern, as previously described (Stylianou, Jenner et al., 1990b). Magnifications: A x40; B x100; C and D x20.

6.2 EXTRACELLULAR MATRIX

The extracellular matrix was compound of fibroblasts and the extract from rat tail collagen. Satisfactory fibroblast isolation only required omental samples to be minced thoroughly and digested with trypsin as described in materials and methods. 40 specimens of omental tissue were used. They all yielded adequate numbers of fibroblasts for use in the 3D model. Cells grew in a spindle shaped fashion as shown in figure 14. Gels containing rat tail collagen and fibroblasts were incubated for 24 hours. They were analysed by light microscopy prior to detachment from the wells. Figures 9A, B, below, demonstrated satisfactory fibroblast growth, with a bipolar or multipolar (stellate) morphology within the extracellular matrix made of rat tail collagen. Once disengaged from the tissue culture wells, fibroblasts initiated gel contraction until a dense matrix was fully formed within 5 days. Thereafter mesothelial cells were seeded on these collagen lattices.

Rat-tail collagen was the best choice for an in vitro extracellular matrix. It had been used successfully by other authors, was cheap and immediately available. The newly formed extracellular matrix allowed mesothelial cells to grow as a monolayer, and provided a suitable matrix for fibroblast proliferation within.

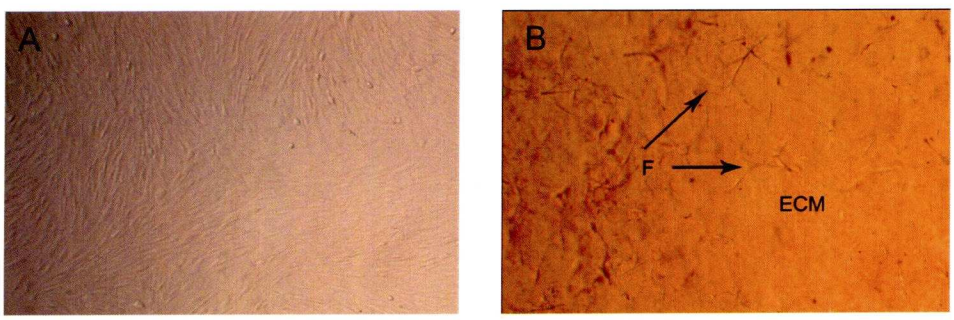

Figures 9A, 9B (A) Fibroblasts grow spindle-shaped to full confluence (magnification 4x). (B) Fibroblasts (F) within the extracellular matrix (ECM) had a bipolar or multipolar shape before contraction of the ECM (magnification 10x)

6.3 LIGHT MICROSCOPIC CHARACTERISATION OF THE MODEL

6.3.1 H&E

A total of 50 peritoneal models of invasion were created. Mesothelial cells seeded onto the upper surface of the above matrices proliferated over five days. Thereafter, a full 3D model of peritoneum was formed. 3D models were examined by light microscopy using both Haematoxylin, Eosin and immunocytochemistry techniques, to characterise cells and confirm findings previously reported by Jayne et al (Jayne, O'Leary et al., 1999b). Mesothelial cells did not invade into the matrix (Fig 10A, B). Instead they formed a confluent monolayer over the extracellular matrix. Fibroblasts grew within the extracellular matrix only. They did not grow within or above the mesothelial monolayer. Although, no physical basal membrane was visible between mesothelium and extracellular matrix, mesothelial cells were never seen within the extracellular matrix, thus implying that a barrier was present, which prevented these non cancer cells from invading the models.

6.3.2 IMMUNOCYTOCHEMISTRY

Immunocytochemistry was crucial to confirm the nature of the cell lines involved in the 3D model. Mesothelial characteristics on the surface monolayer were identified as follows: (positive staining for cytokeratins 8, 18, vimentin, negative staining for von Willebrand factor and Ber EP4). Cytokeratins tipically stained epithelial cells, von Willebrand factor stained endothelial cells and BerEP4 stained epithelial cells of ectodermal origin. As mesothelial cells are embriologically mesodermal in origin, they did not stain with this antibody.

Fibroblasts within the extracellular matrix were also tested (positive staining for vimentin, negative staining for cytokeratins 8, 18, Ber EP4 and von Willebrand factor) (Figures 11 A-D). Positive control tests were performed on samples of human appendix, uterus. Cytokeratins 8, 18, Ber EP4 stained epithelial cells and von Willebrand factor stained blood vessels.

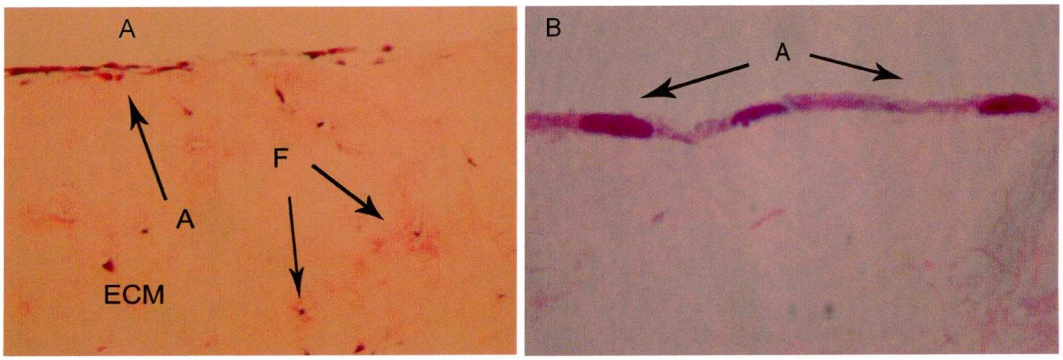

Figures 10A, 10B Light microscopy images of H/E paraffin stained models demonstrate the features of an in vitro 3D model of peritoneum. (Fig A, magnification 10x) HPMC (A) grow onto the ECM surface. Fibroblasts (F) grow within ECM. (Fig B, magnification 40x) shows a formed mesothelial monolayer (A). HPMC do not invade the ECM.

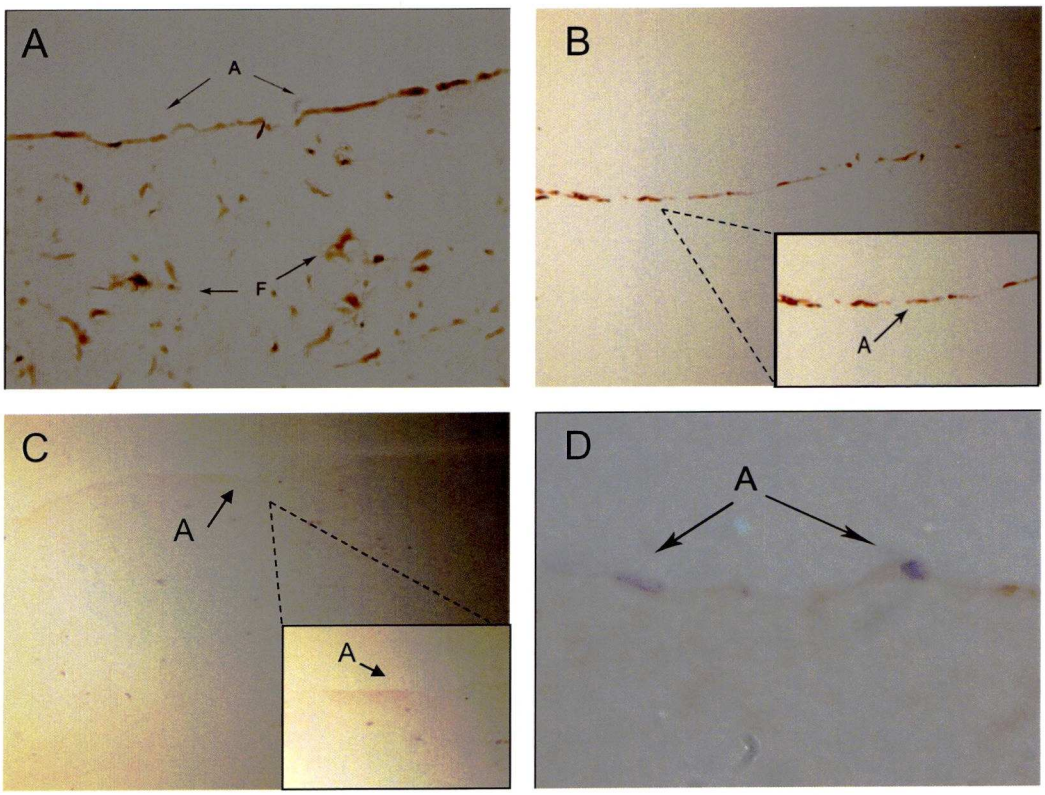

Figures 11 A-D Immunocytochemical features of HPMC and fibroblasts in a 3D model. Figure A, magnification 10x shows positive staining for both HPMC (A) and fibroblasts (F) with vimentin. Figure B, magnification 10x, and magnified inset, Cytokeratins 5, 8, 18 stained HPMC (A) but not fibroblasts (F) within the 3D model. Figure C, magnification 10x and magnified inset Factor VIII did not stain HPMC (A) nor fibroblasts (F). Fig D magnification x100, Ber EP4 did not stain HPMC (A) cells.

7 CHARACTERISTICS OF DIFFERENT INVASION MODELS

The 3D in vitro models of peritoneum were invaded with cancer cells, in order to study the invasive characteristics of these cells and their interaction with the host mesothelial cells. The ultimate aim was to show whether there was any association between observed microscopic findings and gene expression levels obtained from microarray studies.

Four different cancer cell lines were used. Three different concentrations of cancer cells (10^4, 10^5, 10^6 cells/ml) were inoculated in the models. Two models were made for each concentration and cell type. The 24 models were made in duplicate. Furthermore two models of normal, un-invaded peritoneum were made. Thus a total of 50 individual models of were created (appendix section, Table16).

With regards to the cancer cell lines, HT29 and SW480 were colonic in origin while TMK came from a gastric cancer and KATO from metastatic gastric cancer. HT29 was established from a primary well differentiated colonic adenocarcinoma (Wang, Cheong et al., 1999) in 1964 by D Fogh (Chen, Drabkowski et al., 1987). KATO III gastric cancer cell line was established by Sekiguchi in 1978 from a metastatic pleural effusion and when grown in hamsters it behaved as a poorly differentiated tumour (Sekiguchi, Sakakibara et al., 1978). TMK gastric cancer cell lines were originally extracted from a poorly differentiated gastric adenocarcinoma (Ochiai & Tahara, 1986). SW480 was derived from a primary Dukes B colonic carcinoma, from a 50 year old male patient (Hewitt, McMarlin et al., 2000). All cancer cell lines have been used in numerous studies about gastric (Kasuga, Tabuchi et al., 2007;Riles, Erickson et al., 2006) and colonic cancer (Chen, Drabkowski et al., 1987;Kemperman, Wijnands et al., 1997)

Initially it was expected that all cancer cell lines would be gastric in origin and the study would aim at comparing gastric cancer cells with different potential for invasion. Whilst TMK and KATO cell lines arise from poorly differentiated gastric cancer and metastatic cancer as stated above, there were no locally available well or moderately differentiated gastric cancer cell lines. Gastric and

colorectal cancers originate from different organs, behave differently and have overall different prognosis. Gastric cancers tend to invade locally and spread into the peritoneum and they can also metastasise via lymph nodes or bloodstream to distant organs (Dicken, Bigam et al., 2005). Haematogenous metastasis to the liver and invasion of adjacent organs are common patterns of spread in colorectal cancer (Ruo, Gougoutas et al., 2003). Having acknowledged this difficulty, the two colonic cancer cell lines were the best available choice, because of their well (HT 29) and moderately (SW480) differentiated nature. However, their main drawback was that any difference in behaviour in a 3D model of peritoneum, or differences in gene expression compared to gastric cancer cell lines could be attributed to anatomical or pathological reasons rather than intrinsic invasive potential only.

On the 3D in vitro models, the four cancer cells showed different patterns of invasion. HT29 cells grew on the mesothelial cell surface but did not invade regardless of tumour load (Fig 12). They did not seem to be able to break the mesothelial monolayer. This behaviour corresponded with this tumour's well differentiated nature. SW480 showed the most variable invasion pattern. At lower initial seeding concentration (10^4 cells/ml) SW480 behaved similarly to HT 29. However SW480 was able to invade and form rudimentary glandular structures at higher tumour load (10^6 cells/ml). This feature was unique to SW480 and confirms observations previously reported by Jayne et al. (Jayne, O'Leary et al., 1999b).

The TMK I and KATO III cells were visibly demonstrated a more invasive behaviour on light microscopy. Both cell lines penetrated through the mesothelial cell layer even at the lowest initial tumour load. Furthermore both TMK and KATO could digest the extracellular matrix and form distant metastatic deposits within. In addition it was noted that fibroblasts would orientate themselves towards the direction of the tumour during invasion (Fig 12).

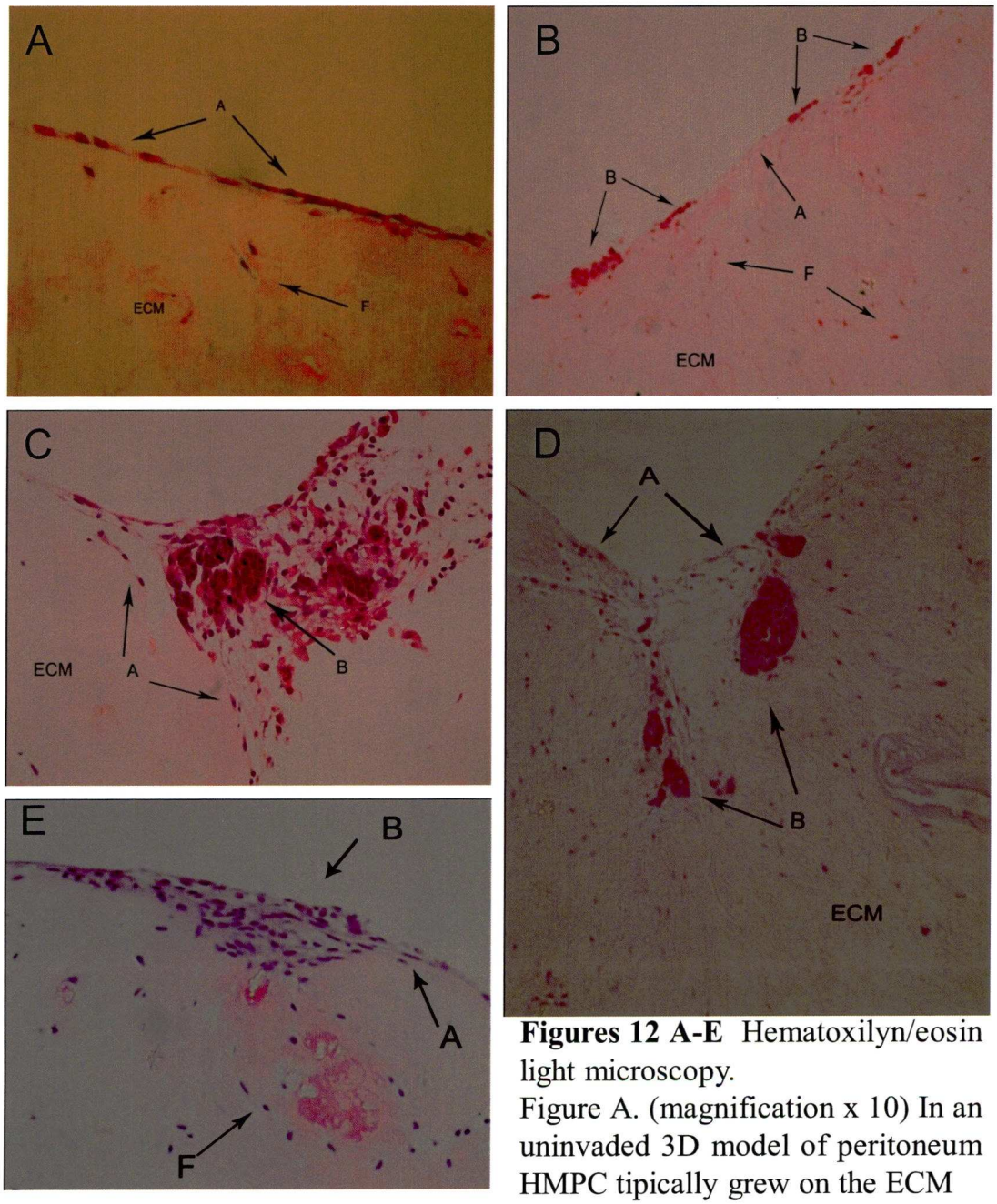

Figures 12 A-E Hematoxilyn/eosin light microscopy.
Figure A. (magnification x 10) In an uninvaded 3D model of peritoneum HMPC tipically grew on the ECM as a characteristic monolayer, fibroblasts (F) within the ECM. Figure B, magnification x10, HT29 cells (B) grew on the peritoneal surface (A) but did not invade through ECM; fibroblasts (F). Figure C, magnification x 20 SW480 cells (B) grew on the mesothelial surface (A) forming rudimentary glandular tissue. Figure D, magnification x 10 TMK cells (B) invaded through the mesothelial monolayer (A), and into the ECM. Fibroblasts (F) oriented towards the invading cells. Figure E, magnification x 10, Kato cells invaded both surface and ECM in the same fashion.

7.1.1 IMMUNOCYTOCHEMISTRY

All 50 3D models were analysed by immunocytochemistry techniques including use of epithelial antibodies (BerP4, CAM52, EMA, cytokeratins 8, 18), anti-vimentin, adhesion molecules (I-CAM, V-CAM, PE-CAM) antibodies and antibodies against extracellular molecules to further characterise basal membrane and extracellular matrix (collagens III and IV, laminin and fibronectin). Observed staining intensities are summarised in table 10 below and microscopic images in figures 14-17.

All four cancer cell lines stained with CAM52, Cytokeratins 5, 8, 18, Ber EP4, and EMA. Thus characterisation for all epithelial cancer cell lines was satisfactory. Mesothelial cells from non un-invaded models reproduced the results already stated above. The fact that Ber EP4 did not stain mesothelial cells confirmed the mesodermal nature of these cells.

ICAM molecule was expressed by all invasion models as well as normal peritoneum, with varying levels of intensity. V-CAM and PE-CAM only stained (very weakly) KATO models.

Collagens, fibronectin and laminin were expressed variably by almost all models. No convincing features of basal membranes were present, however some of the invasive models demonstrated the presence of a rudimentary capsule.

TISSUE	Normal peritoneum	HT29	KATO	SW480	TMK
I-CAM	++	+++	+++	+++	+++
V-CAM	none	none	+	+	none
PECAM	none	none	+	none	none
BeP4	none	++	++	++	+++
CAM52	+++	+++	+++	++	+++
EMA	none	++	+	+++	+
CYTOKERATINS 5,8,18	++	++	++	++	++
VIMENTIN	++	+++	++	+++	+++
COLLAGEN III	none	++	++	++	none
COLLAGEN IV	++	++	+++	++	++
LAMININ	+	+	++	++	++
FIBRONECTIN	++	++	++	+++	++

Table 10 Immunocytochemistry of 3D peritoneal models. Staining intensities are expressed as + weak, ++ positive, +++ strong.

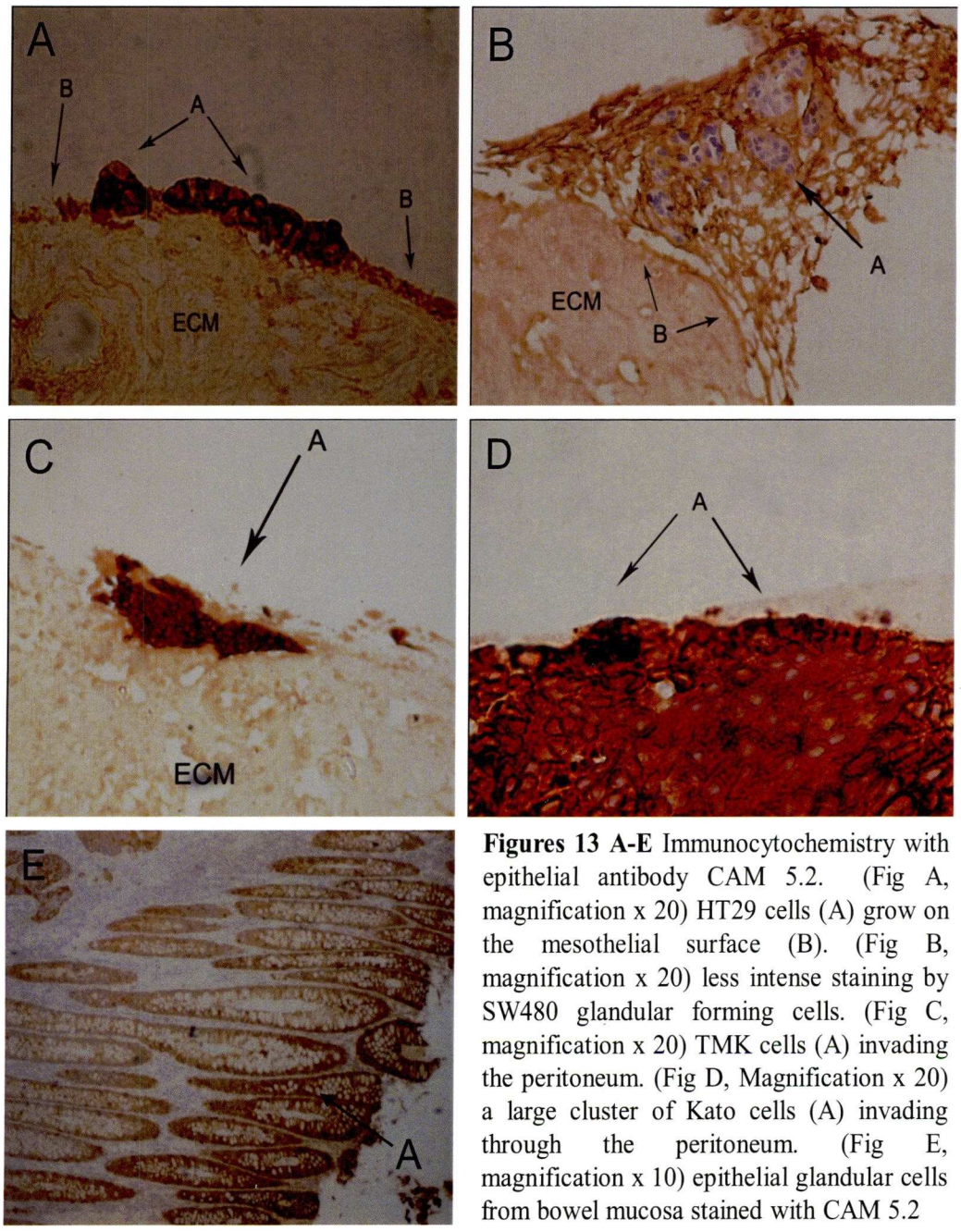

Figures 13 A-E Immunocytochemistry with epithelial antibody CAM 5.2. (Fig A, magnification x 20) HT29 cells (A) grow on the mesothelial surface (B). (Fig B, magnification x 20) less intense staining by SW480 glandular forming cells. (Fig C, magnification x 20) TMK cells (A) invading the peritoneum. (Fig D, Magnification x 20) a large cluster of Kato cells (A) invading through the peritoneum. (Fig E, magnification x 10) epithelial glandular cells from bowel mucosa stained with CAM 5.2

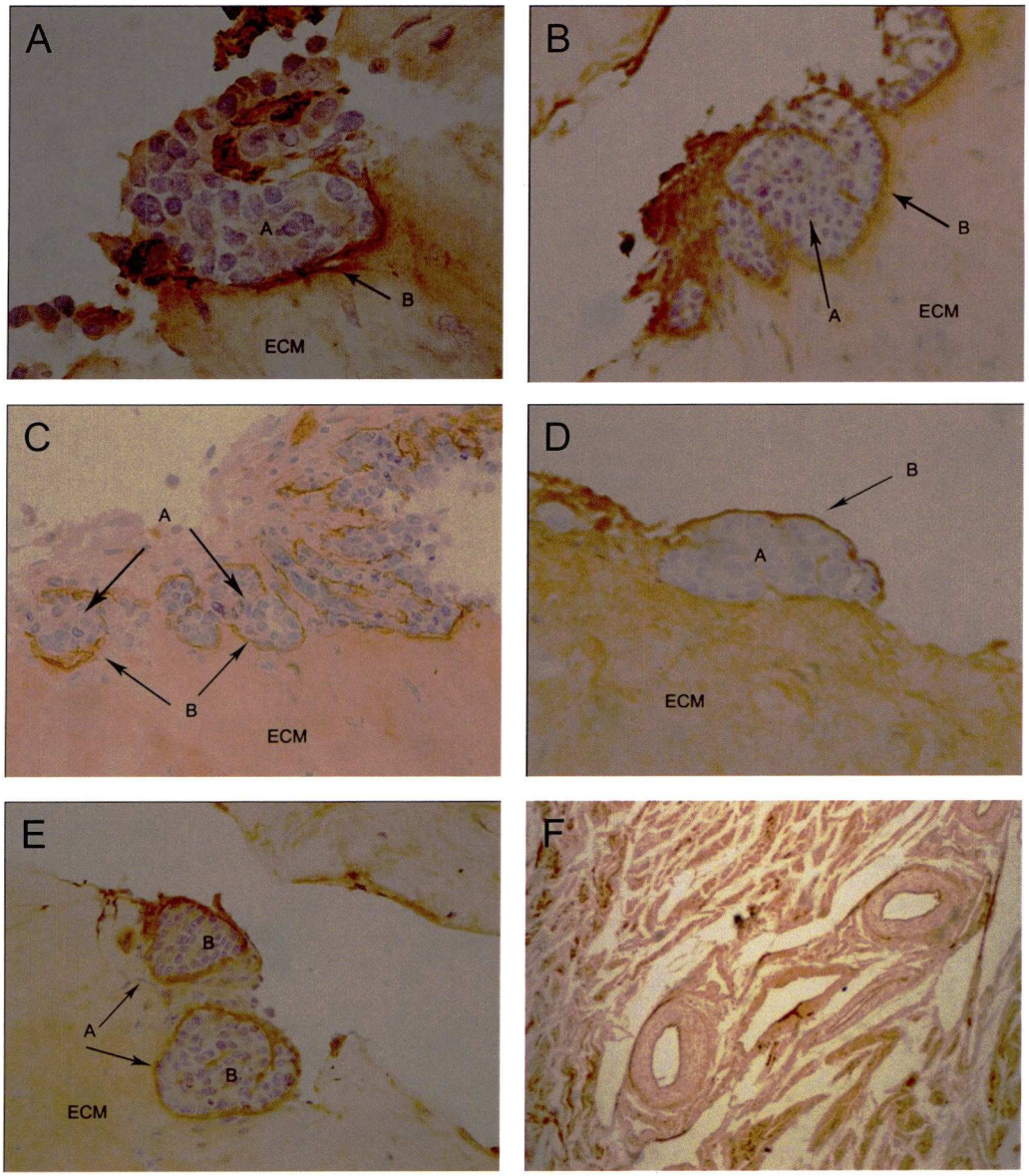

Figures 14 A-F Immunocytochemistry demonstrates the presence of staining around groups of cancer cells resembling a membrane or capsule. Figure A, KATO cells (A) stained with collagen IV (B), magnification x 40; Figure B, TMK cells (A) stained with collagen III (B), magnification x 20; Figure C, TMK cells (A) stained with fibronectin (B), magnification x 20; Figure D, HT29 cells (A) stained with fibronectin (B), magnification x 10; Figure E, TMK cells (B) stained with laminin (A), magnification x 20; Figure F positive control, uterus, stained with fibronectin.

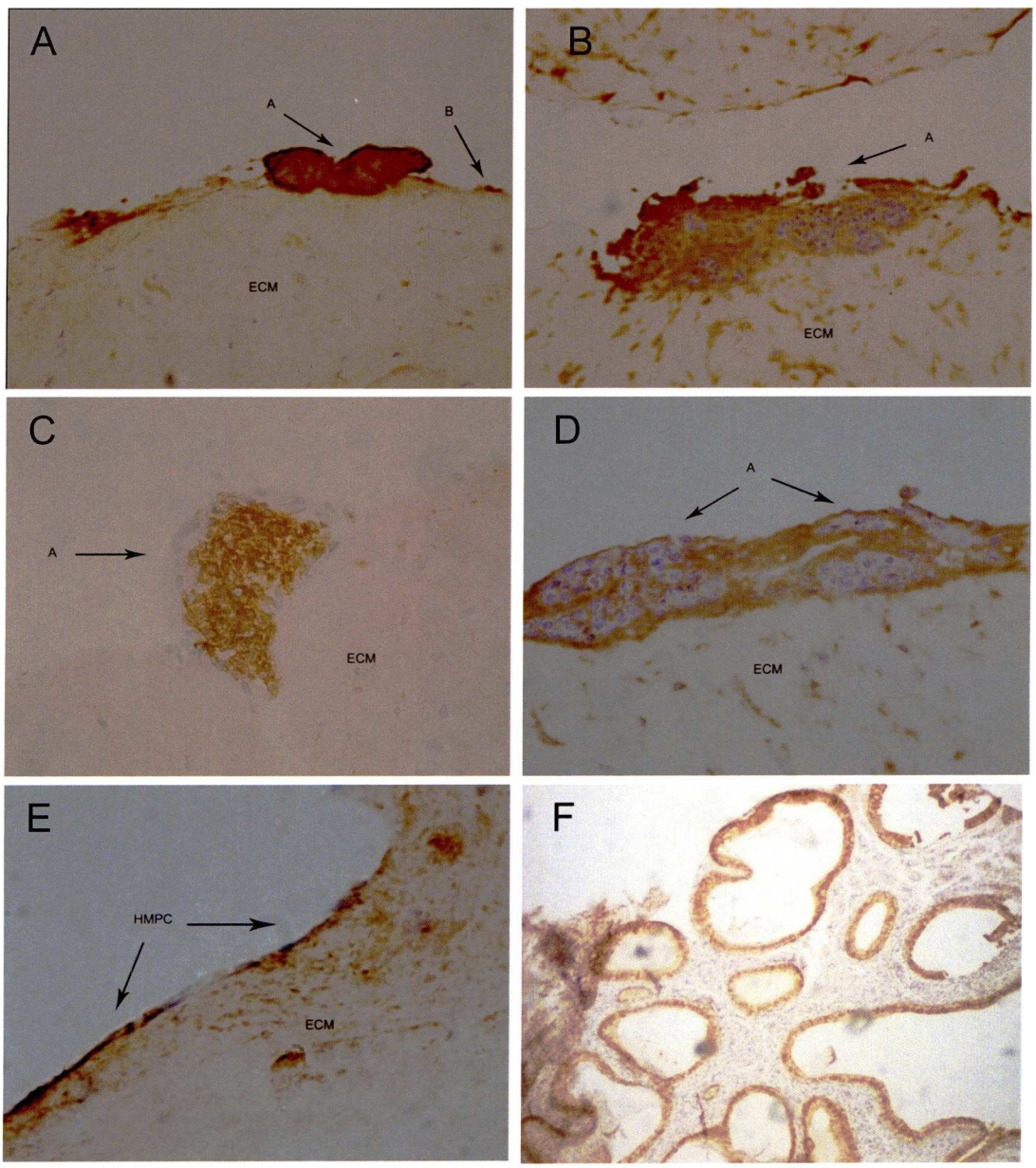

Fig 15 A-F Peritoneal model immunocytochemistry with ICAM antibody. All figures magnified x 10. Figure A peritoneal model invaded by HT29 cells. Figure B peritoneal model invade by TMK cells. Figure C peritoneal model invaded model by SW480 cells. Figure D, peritoneal model invaded by KATO cells. Figure E uninvaded peritoneal model. Figure F positive control on cervix. All of the models demostrated positive staining for ICAM. In this particular model of invasion it was not possible to demonstrate an association between invasiveness and ICAM levels as previously reported. In fact normal peritoneum as well as cervix as positive control, both expressed ICAM at local level

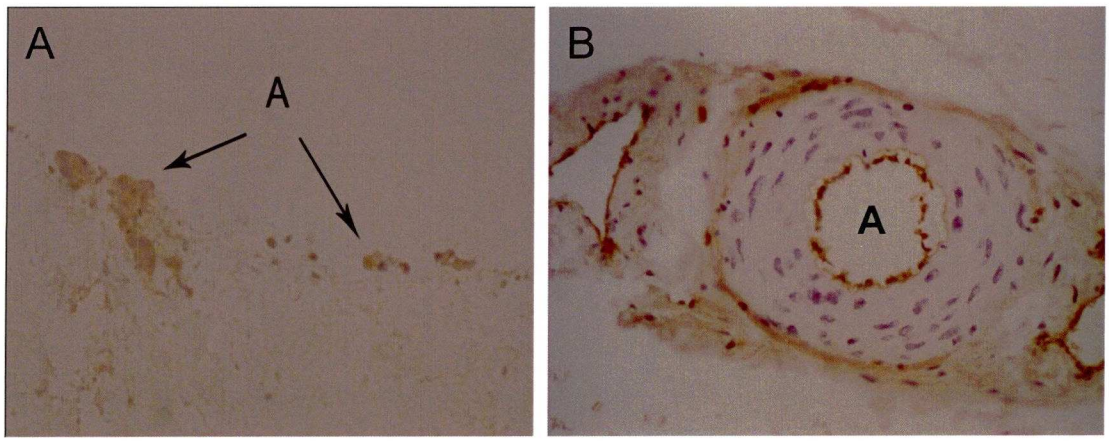

Figures 16 A,B Immunocytochemistry of endothelial adhesion molecule PECAM. Fig A, magnification x 10, Kato cells (A) produce very weak staining, compared to endothelia (A) from control sample of uterus (Fig B, magnification x10)

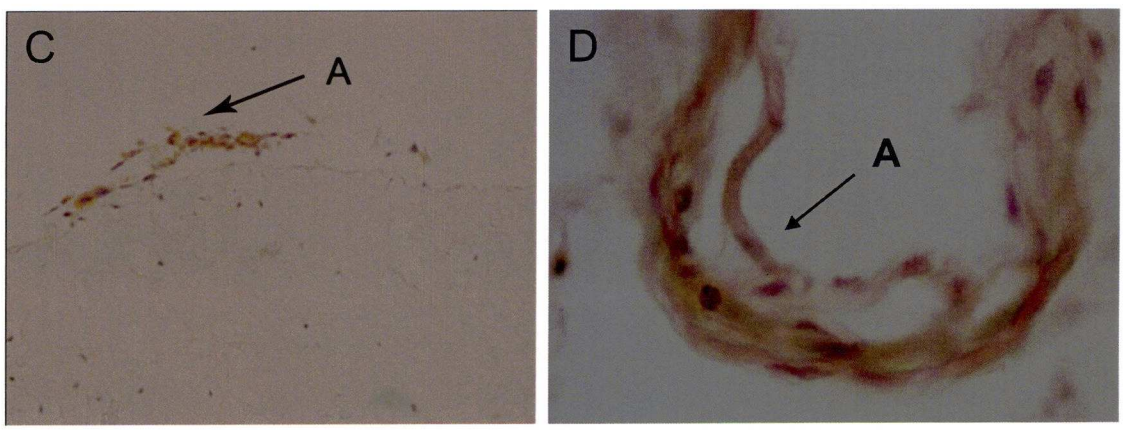

Figures 17 A,B Immunocytochemistry of endothelial adhesion molecule VCAM. Fig C, magnification x 10, SW480 cells (A) produce very weak staining, compared to endothelia (A) from control sample of uterus (Fig D, magnification x 40)

8 LASER CAPTURE MICRODISSECTION

In order to analyse the molecular events taking place in the 3D models, it was necessary to separate populations of invading cancer cells from host mesothelial cells. The best technology available to achieve this was laser capture microdissection (LCM). Since it was first described by Emmert-Buck, Bonner et al in 1996, LCM has been developed to automate and standardise microdissection. The principle of LCM involves placing a thin layer of transparent film over the tissue, which is then visualised in a microscope equipped with the laser; focussed pulses of carbon dioxide laser are applied; once the film is removed from the tissue it will contain the cells of interest. This technology has greatly increased the reproducibility and accuracy of the selection of specific target cells from a complex tissue for subsequent molecular analysis (Bonner, Emmert-Buck et al., 1997;Emmert-Buck, Bonner et al., 1996;Simone, Bonner et al., 1998).

To study the molecular biology of peritoneal metastasis in a 3D model of peritoneum, 5μm sections of all models were stained with haematoxylin eosin, prior to laser capture of selected cells. For every invasion model, cancer cells and mesothelial cells were captured separately. Figure 19 demonstrates LCM results. Samples of cancer cells and mesothelial cells from all invasive models and mesothelial cells from a non invaded model were collected. It was not possible to precisely quantify numbers of captured cells per sample. Each of the 50 peritoneal models underwent laser capture once Table. The results demonstrated that use of LCM in this 3D model of peritoneal invasion did indeed allow isolation of pure populations of cells.

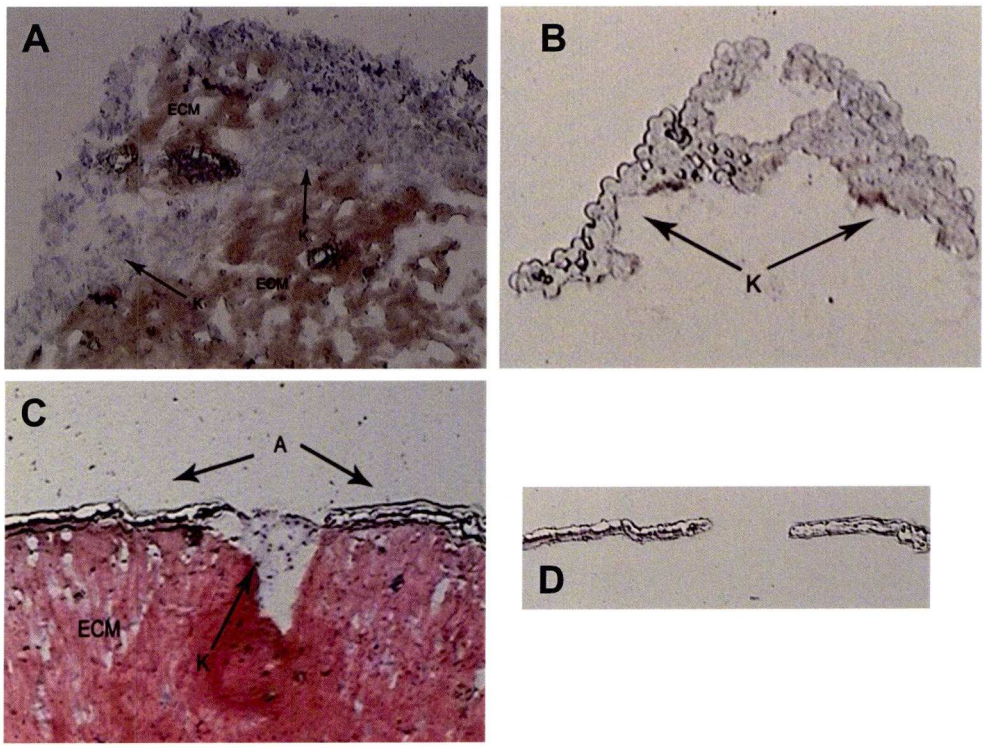

Figures 19 A-D (H/E, magnification x 10) LCM of cancer cells and host mesothelial cells is demonstrated. Figure A, Kato cells (K) invaded the peritoneum, destroying mesothelial monolayer and growing within the ECM. Figure B, Kato cells were captured with LCM caps and isolated from the rest of the model. RNA was then extracted from the caps and amplified. Figure C neighbouring mesothelial cells from an invaded model were captured. These were separated from the model as shown in fig D. This method allowed selective capture of cancer cells and host mesothelial cells in the 3D model of in vitro peritoneum.

9 MICROARRAY STUDIES IN A 3D MODEL OF PERITONEUM

As stated before the hypothesis was that microscopically observed invasive behaviour in 3D models of peritoneum, would be associated with gene expression. The study of peritoneal metastasis in humans is difficult because of the nature of the clinical context. Most patients with peritoneal metastases are debilitated and have very limited life expectancy, making clinical studies very challenging. The 3D model of peritoneum which has a close resemblance to the human peritoneum was a suitable alternative to conduct gene expression studies. To my knowledge this kind of work had never been carried out before.

The experiments described here included: RNA extraction from LCM samples described above, RNA amplification and labelling, hybridisation onto the microarray platforms, scanning of resulting images and microarray analysis.

9.1 AMPLIFICATION

Before amplification of RNA extracted from cells captured from the 3-D peritoneal models was performed, attempts were made to prove and validate the method of amplification proposed was efficient and yielded good quality aRNA, bearing in mind that it was not possible to assess the neither quantity nor quality of extracted RNA from LCM samples. Using total universal reference RNA, (Stratagene Universal Human Reference RNA, La Jolla, CA, US www.stratagene.com), amplification of as little as 1ng of starting RNA yielded enough RNA (mean aRNA concentration 0.70 µg/µl, as shown in Figure 20 A. Below 1ng amplification values fell dramatically. These results were consistent with previously published data by Stirewalt et al (Stirewalt, Pogosova-Agadjanyan et al., 2004).

RNA quality was tested by spectrophotometry and gel electrophoresis. Ratios ranged between 1.81 and 2.19 (Mean: 1.81). Though ratio values for amplifications below 1ng still were within the above range, electrophoresis

demonstrated no smear for the amplified messenger RNA (Fig 20 B). This again showed that this method is not reliable when attempting to amplify less than 1ng of total RNA.

Having validated this published protocol, the actual RNA from LCM samples was amplified. A total of 12 RNA samples from laser-captured cancer cells, host mesothelial cells and HMPC from uninvaded models were amplified in duplicate. (Amplification raw data available in appendix sections 13.1, 13.2). As the starting amount of total RNA was not known before LCM amplification, it was uncertain whether one round of amplification would suffice. The results of one versus two rounds of amplification, both in terms of the amount of product (Tables 12A, B) and range of transcript sizes, assessed by gel electrophoresis, are shown below (Fig 21A, B). In conclusion, all LCM samples needed two rounds of amplification to reliably achieve adequate yields of good quality aRNA.

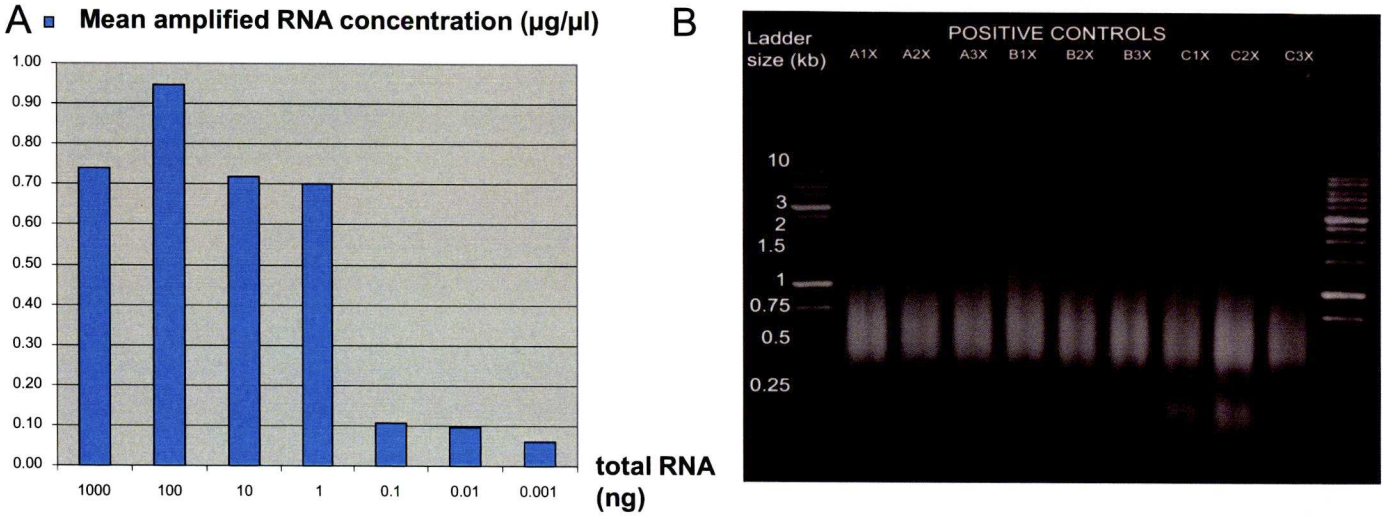

Figures 20 A,B Amplification following the published method by Stirewalt; with Reference total RNA was reliable when starting material was equal or above 1ng. Fig 47 (X axis: Total RNA starting material) (Y axis: amplified RNA mean concentration) Amplification was far less successful with less than 1ng of starting material, as shown in last 3 columns. Fig 48 Gel electrophoresis of amplified RNA. First lane, 1kb ladder; lanes A1X-A3X amplified RNA from 1µg of starting material; lanes B1X-B3X amplified RNA from 100ng; lanes C1X-C3X, amplified RNA from 10 ng. Amplified RNA yielded smears between 0.4-0.8 kb.

A) FIRST ROUND OF AMPLIFICATION

total aRNA 1st round	Mean	Median	SD	Max	Min
Concentration	0.46	0.19	0.51	2.13	0.003
Amount in 100µl	36.61	15.50	41.09	170.54	0.27

B) SECOND ROUND OF AMPLIFICATION

total aRNA 2nd round	Mean	Median	SD	Max	Min
Concentration	1.36	1.38	0.31	1.87	0.57
Amount in 100µl	129.07	132.61	30.85	177.86	53.92

Tables 12 A, B Results of first and second rounds of amplification. After a first round, RNA yields were often inadequate. Following a second round, amounts close to or above 1µg/µl were produced

A) FIRST ROUND OF AMPLIFICATION **B) SECOND ROUND OF AMPLIFICATION**

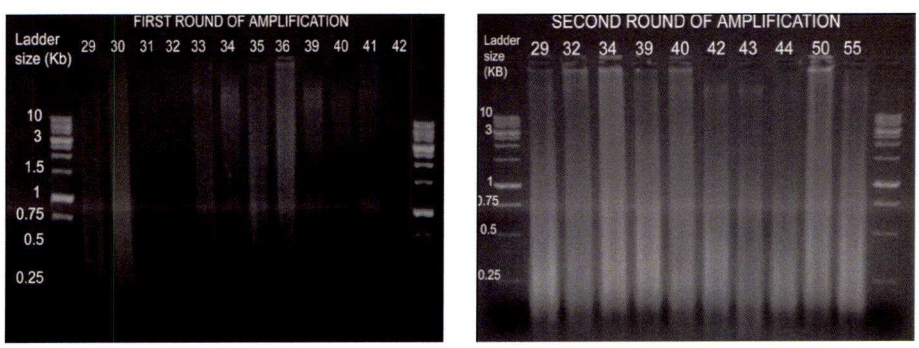

Figures 21 A, B Gel electrophoresis of amplified RNA from LCM samples. (A) Only samples in lanes 30, 33, 35, 36 produced a smear in the gel. Sizes varied amongst samples. (B) All samples produced smears between 0.25 and 1 kb after a second round of amplification. Although amplification in one round was possible, overall 2 rounds produced better quality results.

9.2 RNA LABELLING

Before labelling samples, RNA concentration and purity was checked by spectrophotometry. Reference RNA produced a mean start concentration of 0.74µg/µl (SD 0.16), and ratios between 1.8-2.1. LCM samples from peritoneal models produced a mean RNA start concentration of 1.19 µg/µl (SD 0.26), and ratios between 1.8-2.4. Individual sample results are available in the appendix section, tables 19, 20. In all cases there was enough starting material to commence the labelling procedure. Both peritoneal model RNA and reference RNA was of similar high quality, as assessed by electrophoresis. This was encouraging as degradation of RNA, particularly from peritoneal samples, was a concern.

Each sample was labelled in the same way, but spectrophotometric assessment of label incorporation demonstrated some variability whether coupling was performed with Cy3 or Cy5. Most striking was the variability in RNA loss across labelling reactions. As seen in tables 19, 20 (Appendix) recovery of labelled RNA was sometimes very poor and some samples became unsuitable for hybridisation. Some differences were noticed between dyes. Thus, on the whole, Cy3 coupling was slightly better than Cy5 as shown in table 12. This difference in dye coupling efficiency has already been described, and reported to be due to more prominent quenching of Cy5 ('t Hoen, de et al., 2003). The same amount of Cy3-sample and Cy5-reference RNA were combined for each hybridisation on each slide in all cases.

A) Cy3 LABELED SAMPLES

	Ratio	RNA C	Yield	Dye incorporation	RNA loss (%)	RNA to combine
Mean	2.00	0.12	11.54	34.21	42.32	8.52
St dev	0.19	0.05	4.66	9.72	23.29	3.53
Range	1.46-2.29	0.03-0.21	2.58-30.37	10.53-56.96	1.84 -87.08	2.58-15.54

B) Cy5 LABELED REFERENCE

	Ratio	RNA C	Yield	Dye incorporation	RNA loss (%)	RNA to combine
Mean	2.02	0.11	10.30	26.05	48.49	8.52
St dev	0.17	0.04	4.15	8.68	20.75	3.53
Range	1.77-2.23	0.06-0.19	5.32-17.75	12.73-36.85	11.27-73.4	2.58-15.54

Tables 12 A, B Samples were labeled with Cy3 and Reference was labeled with Cy5. Each variable was expressed in the following units: RNA C (concentration: µg/µl, Yield referred to total RNA per sample expressed as µg/100µl, Dye incorporation n° dye molecules/1000 nucleotides, RNA to combine was referred as µg per sample or µg/100µl. RNA loss was similar regardless of dye. However incorporation was slightly better with Cy3

9.3 HYBRIDISATION ON MICROARRAYS

Hybridisation is the process of applying the previously labelled aRNA from all samples into the microarray slides. As a result genes from the samples of interest will couple or hybridise to complementary oligonucleotides printed on the MWG cancer array slides. This step is crucial since poor hybridisation generated from poor quality samples or slides would generate invalid data if any. Previous attempts at in-house manufacture of spotted microarray slides by colleagues proved unsuccessful. For this reason it was decided, despite the very high cost, to perform all microarray experiments in commercial slides.

Equally important to processing the samples is the adequate choice on the number of hybridisations per sample including biological and technical replicates in a given number of slides. This is known as hybridisation design. This process is crucial to provide not only a cost effective use of slides, but to potentially obtain the best results from the experiments. In this project the reference design was preferred. It is a very popular method which can be found in many microarray publications. The principle is based on the level of expression of any gene in a sample which can be related to the expression of that gene in the common reference, as measured on that slide. Subsequently, expression levels of a gene on different slides may be compared using the common reference to control for sources of variability, amongst spots that affect both channels similarly (Dobbin & Simon, 2002b). The reference design is a practical and popular choice for microarray studies using two colour platforms (Kerr, Serikawa et al., 2007). Total universal reference RNA containing total RNA from 10 different human cell lines (Stratagene Universal Human Reference RNA, La Jolla, CA, US www.stratagene.com) was used as the reference to perform the hybridisations.

Experiments were performed as summarised in Table 13. 3 Initially 50 slides were purchased, however three slides had to be discarded. For each cancer and mesothelial cell model there were two independent biological replicates yielding 18 different RNA samples. For each sample two technical replicates at least were performed. Some samples had three.

CANCER CELLS	HT 29	SW 480	TMK	KATO
Biological replicates	2	2	2	2
Technical replicates	2;3	3;3	3;3	3;3
Total number of samples	5	6	6	6

MESOTHELIAL CELLS	HMPC	HT 29	SW 480	TMK	KATO
Biological replicates	2	2	2	2	2
Technical replicates	2;3	1;3	2;3	2;3	2;3
Total number of samples	5	4	5	5	5

Table 13 Replicate classification. For each sample there were two biological replicates and these would provide one, two or three technical replicates. Tehcnical replicates are shown as number of replicates per biological sample, separated by (;).

After hybridisation and incubation each plate was washed and then scanned. Examples of the images generated showing combined signal for Cy3 and Cy5 is shown below (Figs 22A, B). Overall the results were very satisfactory. Using relatively low gains, the intensity at which the scanner provided an image, it was possible to produce good quality images, with even spot distribution, low background noise and good spot intensities throughout each array. In fact only three slides with poor image quality were discarded. Below a typical image of a cancer array is displayed to illustrate this. The quality of all 47 arrays was similar.

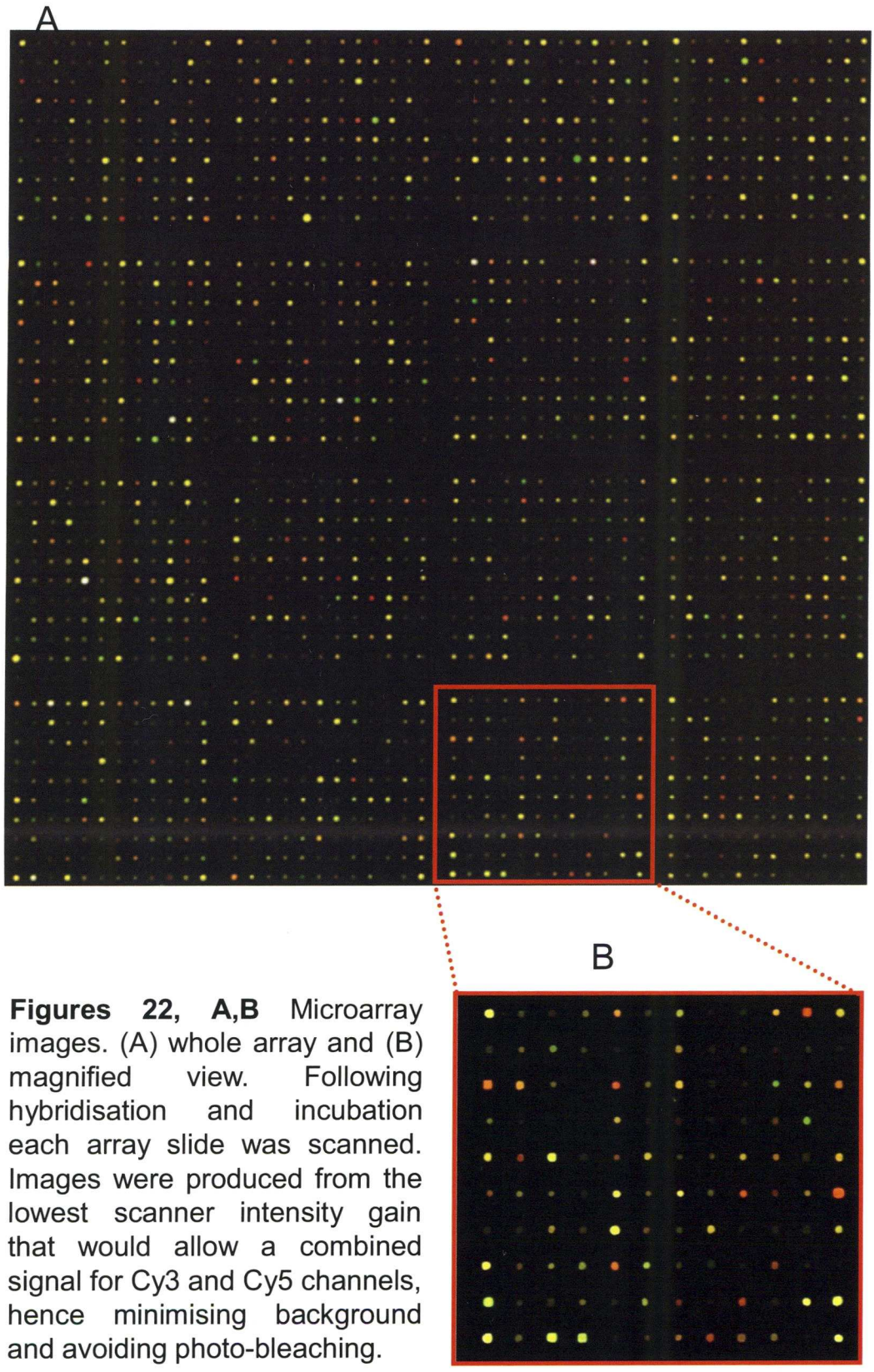

Figures 22, A,B Microarray images. (A) whole array and (B) magnified view. Following hybridisation and incubation each array slide was scanned. Images were produced from the lowest scanner intensity gain that would allow a combined signal for Cy3 and Cy5 channels, hence minimising background and avoiding photo-bleaching.

9.4 MICROARRAY ANALYSIS

The first step in microarray analysis is to convert the images obtained by the scanner into numbers. This process is facilitated with the use of computer software which performs this process, known as feature extraction. The programme determines which pixels within the scanned area are part of a feature or spot and which are part of the background, outside the spots. The best image quality translates into most successful results. For this purpose, scanned images were analysed with Genepix Pro 6.0 software, Molecular Devices Corporation, California, www.moleculardevices.com/logos). At the time this programme was the only of its kind that had an automatic spot detection feature, thus reducing error in the process of spot alignment, commonly faced during manual grid alignment. Using a compatible gene identification file supplied by MWG Biotech, London, automatic spot or feature detection was used, and data from both channels was linked to the appropriate gene annotation information. Thus, at this point images were translated into numbers. Microarray spot quality control was performed following the parameters, described in materials and methods. These allowed exclusion of poor spots based on poor signal, which would provide false negative results. Also, excessive noise misinterpreted as signal could potentially produce false positives. Furthermore, poorly shaped spots or those with non-uniform pixel distribution were too excluded. Such exclusion process was known as flagging. Any flagged spots were subsequently filtered and excluded from further analysis.

Further analysis was carried out with BRB-Array tools (version 3.3.0) described by Simon et al (Simon, Lam et al., 2007). This is a free software package from the Biometric Research Branch, Division of Cancer Treatment and Diagnosis, National Cancer Institute, Rockville, Maryland, USA. It is free and available online to download as application to be used with Microsoft Excel. Once each array file had been processed by Genepix as above, including flagging, but not normalised, these were loaded onto BRB as text files, which contained information on gene ID, median and standard deviations for signal

intensity of each spot and its background. In addition the programme required a Microsoft Excel experimental descriptor file. This contained the names of the samples to which the files would subsequently be linked. The files were then loaded into BRB-Array tools in class comparison mode. Data normalisation was performed before the analysis. A submenu named "filter and subset the data" provided the normalisation options. The programme offered two options: to normalise using the median over house-keeping genes or to normalise over the entire array, using median array as reference. In this project, normalisation was performed over the entire array. Median centring, as previously described by Eisen et al (Eisen, Spellman et al., 1998), allows removal of any systematic bias in expression between different cell-type models and facilitates comparison across columns. Once the data was flagged and normalised, the analysis was performed in two different approaches, hierarchical clustering and class comparison.

Cluster analysis was performed on all the gene expression profiles generated in the arrays, for both the cancer and the host mesothelial group. The results are show in the figure below. This conventional analysis looks at the level of similarity/dissimilarity between individual samples. The results are expressed as a dendrogram (Figures 23, 24), where the distance between branches is proportional to the level of "relatedness" detected by the software.

Two main findings were apparent amongst the results. All technical replicates demonstrated high index of correlation, appearing next to each other within the dendrogram. These results were very encouraging for both the cancer and host mesothelial cell groups. Considering that these technical replicates were identical samples, lead to the conclusion that the experiments were performed in a robust and consistent manner. The process of laser capture, RNA isolation and amplification, label and hybridisation were performed on different days, further reinforcing the strength of these results. Unfortunately these findings were not reproduced within biological replicates. Within the cancer cell group, none of the biological replicates appeared to be linked to one another. Only samples 15 and 39, both SW480 invasion models showed slight correlation. If gastric versus colorectal cancer were compared, samples 33 (TMK) and 51 (KATO), both gastric cancers had a correlation value near 0.5. Samples 15 (HT 29) and 21 (SW 480) correlated somewhat, with a value near 0.2. Another interesting

finding is the position within the dendrogram of samples 9 (KATO) and 45 (HT 29). The possibility of both being mislabelled cannot be completely excluded. If that was the case, the final result would be that gastric and colonic cancers group together within the dendrogram. However the process of labelling was rigorous.

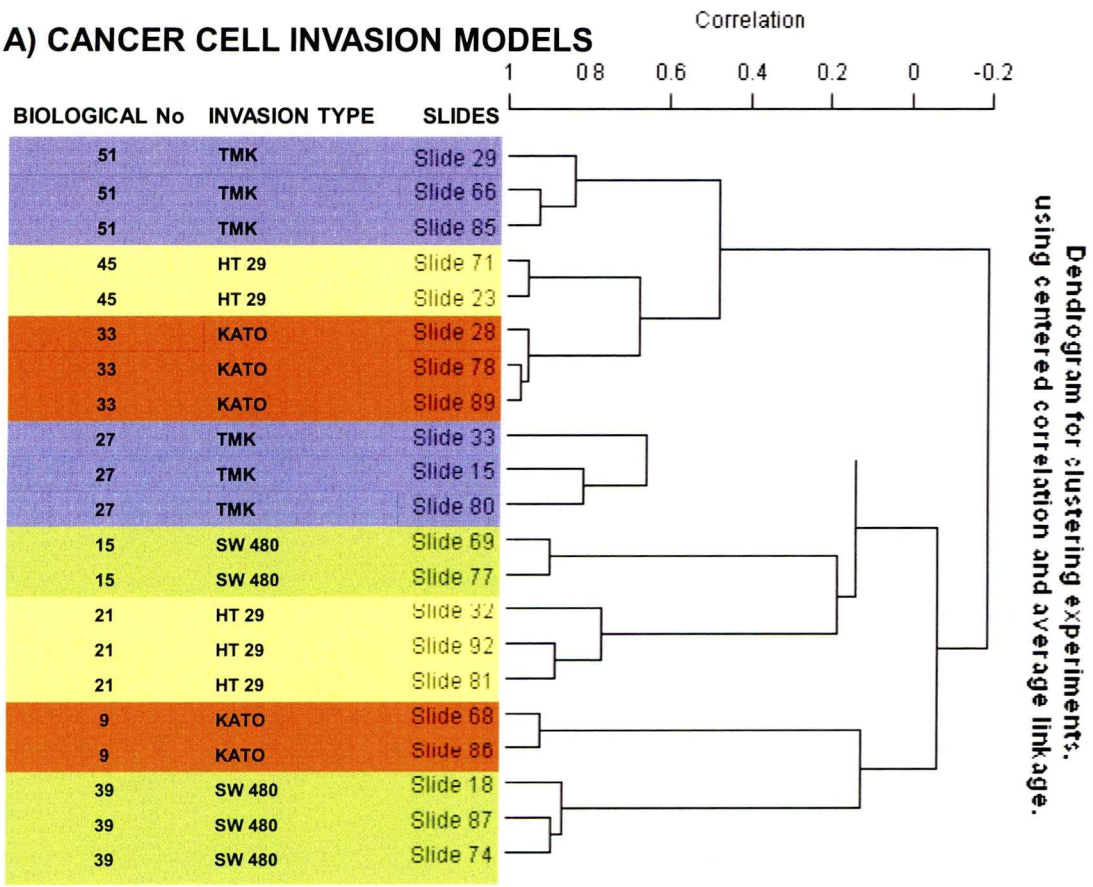

Figure 23 A Cancer cell dendrogram Heat map showing cluster analysis performed on gene expression data generated from arrays, for the cancer cells. Samples were clustered by comparing their expression profiles across the set of genes. This approach identifiesH the level of similarity/dissimilarity between individual samples and results were expressed as a dendrogram. The distance between branches is proportional to the level of "relatedness" between samples detected by the software.

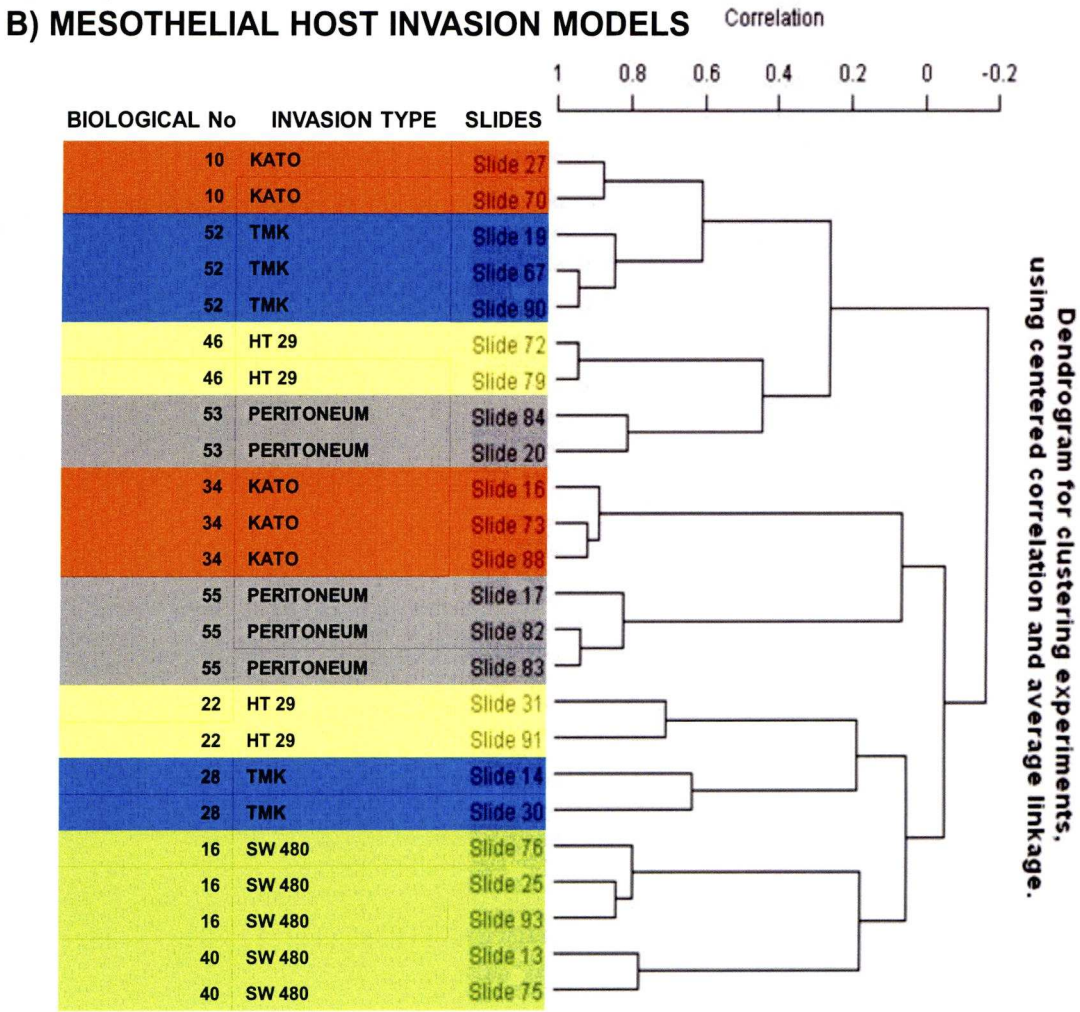

Figure 23 B Mesothelial host cell dendrogram Heat map showing cluster analysis performed on gene expression data from the arrays, for the host mesothelial cells. Samples were clustered by comparing their expression profiles across the set of genes. The software identified the level of similarity/dissimilarity between individual samples and results were expressed as a dendrogram. The distance between branches is proportional to the level of "relatedness" between samples detected by the software.

Within the host mesothelial group the results were similar. Technical replicates again grouped next to each other. Only biological samples of peritoneum invaded by SW 480 grouped together. Although host mesothelial cells invaded by HT 29 were grouped next to uninvaded peritoneum, at least one

model invaded by KATO cells also grouped next to uninvaded peritoneum. Overall there was no clear correlation amongst samples, except for SW 480, regarding tissue type or invasion pattern.

The most immediate criticism would be the lack of microarray experiments due to costs. If it was possible to produce far more biological samples, including whether available, invaded models by other gastric and colonic cancer cell lines, the results would be more robust.

Further analysis was performed by the class comparison approach, which allowed identification of differentially expressed genes among samples, both biological and technical replicates. The principle of class comparison is based on the use of statistical methods in order to test a hypothesis and determine which genes are statistically significant (different) across the groups of interest. This statistical approach aimed at identifying gene changes associated with the biological processes taking place, while minimising false discovery rates or the presence of false positive results. The class comparison analysis was performed with the F test (a generalisation of the t-test which allows comparisons amongst groups) separately for each gene using normalised log ratios from the arrays. The random variance version of the F-test was used, because the number of samples per class was small. Random variance tests take into account information among genes of the within-class variance in log-ratios.

Another issue commonly faced during microarray analysis is the finding of a proportion of genes which may appear differentially expressed although they are not of biological significance, also known as false discovery rates. When multiple independent tests are carried out on a given sample, the likelihood of false discovery doubles with each additional test. Although mathematical approaches such as Bonferroni's correction test, where the accepted test-wise p value is divided by the number of independent tests (Bonferroni CE, 1936), try to compensate for this, they may prove to restrictive in microarray analysis, resulting in reduced false discovery rates at the price of also reduced biologically significant data. Other statistical approaches use more conservative correction for multiple testing than Bonferroni's. These rank results based on their p values and accept as best those with the smallest p values, until they satisfy certain mathematical characteristics, known as step down analysis (Benjamini Y & Hochberg Y, 1995;Holm, 1979). While these approaches improve sensitivity

they compromise on false discovery rate. More recently, permutation tests have been developed to calculate false discovery rates in class comparisons. (Radmacher, McShane et al., 2002). In this approach each individual sample is analysed by comparing it to other samples belonging to different classes, identifying genes that are differentially expressed and ranking these in order of p value. Then the same sample is given the "wrong" classifier, and the comparisons are repeated generating a list of "differentially expressed" genes and their associated p values. Assuming a perfect dataset, in this second permutated analysis, there should be no significantly different genes. The number and significance of the "differences" observed during the permutated analysis allows the software to calculate the level of error present in the dataset. (In contrast the previously mentioned step down analysis only estimates the error). By analysing the dataset reiteratively, the number of false discoveries can be controlled much more tightly and accurately while maximising sensitivity. The algorithms used for these calculations have been tested extensively on both simulated data and publicly available real life gene expression data (Korn EL, Troendle JF et al., 2004).

In this project the p-value was set at $p<0.001$ with a maximum false discovery rate set at 10 genes or 10% of the total of the genes identified as differentially regulated, in order to maximise the sensitivity of the study and minimise the rate of false discoveries. In the cancer cell group 139 genes were differentially regulated. Within the host mesothelial cell group 104 were included (Appendix sections 13.3, 13.4). Genes were selected that would be differentially expressed in either ascending or descending order regarding the invasive behaviour of the class they belong. The results are displayed below in tables 14, 15. The cancer cell group displayed four genes of interest, three of them up-regulated and one downregulated with malignancy. In the host mesothelial cell group 15 genes were up-regulated and 3 were down-regulated.

CANCER CELL GENE EXPRESSION

GENE NUMBER	GENE ID	DESCRIPTION	HT 29	SW 480	TMK	KATO	PARAMETRIC p-VALUE
27	NM_003472	dek oncogene dna binding;	0.16	0.50	1.55	1.93	2.10E-06
109	NM_004585	retinoic acid receptor responder tazarotene induced 3; rarres3	0.63	2.40	3.63	5.49	0.0003
111	NM_022118	cutaneous t-cell lymphoma tumor antigen se70-2; se70-2	0.27	0.27	0.28	0.89	0.0003
62	NM_033018	pctaire protein kinase isoform a; pctk1	1.52	1.12	0.52	0.20	3.27E-05

Tables 14, 15 Gene expression levels for cancer cells (14) and host mesothelial cells (15, next page). Results are expressed as geometric mean of ratios. BRB array tools was the software of choice. Univariate F-test with a random variance model were used. Permutation p-values for significant genes were computed based on 10000 random permutations. The highest parametric p-value was 0.01 for cancer cells and 0.03 for host mesothelial cells. False discovery rates were 0.004 for cancer cells and 0.01 for host mesothelial cells. Results shown here are those genes which follow either a ascending (red) or descending (green) pattern of gene expression, depending on the degree of invasion of cancer cells previously shown in the microscopic findings. Overall gene results are enclosed in the appendix section.

HOST MESOTHELIAL CELL GENE EXPRESSION

GENE NUM	GENE ID	DESCRIPTION	Mesothelial cells only	Mesothelial cells plus HT 29	Mesothelial cells plus SW 480	Mesothelial cells plus TMK	Mesothelial cells plus KATO	PARAMETRIC p-VALUE
1	NM_001444	Fatty acid binding protein 5 psoriasis-associated; fabp5	16.24	0.39	3.62	3.84	14.61	< 1e-07
2	NM_000249	Mutl homolog 1; mlh1	5.60	0.64	1.00	1.14	3.30	< 1e-07
11	NM_000611	cd59 antigen p18-20 identified by monoclonal antibodies 16.3a5 ej16 ej30 el32 and g344 cd59.	2.97	0.26	0.45	0.61	2.99	3.00E-07
19	XM_087218	similar to tropomyosin cytoskeletal type tm30-nm; loc151471	1.84	0.70	2.12	2.81	3.47	2.20E-06
22	NM_006519	t-complex-associated-testis-expressed 1-like 1; tctel1	3.40	0.80	0.91	2.25	8.68	2.50E-06
55	NM_005053	rad23 s. cerevisiae homolog a; rad23a	2.92	0.80	2.47	2.50	3.42	0.0001
60	NM_006087	tubulin beta 5; tubb5	2.24	0.96	1.75	2.80	4.75	0.0001
67	NM_003172	surfeit 1; surf1	0.61	0.30	1.22	1.33	2.20	0.0002
74	NM_004039	annexin a2; anxa2	1.73	0.50	0.96	1.18	2.70	0.0003
78	NM_080648	Apex nuclease;	1.64	0.44	2.50	2.50	3.25	0.0003
91	K00558	Alpha tubulin; replicated spot	3.51	1.50	2.01	2.51	5.73	0.0006
92	K00558	Alpha tubulin_2; replicated spot	4.06	1.72	2.31	3.04	5.69	0.0006
99	NM_004939	deadh asp-glu-ala-asphis box polypeptide 1; ddx1	2.16	0.44	0.66	1.85	3.67	0.0007
100	K00558	Alpha tubulin; replicated spot	5.50	1.95	2.28	3.40	7.26	0.0008
104	NM_002166	inhibitor of dna binding dominant negative helix-loop-helix protein; id2	2.59	0.70	1.12	3.51	3.86	0.0009
59	X61498	nf-kb subunit	1.86	2.03	1.91	1.24	0.96	0.0001
64	NM_001731	b-cell translocation protein 1; btg1	1.73	1.94	0.68	0.53	0.10	0.0002
101	NM_004318	aspartate beta-hydroxylase isoform a; asph	0.86	1.46	1.05	0.69	0.41	0.0008

10 GENETIC CHARACTERISATION OF DIFFERENT INVASIVE PHENOTYPES IN A 3D MODEL

10.1 CANCER CELL GENE EXPRESSION

When results of microarray studies had been normalised and analysed as described above, genes were selected as potentially relevant to peritoneal metastasis and invasion based on the correlation between gene expression and the observed invasive behaviour of the cancer cells in the models described earlier. A total of 139 genes were identified following analysis, using the F-test with a univariate random variance model. Nominal significance of each univariate test was less than 0.001 and false discovery rates were also less than 0.001. Genes selected from the above included those following a gradient pattern of expression. They were either up or downregulated depending on degree of invasion, previously shown in light microscopy. Only three genes from cancer cells followed an ascending and one a descending pattern of expression. For instance, the protein kinase, pctk1, (NM_033018), was differentially more expressed in HT 29 and gradually less with other more invasive lines. Conversely, DEK oncogene (NM_003472) was gradually more expressed in Kato cells type than the other cell types. Cutaneous t-cell lymphoma tumour antigen se70-2 (NM_022118) and retinoic acid receptor responder tazarotene induced 3; rarres3 (NM_004585) were differentially far more expressed by the malignant cell lines TMK and KATO than HT 29 and SW480.

Although the role of DEK and relevance to clinical practice is poorly understood there were some studies reporting its involvement with cell cycle and senescence. DEK oncogene encodes a protein which binds to cruciform and superhelical DNA and induces positive supercoils into closed circular DNA and is also involved in splice site selection during mRNA processing. Chromosomal aberrations involving this region, increase expression of this gene and the presence of antibodies against this protein were all associated with various diseases. Wise-Draper et al found the human DEK proto-oncogene to behave as a senescence inhibitor, in their studies with Human Papilloma viral oncogenes E6

and E7. Specifically DEK message and protein levels were repressed during cervical cancer cell senescence when induced by either E2 overexpression or E6/E7 interference. They reported that DEK contributed to extended cell life span and potential elevated risk of carcinogenic progression over time(Wise-Draper, Allen et al., 2005).

Retinoids are involved in cell growth and differentiation activities. This is mediated by specific nuclear receptor proteins that are members of the steroid and thyroid hormone receptor superfamily of transcriptional regulators. Growth inhibitor retinoic acid receptor responder, tazarotene, is used in the treatment of hyperprolipherative skin conditions such as psoriasis (DiSepio, Ghosn et al., 1998). It is also thought act as a tumour suppressor or growth regulator in gastric epithelial cells, and their inhibition by hypermetilation, common in the elderly, cause this and other genes to lose their role, making gastric cancer more likely in that age group (So, Tamura et al., 2006).

The protein kinase, pctk1, (NM_033018) gene encodes for a protein which belongs to the cdc2/cdkx subfamily of the ser/thr family of protein kinases. It may play a role in signal transduction cascades in differentiated cells. However, its role in gastrointestinal cancer is unknown.

In summary, very few genes demonstrated a pattern of expression that could be associated with observed microscopic findings. Despite the relevant findings described above, further experiments could provide a more robust answer to the molecular biology of peritoneal metastasis.

10.2 HOST MESOTHELIAL CELL GENE EXPRESSION

A total of 104 genes were identified following analysis, using the F-test with a univariate random variance model. Nominal significance of each univariate test was less than 0.001 and false discovery rates were also less than 0.001. Within the results a number of genes were selected which followed a gradient pattern of expression. They were either up or downregulated depending on degree of invasion, previously shown in light microscopy. This resulted in 18 genes being selected (table 15). 15 genes were significantly upregulated in the

most aggressive cancer cell lines (Kato and TMK), and 3 showed a decreased gradient of expression. It was expected that non invaded HPMC (mesothelial cells only) would behave as the baseline and that once invasion took place genes would show an ascending or descending pattern of expression. However this did not happen and the reasons for this were unclear. Overall HPMC expression levels mostly fell in between those of host mesothelial cells invaded by cancer cells.

Using the gene annotation tool from BRB array tools, gene functions were sought and their relevance to the process of invasion identified whether possible. Fatty acid binding protein psoriasis-associated; fabp5 (NM_001444) has a high specificity for fatty acids. This gene encodes the fatty acid binding protein found in epidermal cells, and was first identified as being upregulated in psoriasis tissue. Fatty acid binding proteins are a family of small, highly conserved, cytoplasmic proteins that bind long-chain fatty acids and other hydrophobic ligands. It is thought that FABPs roles include fatty acid uptake, transport, and metabolism. FABPs have been reported to be involved in the primary response of liver parenchymal cells to Western-type diet feeding, and may play an important role in the primary protection against the cellular toxicity of cholesterol, free fatty acids, and lipid oxidants (Hoekstra, Stitzinger et al., 2006). However there are no reports linking this gene with neoplasia. Although it was not possible to link this gene to the process of invasion, HPMC showed highest levels than any other invaded host mesothelial cell, or in fact than any gene in the list. Mesothelial cells invaded by Kato showed very high levels of expression, while other cell lines had much lower levels ($p<1e-07$).

Mutl homolog 1 (mlh1, NM_000249) was identified as a locus frequently mutated in hereditary nonpolyposis colon cancer (HNPCC). Defects in mlh1 are the cause of hereditary non-polyposis colorectal cancer type 2 (hnpcc2). Most families with clinically recognized HNPCC have mutations in either mlh1 or msh2 genes. HNPCC is an autosomal, dominantly inherited disease associated with marked increase in cancer susceptibility, characterized by a familial predisposition to early onset colorectal carcinoma and extra-colonic cancers of the gastrointestinal, urological and female reproductive tracts. HNPCC is reported to be the most common form of inherited colorectal cancer in the western world, and accounts for 15% of all colon cancers. Lower expression of

this gene is associated with development of colonic adenomata and colorectal carcinoma (Sidelnikov, Bostick et al., 2009). In the 3D models of invasion Mlh1 was least expressed by HPMC invaded by HT 29, then SW480, TMK, Kato and highest levels were found on uninvaded peritoneum ($p<1e-07$).

A gene involved in DNA damage and repair was Rad 23a. The protein encoded by this gene is one of two human homologs of Saccharomyces cerevisiae Rad23. This protein is involved in DNA damage recognition, nucleotide excision and repair. Thus it provides subsequent regulation of protein stability. Rad 23 proteins are known to regulate p53 stability in unstressed cells and control apoptosis (Kaur, Pop et al., 2006). Little is known about the precise mechanism of action of Rad23 in gastrointestinal cancer. However a few reports exist involving other neoplasms. Shen et al found positive correlation between expression of a Rad23 polymorphism and development of lung cancer in a population highly exposed to indoor smoky coal emissions (Lee, Shen et al., 2007). Steinberg et al found that downregulated Rad23 UV excision repair gene and the Growth Arrest and DNA Damage gene (GADD45) were found in patients with melanoma (Steinberg, Hubbard et al., 2009).

Annexin A2 was more expressed by host mesothelial cells invaded by the invasive gastric cancer cell lines TMK and Kato, and less by HT29 and SW480. Annexins are a family of calcium dependent proteins with the ability to bind membrane phospholipids and other anionic polymers, mostly glycosaminoglicans, such as heparin and heparin sulphate and have been implicated in many functions such as cell signalling, ion transport, inflammation, apoptosis, fibrinolysis and angiogenesis (Shao, Zhang et al., 2006). The role of these genes in neoplasia has been documented. Lenighk et al reported that downregulated levels of annexin 2 were present in prostate cancer compared to normal prostate epithelia or benign prostatic disease (Lehnigk, Zimmermann et al., 2005). Sharma et al reported that annexin 2 was a promoter of breast cancer growth and angiogenesis via conversion of plasminogen to plasmin (Sharma, Koltowski et al., 2006). More interesting is a role for annexin described as vascular carcinomatosis or tumour proliferation on the vascular intima that replaces normal epithelium (Madoiwa, Someya et al., 2007). This was described by Madoiwa et al in a small study with three patients suffering metastatic renal cell carcinoma. These patients presented with coagulopathy with low plasma

fibrinogen and high levels of products of degradation of fibrinogen and fibrin. Areas of vascular carcinomatosis presented high levels of annexin 2. Annexin 2 has also been linked to gastric carcinoma, and correlation found with lymph node invasion and metastasis (Emoto, Sawada et al., 2001). However there are no reports to date of annexin 2 in peritoneal metastasis. Host mesothelial cells showed an upregulated pattern of expression in response to invasiveness. Non invaded peritoneum however, showed higher level of expression than HT29, SW480 and TMK invasive models.

α-tubulins 1, 2 and β-5 all were differentially expressed by peritoneal cells from invaded and non-invaded models. α-tubulin 1 had a replicated spot. Gene expression levels in both spots showed a similar pattern. This was not the case with α-tubulin 2, where only 1 spot showed a differential pattern of expression. Tubulins form structures known as microtubules which are an important component of the cytoskeleton along with microfilaments (actins) and Vimentin (Source: Entrez Gene,www.ncbi.nlm.nih.gov). These genes play therefore an important role in maintaining cellular adhesion. Adhesion is essential for the maintenance of tissue architecture. Loss of adhesion is a feature common in many tumours. A visible finding during peritoneal invasion was the loss of the mesothelial monolayer, thus allowing cancer cells to enter the extracellular matrix. This was most marked on the TMK and Kato invasion models. In contrast gene expression patterns did not quite reflect the same picture. While there was a gradient of expression, this was opposite to the microscopic findings. The expected result would be a down-gradient of expression. Also non invaded models showed higher expression levels than the colonic invasion models but lower than Kato which was again contrary to the microscopic findings.

Another gene of interest was the inhibitor of DNA binding dominant negative helix-loop-helix. The protein encoded by this gene belongs to the inhibitor of DNA binding (ID) family, members of which are transcriptional regulators that contain a helix-loop-helix (HLH) domain but not a basic domain. Members of the ID family inhibit the functions of basic helix-loop-helix transcription factors in a dominant-negative manner by suppressing their heterodimerization partners through the HLH domains. This protein may play a

role in negatively regulating cell differentiation (Source: Entrez, NCBI, www.ncbi.nlm.nih.gov.)

A probable gene of interest previously isolated in B cell chronic lymphocytic leukaemia cells is B cell translocation gene 1 BTG1 (NM_001731). This gene was upregulated in HT29 and SW480 compared to uninvaded peritoneum and downregulated in TMK and Kato. BTG1 belongs to a family of antiproliferative genes. Its expression is maximal in the G0/G1 phases of the cell cycle and downregulated when cells progress through G1 (Source: Entrez, NCBI, www.ncbi.nlm.nih.gov.). A role in angiogenesis has been reported for this gene as its up regulation led to endothelial cell proliferation and neovascularisation in an in-vitro model of angiogenesis (Iwai, Hirata et al., 2004). There is no published data linking this gene with gastrointestinal malignancy.

Aspartate β-hydroxylase isoform a (asph, NM_004318) gene is thought to play an important role in calcium homeostasis, by regulating calcium release from the endoplasmic and sarcoplasmic reticulum. The gene is expressed from two promoters and undergoes extensive alternative splicing, thus leading to varied functional properties. Some isoforms have been implicated in metastasis, though there are no reports regarding peritoneal metastasis. The gene has been reported in gastrointestinal cancer, mostly in cholangiocarcinoma, where the gene was detected in these patients with RT-PCR (Feldmann, Nattermann et al., 2006).

Overall, a number of genes were identified with patterns of expression which corresponded with the previously shown microscopic findings. Some relevant cell roles and functions were identified including adhesion, cell cycle control, angiogenesis, apoptosis, cell signalling and transport. It was not possible to assess how those changes in invaded host mesothelial cells related to a non invaded model. The most likely explanation is that the number of both biological and technical replicates was inadequate. Further experiments would probably strengthen the data and possibly provide other potential candidate genes not identified here.

However it has been possible to demonstrate that the in vitro 3D model of peritoneal invasion is a suitable source to study peritoneal metastasis using microarray technology.

11 REAL TIME PCR VALIDATION

Extensive data in the literature indicates that multiplexed hybridization based DNA/RNA measurements, including those obtained with microarrays, are often unreliable. This is due to many factors; in case of oligonucleotide arrays the primary concerns are about the specificity of the gene specific oligo present on the array and errors introduced during the complex multi-step sample amplification procedure. In addition, the high number of parallel observations made during array experiments raises the possibility of randomly occurring false positive results. Thus, findings from microarray experiments are often regarded as "trends", which require further validation by alternative, preferably non-hybridization based approaches. Depending on the constraints of the experiments immunohistochemistry, RNAse protection assays or quantitative PCR are used most frequently for the purposes of this confirmatory work. However, as RNAse protection assays require large amounts of starting material, they could not be performed with laser captured samples. Given that the laser capture process removed the relevant cells from the models, antibody based detection systems could not be used either. To independently confirm the findings of the array hybridization studies quantitative real time PCR experiments were carried out. Due to the limited amounts of starting material, as well as monetary and time limitations, it was impossible to confirm every array finding. Based on a preliminary analysis of the data three genes of potential interest were selected and gene specific primer/Taqman probe sets for these were obtained from a commercial source. The abundance of the mRNA species of these genes was quantified in the samples. The results of this work are presented here.

To test whether the primer sets designed by Qiagen (Qiagen, Crawley, West Sussex, UK, www.qiagen.com) were working and to check the efficiency of the amplification, universal reference RNA (Stratagene Universal Human Reference RNA, La Jolla, CA, US www.stratagene.com) was reverse transcribed and a dilution series of the cDNA product was set up, as described in the Materials and Methods section. Quantitative PCR reactions were run amplifying

aliquots of these pre-diluted standard samples with the gene-specific primer sets to establish a standard curve and calculate the efficiency of the amplification process. Thereafter, cDNA derived from laser captured samples was run, together with the standard curve, to measure mRNA levels in individual laser captured samples as detailed in Materials and Methods. Quantitative PCR experiments were multiplexed (dual channel) single tube amplifications, to eliminate pipetting errors. The housekeeping gene used throughout was GAPDH, with primers and Taqman probe from the same commercial source.

11.1 RT PCR RESULTS

There were three genes selected for real-time PCR validation based potential relevant pathways in the process of peritoneal metastasis (ECM proteolysis, apoptosis and cystoskeletal disruption). These were cathepsin k (NM_000396), vimentin (NM_003380) and caspase 8 (NM_033356). Following the analysis of microarray data with BRB array tools, only one gene from the above, cathepsin K was differentially expressed by cancer cells. Geometric mean values for HT29 (0.16), SW480 (0.16) and KATO (0.13), were similar, whereas TMK cancer gene expression levels were considerably higher (1.90), $p<1e-07$. However cathepsin K was not found to be differentially expressed by invaded host mesothelial cells. Therefore, the results of RT PCR presented here could not be associated to the microarray data. RT PCR results are presented to show that RT PCR, regarded as a gold standard test, may be performed to confirm gene expression results extracted from microarray data. This would be a requirement for publication of microarray studies in most high impact journals.

11.1.1 Cathepsin K

Cathepsin K is a lysosomal cysteine proteinase. Under physiological conditions the protein is primarily present in osteoclasts where it contributes bone remodelling, as mentioned earlier, this gene is expressed in certain tumours, including breast cancers, where it has been suggested to contribute to invasiveness.

During initial primer/Taqman probe testing the abundance of this message was higher than that of the housekeeping gene. During the amplification of the commercial reference mRNA sample the cathepsin k amplification curve (figure 24 A) crossed the detection threshold (C_t) sooner than the GAPDH curve (figure 24 B) indicating that the abundance of this mRNA was higher than that of the housekeeping gene used.

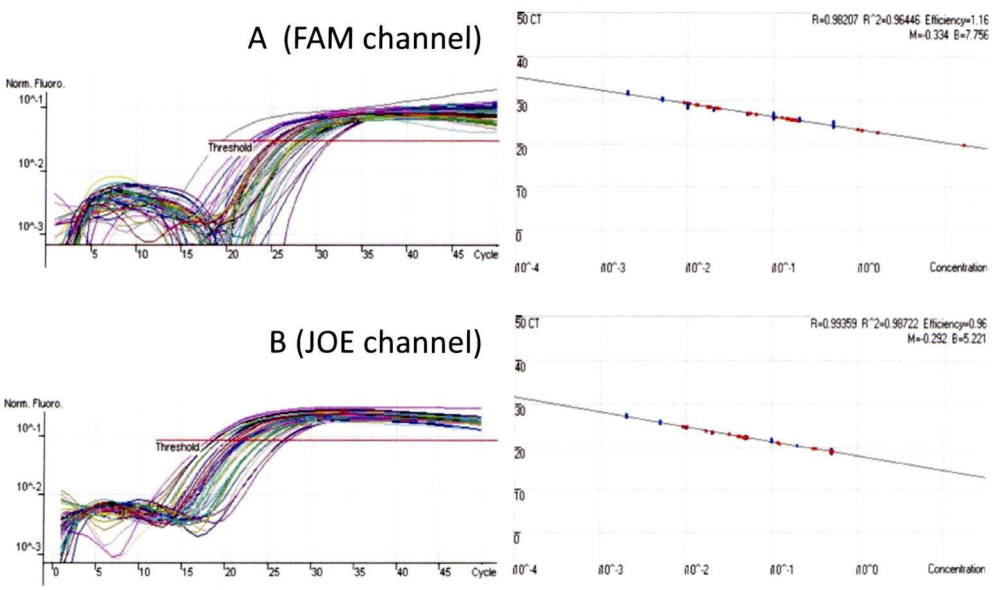

Figures 24 A,B Threshold fluorescence values for cathepsin K determined by Rotorgene, following the log-transformation of fluorescence measurements for each channel (A Fam channel, B Joe channel). (X axis shows number of cycles at which threshold values are reached, Y axis shows fluorescence values in log scale. Standard curves for each channel, on the right, generated using 2-fold serial dilution of the reverse transcribed Universal mRNA standard. Panel A, cathepsin K amplification, panel B GAPDH housekeeping amplification (Y axis, CT is the threshold cycle; x axis is the concentration in log scale) red dots are the gene of interest, blue dots are reference RNA.

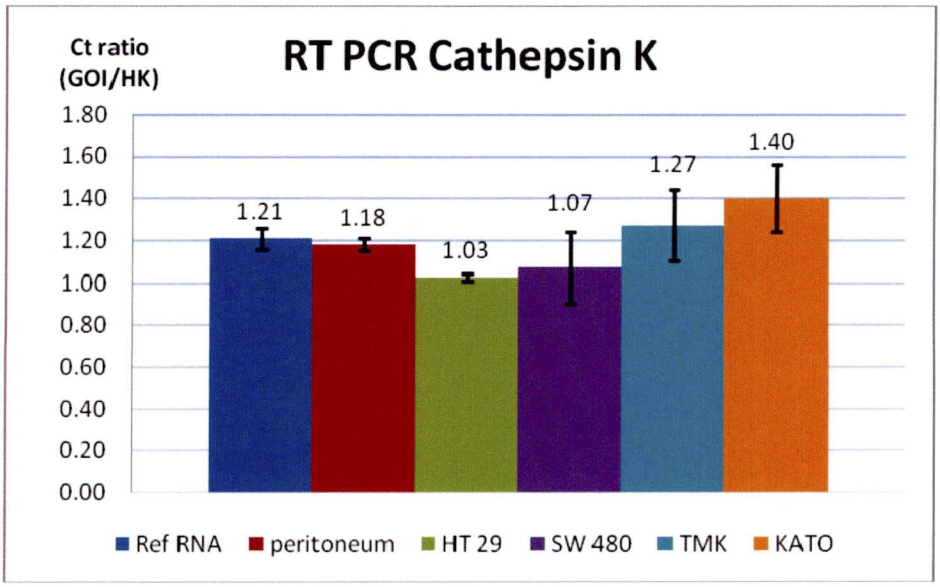

Fig 25 Host mesothelial cell cathepsin K expression in the 3D models. Bars show Ct detection threshold ratios between the gene of interest (GOI) versus housekeeping gene (HK) Cathepsin K/GAPDH ratios for the samples. Error bars show standard deviation for each group of samples. Numerical data available in appendix

The analysis of the standard curves shown in Figures 24 A, B (data in appendix section13.6) indicated that the amplification of the cathepsin k gene was slightly less efficient than that of GAPDH (R Fam channel 0.98, R Joe channel 0.99). The mesothelial cell derived cDNA samples derived from non-invaded and invaded peritoneal models were run together with the dilution standards. The analysis of these curves has shown that the detection threshold (C_t) for the cathepsin k gene product was 1.2 cycles higher than that of GAPDH in the universal reference RNA sample. Similarly, in the non-invaded mesothelial samples the difference in C_t values was 1.18. In contrast the expression was higher in both TMK and KATO invading models. However HT 29 and SW480 invasive models showed lower levels of cathepsin K than non invaded peritoneum (Fig 25). These data confirm that although the expression of Cathepsin K showed a gradient pattern of expression in invaded mesothelial cells the level, only KATO and TMK were slightly higher than reference RNA or normal peritoneum. As this gene was not differentially expressed by the microarrays, it was not possible to establish any association.

11.1.2 Vimentin

Vimentin is an important component of the cytoskeleton along with microfilaments (actins) and microtubules (tubulins), (Source: Entrez Gene, www.ncbi.nlm.nih.gov). Invaded mesothelial cells had shown a pattern of inverse association of expression versus microscopic level of invasion, in previous microarray analysis. Current analysis did not show this gene to be differentially expressed by invaded mesothelial cells

Vimentin primer/Taqman probe testing the abundance of this message was higher than that of the housekeeping gene. Amplification figures and standard curves (figures 26A, B) (data in appendix 13.7) for this genes showed that vimentin gene (FAM channel) crossed the detection threshold (C_t) sooner than the GAPDH, although this difference is less obvious than for the previous gene cathepsin K. A separate grey curve not crossing the detection threshold in the FAM channel corresponded to a negative control. The standard curves also showed that vimentin amplification was slightly less efficient (R=0.93), than of GAPDH (R=0.96).

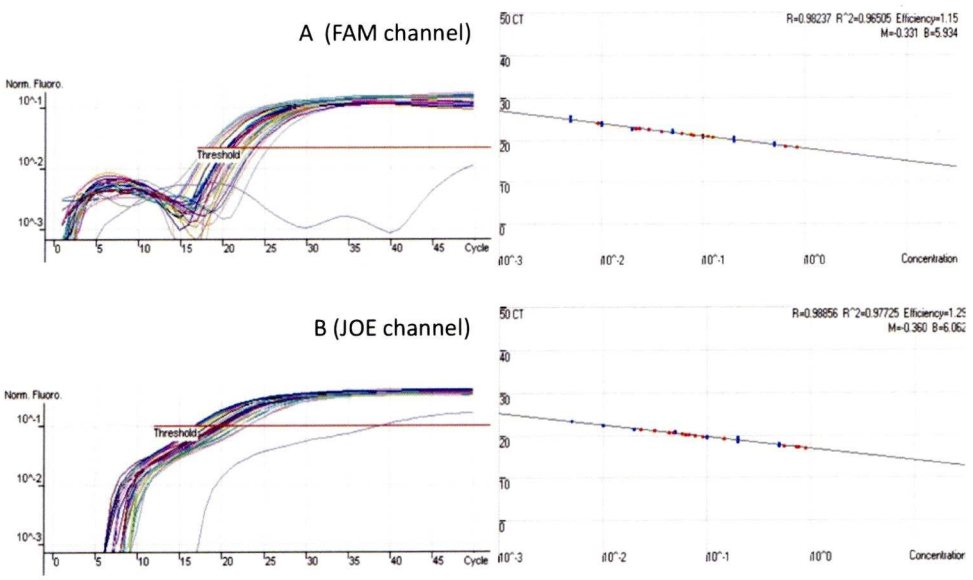

Figures 26 A,B Threshold fluorescence values for vimentin determined by Rotorgene, following the log-transformation of fluorescence measurements for each channel (A Fam channel, B Joe channel). (X axis shows number of cycles at which threshold values are reached, Y axis shows fluorescence values in log scale. Standard curves for each channel, on the right, generated using 2-fold serial dilution of the reverse transcribed Universal mRNA standard. Panel A depicts the amplification results of the vimentin k target gene while panel B shows the GAPDH housekeeping gene curves measured in the same test tubes.

Below are shown the detection threshold (Ct) ratios for vimentin (Fig 27). Although abundance of vimentin was higher than that of the housekeeping gene used, Values were fairly similar across the samples, and on this occasion there was no obvious gradient of expression. On this occasion no uninvaded peritoneal models had been run along the samples for comparison. Although they would have not necessarily contributed to the results, it is acknowledged that their analysis should have been included for the sake of completion.

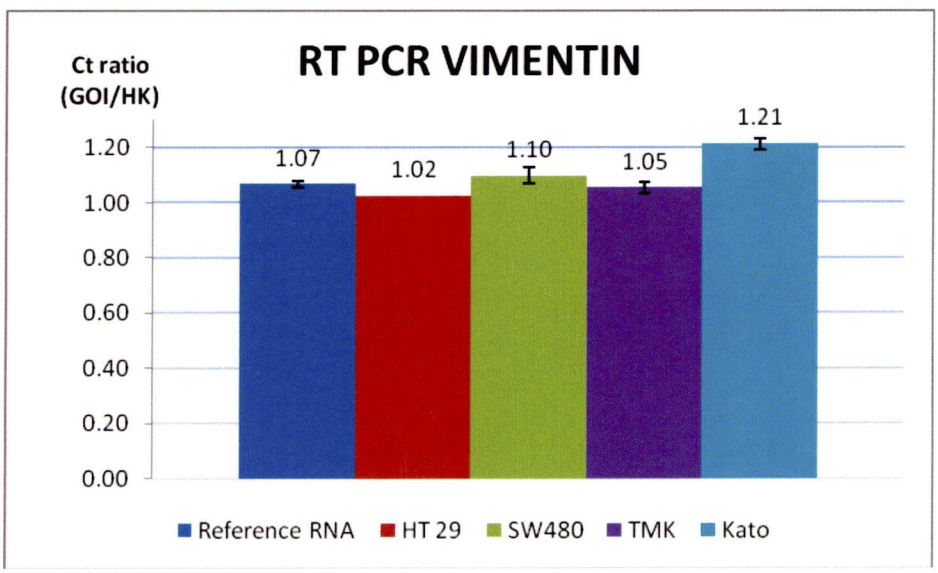

Fig 27 Host mesothelial cell vimentin expression in the 3D models. Bars show the Ct detection thresholds between the gene of interest (GOI) Vimentin and the housekeeping gene (HK) GAPDH, for the samples. Error bars show standard deviation for each group of samples. No Standard deviation available for HT 29 as only two models were run. Numerical data available in appendix

11.1.3 Caspase 8

Caspase 8 is an apoptosis related gene, directly involved in the extrinsic pathways in apoptosis. This pathway is activated following ligand binding to receptors of the tumor necrosis factor (TNF) superfamily, and activation of the caspases. Disruption of the normal apoptotic pathways may lead to the development of cancer (Hajra & Liu, 2004). This gene had also been expressed

by invaded mesothelial cells in previous microarray analysis. However following current analysis this gene was not differentially expressed.

The primers and Taqman probe amplifying the Caspase 8 gene were tested identically to that described for the two previous genes. However, as shown in Figure 28A, B while the universal reference RNA showed good amplification with these reagents, none of the laser dissected mRNA samples showed measurable levels of Caspase 8. Figure 28A demonstrated how a series of reactions went above the threshold, after 25 to 30 cycles. These corresponded to the reference RNA. None of the samples yielded results above the threshold. Equally the standard curve failed to show any of the samples amplification, normally represented by red dots. Results in the Joe channel (Fig 28B) showed better results for GAPDH amplification in both reference RNA and samples. In summary assays for CASPASE 8 did not return technically acceptable results for samples; further analysis of these amplifications was subsequently not carried out.

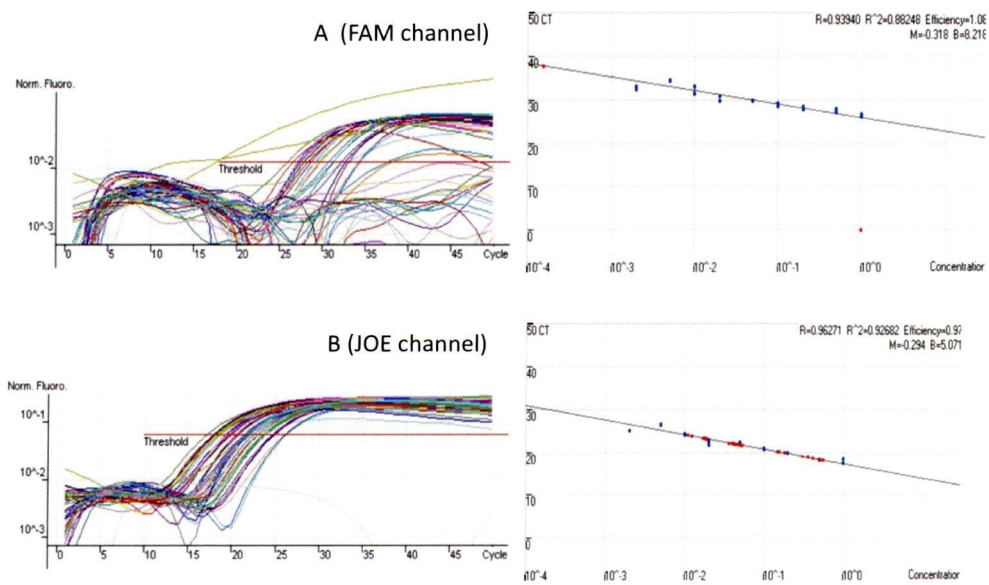

Figures 28 A,B Threshold fluorescence values for caspase 8 determined by Rotorgene, following the log-transformation of fluorescence measurements for each channel (A Fam channel, B Joe channel). (X axis shows number of cycles at which threshold values are reached, Y axis shows fluorescence values in log scale. Standard curves for each channel, on the right, generated using 2-fold serial dilution of the reverse transcribed Universal mRNA standard. Panel A depicts the amplification results of the caspase 8 target gene while panel B shows the GAPDH housekeeping gene curves measured in the same test tubes.

11.2 SUMMARY

The results of the PCR validation studies were disappointing in that they could not validate any of the present data. The process of optimisation of the real-time PCR reactions is costly and time-consuming and it is unfortunate that these experiments were limited both by costs, and by the time available to complete the work. This meant that the genes for the purposes of the PCR confirmation were selected based upon a previous rudimentary analysis not at the completion of the current full analysis of the comprehensive array dataset. This, unfortunately, greatly limited the biological relevance of the selected genes. Thus there were practical reasons why many of the intending validation experiments were not completed and did not yield useful results.

12 DISCUSSION

A three-dimensional model of peritoneum was the platform of choice to study the molecular biology of peritoneal metastasis. Immunocytochemical studies and analysis of gene expression in both cancer cells and mesothelial cells were conducted to investigate the mechanisms of peritoneal metastasis.

The optimal method for isolation of HPMC isolation was determined and 3D model was constructed, as described by previous authors, and characterised by light microscopy and immunocytochemistry.

HPMC isolation was a complex process. Despite previous reports in the literature, which reported successful HPMC isolation, it was necessary to compare some of the published methods to consistently obtain HPMC cells from tissue samples. Previously, tissue culture models of the peritoneum had been developed using isolated human mesothelial cell monolayers alone, or in combination with a variety of connective tissue supports (Jayne, Perry et al., 2000;Sawada, Shii et al., 1994) . Though HPMC could be obtained from commercial sources (Coriel Cell Repositories, Camden, New Jersey)(Casey, Koch et al., 2003), most authors harvested HPMC from omental tissue (Stylianou, Jenner et al., 1990;Zhang, Pettengell et al., 1999) or peritoneal effusions (Rieppi, Vergani et al., 1999;Sakata, Shigemasa et al., 2002) obtained from local clinical sources. Satisfactory isolation and growth of HPMC is crucial to the success of any tissue culture model used. Commonly encountered problems include poor yield of HPMC from different isolation techniques, and contamination of HPMC with fibroblasts which grow much more rapidly and dominate the combined cell preparations making them unsuitable for use in studies aimed at understanding mechanisms of disease in the peritoneum.

Isolation of HPMC from omentum usually requires protease digestion to release HPMC from the underlying connective tissue. Use of different concentrations of trypsin for varying lengths of time has been reported. Some studies reported success digesting omentum with trypsin 0.25% for 20 minutes (Mizutani, Kofuji et al., 2000b) , others used 0.05% trypsin for 5 minutes (Bittinger, Brochhausen et al., 1997).

In order to develop the models, a total of 40 HPMC isolation experiments were performed. 11 samples underwent digestion with 0.05% trypsin for 20 minutes, as described in materials and methods. None of them yielded any results. However when 0.25% trypsin was used instead on 29 omental samples (15 samples digestion time 10 minutes, and 14 samples digestion time 20 minutes) the results were better. Only 4 out of 15 (26%) samples digested for 10 minutes yielded a pure mesothelial population. When omental tissue was digested with trypsin 0.25% for 20 minutes, 10 out of 14 (71%) samples yielded satisfactory growth. Although the overall number of experiments was not large, HPMC isolation with 0.25% trypsin for 20 minutes produced significantly better results than the 10 minutes group. (Fisher's exact test p=0.02).

The fibroblast contamination of isolated HPMC was present in the methods assessed. Though no statistically significant differences were observed among the 0.25% trypsin digestion groups (10 minutes group, 8 contaminated out of 15 (53%); 20 minutes group, 3 out of 14 (21%), fibroblast contamination remains a major issue in performing or interpreting any studies using isolated HPMC. The fibroblast contamination observed might indicate that the peritoneal mesothelial cell monolayer present in the omentum was disrupted at some point during collection, thereby increasing the chances that subsequent trypsin digestion and centrifugation would release fibroblasts in addition to HPMC. To counteract this, after removal from the peritoneal cavity, all omental samples were immediately washed to ensure no sample dried out and tissue manipulation was minimised. It is also possible that trauma to the peritoneal mesothelial cell monolayer occurred during surgery and indeed this is thought to be the mechanism for development of abdominal adhesions as a complication of surgery. Data on the timing of collection of omental samples in relation to the abdominal surgery being performed was not recorded, but it might be appropriate to ensure that omental samples for HPMC isolation should be collected at the beginning of the surgical procedure, to reduce the chances of peritoneal trauma due to the surgical manipulation. In addition to assessing HPMC yield, the data suggest a trend towards increased fibroblast contamination in method B versus method C. The differences observed did not reach statistical significance and need further corroboration. However these results suggest that the method C for HPMC isolation (0.25% trypsin for 20 minutes) was superior.

Invasion into the in-vitro peritoneal model was reproduced using four different gastrointestinal cancer cell lines, each with different degree of differentiation and invasion potential. Assessment by light microscopy, using Haematoxylin eosin and immunocytochemistry techniques allowed to confirm previously reported findings regarding cancer cell and host mesothelial cell behaviour. Unlike cancer cells, HMPC behaved as non-invasive cells by lining the ECM as a monolayer. Although no visible basal membrane was identified by immunocytochemistry, HMPC behaved as if a physical barrier between the monolayer and ECM existed. On the in vitro models, the four cancer cells showed different patterns of invasion. HT29 cells grew on the mesothelial cell surface only; invasion did not progress into the extracellular matrix, which corresponded with this tumour's well differentiated nature. SW480 was able to invade and form rudimentary glandular structures when initial cell concentration was 10^6 cells/ml. This feature was unique to SW480 and confirms observations previously reported by Jayne et al. (Jayne, O'Leary et al., 1999b). The TMK I and KATO III cells were visibly demonstrated a more invasive behaviour on light microscopy. Both cell lines invaded through the mesothelial cell layer. They could digest the extracellular matrix and form distant metastatic deposits within. Fibroblasts would typically orientate themselves towards the direction of the tumour during invasion. These findings had also been previously reported by Jayne et al. (Jayne, O'Leary et al., 1999b).

Immunocytochemistry allowed further cell characterisation within the model. All cancer cell lines stained positively with epithelial antibodies including Ber EP4, which is commonly used in clinical practice to stain carcinoma cells such as breast cancer. Although staining intensities varied, overall characterisation for all epithelial cancer cell lines was satisfactory. Mesothelial cells from non un-invaded models reproduced the results already stated above. The fact that Ber EP4 did not stain mesothelial cells confirmed the mesodermal nature of these cells.

The extracellular matrix and basal membrane of normal peritoneum and invasion models was characterised with vimentin, collagens III and IV as well as laminin and fibronectin. These results reproduced those published by Jayne et al (Jayne, O'Leary et al., 1999b) who showed that fibroblasts and extracellular matrix stained with antibodies such as vimentin, collagens III and IV, laminin

and fibronectin to varying degrees; however, no physical basal membrane could be demonstrated. An interesting finding was the presence of staining around groups of cancer cells resembling a membrane or capsule. This did not happen in non invaded mesothelium. TMK model showed this feature whether stained with fibronectin, laminin or collagen III but not with collagen IV. Moreover KATO III also presented this capsular feature when stained with collagen IV and laminin. HT 29 model did with fibronectin, whereas SW480 models did not demonstrate this feature at all. Although the significance of this capsular formation was uncertain, it seemed more common in the most aggressive cancer models. As mesothelial layers were often destroyed by invading cancer cells and no basal membrane could be demonstrated in this peritoneal model it is difficult to define the relationship between these apparent capsular formations and any pre-existing basal membrane.

The interest in staining the invasion models with adhesion molecule related antibodies was based on the likely relevance of adhesion molecules to the process of peritoneal metastases. ICAM-1 has been reported to be secreted locally by tumours (Alexiou, Karayiannakis et al., 2001;Maruo, Gochi et al., 2002) and suppress immune response. Lymph node and metastatic spread have been correlated with high serum levels of ICAM-1 in various tumours. Some authors have suggested a role for serum ICAM-1 as a prognostic factor of the disease (Maruo, Gochi et al., 2002). ICAM-2 potential for gene therapy has been reported by Tanaka et al(Tanaka, Yashiro et al., 2004)

Therefore ICAM-1 staining was assessed in all invasion models and potential correlation between ICAM-1 expression and invasiveness was sought. Despite current evidence suggesting that ICAM-1 expression has an important role in development of peritoneal invasion and metastasis, no correlation between ICAM-1 expression and invasive behaviour was found. These findings suggested ICAM-1 is always expressed at local level and thus may not be a good marker of invasiveness of metastases in the gastrointestinal tumours studied here. Moreover ICAM-1 was also expressed by non-invaded mesothelial cells.

VCAM and PECAM did not produce any staining in the majority of models. These glycoproteins of the immunoglobulin superfamily are commonly encountered in the surface of endothelia (Parums, Cordell et al., 1990;Wilkinson,

Edwards et al., 1993). As in vitro models lacked any vasculature these results were expected.

Laser capture technology was used to collect cancer cells and mesothelial cells from each model and study their transcriptional responses independently. RNA isolation and amplification was performed and 50 samples of RNA from cancer cells and neighbouring mesothelial cells were hybridised to commercial cancer arrays. Successful microarray studies depend on enough good quality starting material (total RNA) available. RNA yield from cells is variable but 1-2μg of RNA may require extraction of total RNA from approximately 10^5–10^6 cells. Acquiring this number of cells was not possible in this or indeed in many other clinical studies (Li, Adams et al., 2003). Hence it was crucial to identify a robust amplification protocol which would yield sufficient good quality RNA. Numerous methods have been published in the literature. The most popular methods involve either in vitro transcription or SMART technology. The first described method amplified the RNA through in vitro transcription (IVT), usually employing reverse transcription and two amplification cycles. This was first published by Eberwine et al (Eberwine, 1996;Van Gelder, von Zastrow et al., 1990). Its principle involves the reverse transcription of total RNA using an Oligo dT primer bearing a T7 promoter and subsequent in vitro transcription of DNA thus generating thousands of copies of amplified anti-sense or complementary RNA, using a highly specific T7 RNA polymerase. Although this was originally described to start with 40μg of total RNA, optimisation of the protocol throughout the years has made possible to work with far smaller amounts of starting material. This protocol, now considered by many the gold standard, is well documented and commercially available. It is possible to perform subsequent rounds of amplification using random primers and a modified protocol has been reported to successfully amplify as little material as RNA from a single cell (Kamme, Zhu et al., 2004).

Amplification methods based on template switching technology have grown in popularity. These were developed to solve issues such as starting material, reliability of reverse transcription and the need for various rounds of amplification. As reverse transcription may not always transcribe the entire mRNA sequence, the 5' ends of genes could to be under-represented in amplified cDNA. This would often the case for long mRNAs, especially if the first-strand

synthesis is primed only with oligo (dT) primers. Adding the SMART primer to the reverse transcription reaction has been reported to avoid such 3' bias, thus making reverse transcription and subsequent amplification more reliable (Seth, Gorrell et al., 2003a). Amplification starts with nanograms of total RNA and generates large quantities of double stranded cDNA in a single round without in theory the need for further rounds (Kenzelmann, Klaren et al., 2004;Seth, Gorrell et al., 2003b). Thus, where tissue sources cannot provide sufficient amounts of RNA to proceed to microarray or other techniques directly, validated methods of amplification are available and some groups have even combined both switching primer technology and T7 amplification (Ji, Zhou et al., 2004) with successful results.

When the amount of starting RNA is not detectable by conventional means such as spectrophotometry and its quality cannot be checked, it is crucial to choose an amplification method that is reliable, reproducible, robust, and simple. Some authorities have reported successful amplification of RNA from a single cell (Kelz, Dent et al., 2002). Kamme et al (Kamme, Zhu et al., 2004) worked with samples containing some 14 captured cells and using a modification of the protocol from Eberwine (Van Gelder, von Zastrow et al., 1990) they successfully amplified RNA in two rounds of amplification and hybridised their samples on cDNA arrays.

My initial experiments with switching primer amplification, as described by BD Biosciences (www.bdbiosciences.com, Oxford, UK), did not yield satisfactory results. Although a second round using random primers and T7 amplification might have been successful, I was not confident with the results. Stirewalt et al (Stirewalt, Pogosova-Agadjanyan et al., 2004) developed a protocol that combined the reproducibility of linear amplification and the robustness of PCR. Unlike the original SMART protocol, here amplification of DNA takes place only from the 5' end producing large amounts of first strand cDNA. In a separate reaction second strand (complimentary) cDNA is synthesised. Their method was compared to a modified version of the protocol by Eberwine (Stirewalt, Pogosova-Agadjanyan et al., 2004). It was concluded that whilst the reproducibility of both methods was similar, the overall reliability of single linear amplification was superior. The protocol proposed by Stirewalt et al (Stirewalt, Pogosova-Agadjanyan et al., 2004) was used in these studies and

found to be reliable and reproducible. For the second round of amplification I used the original protocol from Eberwine (Van Gelder, von Zastrow et al., 1990) available as the Message Amp kit from Ambion.

Following hybridisation into cancer arrays and microarray analysis as described earlier it has been possible to demonstrate that 3D models of peritoneum may provide valuable information about the molecular biology of peritoneal metastasis. Microarray work in this model has never been done before. The limitations of a 3D model, in terms of lifespan and cellular characteristics, lead to a limited understanding of the results. The lack of a systemic response to the disease translated into a more basic understanding of peritoneal metastasis at the local level. While this may seem incomplete, it may prove advantageous, at least initially, in a field that is poorly understood.

Invading cancer cells and host mesothelial cells only showed a limited number of genes with a pattern of expression that could be associated with the previous microscopic findings. Many functions potentially relevant to the metastatic process were not reflected in the results. There were two main reasons for this. Either a gene or a group of genes were not differentially expressed or if they were, this difference in expression levels was mostly related to one cell group. For example, cancer cells showed a number of proteases, or inhibitors thereof that were differentially expressed in one cell line. This included TIMP-1 and TIMP-2, MMP-17 and cathepsin-k. While they play a crucial role in invasion, their expression levels in the 3D model only demonstrated significant differences in the TMK cell line, except for TIMP-2 which had higher levels in KATO cells. Host mesothelial cells also failed to demonstrate many genes which could be relevant to vital functions such as cell to cell adhesion. While tubulins were shown earlier to be differentially expressed, other genes such as cadherin I were showed higher levels of expression in non-invaded peritoneum, TMK and KATO, compared to SW480 and HT29. Furthermore, non invaded HPMC did not behave as a baseline model. Often gene expression levels from HMPC were similar to those of one or more cancer cell lines, rather that at the highest or lowest point of a gradient. The reasons for this were unclear. It is also acknowledged that the limited choice and availability of cancer cell lines at the time of these experiments is a source of potential bias. It is not possible to demonstrate that results obtained were not influence by the nature of the tissues,

rather than their aggressive behaviour. It is well known that gastric carcinoma usually behaves very differently from colorectal carcinoma. It would have been ideal to compare a series of gastric tumours amongst themselves. Alternatively tumours could have been compared to healthy tissue.

Overall it becomes apparent that further experiments, including more arrays and more cancer cell lines could have provided more robust results. The initial plan was to perform experiments using slides printed in the laboratory; however the quality of these in-house printed slides never reached the required standard, and other arrangements had to be made. The availability of many more microarray slides would have meant more replicates; both biological and technical. However, commercial slides were costly, seriously compromising the number of experiments,.

However the in vitro peritoneal model of peritoneum also had some limitations. While valuable information could be gained about the early stages of invasion of the in vitro models, these were removed from culture after a given number of days. Subsequently any information gained would be based on a given point in time, thus missing changes over a period. If models could survive weeks or months, a more thorough study of peritoneal metastasis during various stages of the disease could be possible. Moreover, only three cell types were present in the model. There were no vessels, no blood supply, no immune system, which translated into a lack of ability to generate a systemic response to invasion, as it would take place in humans. Therefore, some functions which take place at the very local level, such as disruption of HPMC adhesion and proteolysis of the extracellular matrix may be reproduced in an in vitro model, whereas the understanding of those functions provided by a host response such as immunity, angiogenesis, cell repair or apoptosis may be limited.

With regards to the RT PCR, genes relevant to apoptosis, ECM proteolysis and cytoskeletal disruption were tested. The results presented showed that an alternative test could potentially confirm the microarray findings. While negative results were obtained, further experiments with both microarrays and RT PCR could have shown more conclusive results.

However it should also be remembered that there are other reasons why the real-time PCR results may differ from those of the microarrays. Normalisation of results from the PCR experiments was performed using

GAPDH as a single reference gene. This assumes that the expression of this gene is constant in all cells tested, and if this assumption holds then normalisation can be performed to correct for different amounts of starting RNA. Unfortunately, though genes such as GAPDH are expressed as high level by most cells, there is evidence that expression of this gene varies in different conditions and in different cell types (Pfaffl, Tichopad et al., 2004). Hence reliance on expression of a single gene such as GAPDH to help normalise another gene's expression may well lead to spurious results due to alteration in expression of GAPDH itself. If further RT PCR experiments were possible, this problem could be avoided by using several genes as reference or normalisation genes and using an average of the combined expression as the normalisation factor (Pfaffl, Tichopad et al., 2004).

Finally, research on peritoneal metastases could be further expanded by studying particular aspects of the molecular biology. For instance gene expression relevant to a given cell function could be further assessed using custom arrays with related genes. Whilst it may be argued that many cellular functions interact with others, rather than working independently, a thorough study of individual functions could provide more answers than a more general approach.

A disadvantage of any in vitro model is the lack of systemic response to the environment provided by molecules from other cells and organs. A possible avenue for future research could be the incubation within the ECM of endothelial cells and investigation of their ability to form vascular structures. This would give the 3D model a closer resemblance to human peritoneum. Endothelial cells may secrete chemo attracting molecules and angiogenic factors and their role could potentially provide better understanding about local peritoneal response to pathological events such as inflammation, adhesions or neoplasia.

Furthermore, a three dimensional model of peritoneum could also be useful for the assessment of gene functions during invasion. Thus, known genes could be tested in the models by introducing silencing RNA sequences into cancer cells, allow invasion to take place and compare behaviour with non treated models.

13 APPENDICES

3D INVASION MODELS

Model	Number	Model	Number
Kato 104c	5	Kato 105c	31
Kato 104m	6	Kato 105m	32
Kato 105c	7	Kato 106c	33
Kato 105m	8	Kato 106m	34
Kato 106c	9	SW480104c	35
Kato 106m	10	SW480104m	36
SW480104c	11	SW480105c	37
SW480104m	12	SW480105m	38
SW480105c	13	SW480106c	39
SW480105m	14	SW480106m	40
SW480106c	15	HT29104c	41
SW480106m	16	HT29104m	42
HT29104c	17	HT29105c	43
HT29104m	18	HT29105m	44
HT29105c	19	HT29106c	45
HT29105m	20	HT29106m	46
HT29106c	21	TMK104c	47
HT29106m	22	TMK104m	48
TMK104c	23	TMK105c	49
TMK104m	24	TMK105m	50
TMK105c	25	TMK106c	51
TMK105m	26	TMK106m	52
TMK106c	27	peritoneum	53
TMK106m	28	Neg control	54
Kato 104c	29	peritoneum	55
Kato 104m	30		

Table 16 50 models of peritoneum were made. Within the model column, letters "c" and "m" indicate whether cancer cells or mesothelial cells were laser captured. Numbers 104, 105 and 106 corresponded to the initial concentrations of invading cancer cells ($104=10^4$ cells/ml, $105=10^5$ cells/ml, $106=10^6$ cells/ml). Within the number column each number is a unique identifier for each model

13.1 REFERENCE RNA AMPLIFICATION DATA

Name	Total RNA ng	A260	A280	Ratio	aRNA µg/µl	Total aRNA *(µg in 100µl)*
A1X	1000	0.387	0.203	1.906404	0.8514	85.14
A2X	1000	0.264	0.139	1.899281	0.5808	58.08
A3X	1000	0.356	0.185	1.924324	0.7832	78.32
B1X	100	0.505	0.262	1.927481	1.111	111.1
B2X	100	0.413	0.216	1.912037	0.9086	90.86
B3X	100	0.374	0.201	1.860697	0.8228	82.28
C1X	10	0.386	0.201	1.920398	0.8492	84.92
C2X	10	0.258	0.118	2.186441	0.5676	56.76
C3X	10	0.334	0.178	1.876404	0.7348	73.48
F1X	1	0.354	0.187	1.893048	0.7788	77.88
F2X	1	0.243	0.13	1.869231	0.5346	53.46
F3X	1	0.361	0.188	1.920213	0.7942	79.42
M2X	0.1	0.273	0.137	1.992701	0.12012	12.012
M3X	0.1	0.22	0.122	1.803279	0.0968	9.68
X1X	0.01	0.199	0.105	1.895238	0.08756	8.756
X3X	0.01	0.23	0.127	1.811024	0.1012	10.12
Y1X	0.001	0.105	0.051	2.058824	0.0462	4.62
Y2X	0.001	0.171	0.094	1.819149	0.07524	7.524

Table 17 Amplification performed with Reference RNA at various concentrations of starting material. Below 1ng of total RNA, amplification values fell dramatically

13.2 RNA SPECTROPHOTOMETRY BEFORE Cy LABEL

A) PERITONEAL MODELS

	A260	A280	Ratio	Start µg/µl	Start total
MEAN	0.54	0.27	2.01	1.19	113.50
ST DEV	0.12	0.06	0.16	0.26	24.43
RANGE	0.26-0.68	0.13-0.36	1.8-2.45	0.56-1.49	53.3-141.08

B) REFERENCE RNA

	A260	A280	Ratio	Start µg/µl	Start total
MEAN	0.34	0.18	1.90	0.74	70.41
ST DEV	0.07	0.04	0.09	0.16	15.40
RANGE	0.26-0.58	0.14-0.3	1.80-2.14	0.56-1.28	53.50-121.85

Tables 18 A,B Each variable was expressed in the following units: µg/µl, start total µg/100µl

Table 19 Cy3 Sample Label (Columns in black indicate spectrophotometry readings before label, in green after label procedure)

Model	Code	Number	A260	A280	Ratio	Start con	Start µg	20µg vol	Dilution	A260	A280	Ratio	RNA con	Yield	A550	Dye Incorporation	Sample	Loss RNA	RNA to combine	Vol to combine
Kato 106c	NB184/04	9	0.58	0.26	2.28	1.28	121.85	15.59	10	0.44	0.22	1.96	0.17	16.61	0.29	40.14	9.00	16.97	15.50	88.70
Kato 106m	NB184/04	10	0.37	0.19	1.98	0.81	76.91	24.70	10	0.27	0.13	2.13	0.11	10.22	0.14	30.37	10.00	48.89	10.22	95.00
SW480106c	NB138/04	15	0.65	0.36	1.80	1.43	135.85	13.99	10	0.35	0.18	1.92	0.14	13.22	0.21	35.38	15.00	33.88	13.22	95.00
SW480106m	NB138/04	16	0.66	0.33	2.01	1.45	137.94	13.77	10	0.46	0.21	2.17	0.18	17.40	0.28	36.46	16.00	12.98	10.75	58.70
HT29106c	NB186/04	21	0.59	0.29	2.01	1.30	123.10	15.43	10	0.45	0.21	2.12	0.18	17.10	0.32	42.98	21.00	14.50	14.97	83.18
HT29106m	NB186/04	22	0.50	0.25	1.98	1.11	105.13	18.07	10	0.44	0.24	1.81	0.18	16.76	0.27	36.23	22.00	16.21	10.75	60.96
TMK106c	NB185/04	27	0.68	0.32	2.11	1.49	141.08	13.47	10	0.41	0.22	1.86	0.16	15.54	0.23	33.93	27.00	22.29	15.54	95.00
TMK106m	NB185/04	28	0.31	0.16	1.96	0.68	64.58	29.42	10	0.53	0.23	2.28	0.21	20.10	0.30	34.18	28.00	-0.51	10.75	50.82
Kato 106c	NB184/04	33	0.49	0.27	1.86	1.09	103.25	18.40	10	0.20	0.12	1.74	0.08	7.68	0.12	36.58	33.00	61.62	7.26	89.83
Kato 106m	NB184/04	34	0.55	0.28	1.95	1.20	114.32	16.62	10	0.33	0.15	2.27	0.13	12.58	0.20	36.48	34.00	37.11	7.45	56.25
SW480106c	NB138/04	39	0.63	0.29	2.13	1.38	131.04	14.50	10	0.28	0.14	1.97	0.11	10.49	0.22	48.31	39.00	47.56	10.49	95.00
SW480106m	NB138/04	40	0.40	0.22	1.85	0.88	83.60	22.73	10	0.54	0.24	2.28	0.21	20.37	0.28	31.83	40.00	-1.84	7.26	33.85
HT29106c	NB186/04	45	0.26	0.13	2.04	0.56	53.30	35.65	10	0.24	0.11	2.14	0.10	9.04	0.10	26.00	45.00	54.78	7.26	76.24
HT29106m	NB186/04	46	0.56	0.23	2.45	1.23	117.04	16.23	10	0.26	0.12	2.21	0.10	9.84	0.13	29.92	46.00	50.79	7.26	70.06
TMK106c	NB185/04	51	0.67	0.35	1.93	1.47	139.82	13.59	10	0.20	0.09	2.17	0.08	7.68	0.09	27.65	51.00	61.62	7.68	95.00
TMK106m	NB185/04	52	0.57	0.30	1.89	1.25	118.50	16.03	10	0.20	0.10	1.97	0.08	7.49	0.10	29.88	52.00	62.57	7.26	92.11
PM1	NB 690	53	0.40	0.22	1.83	0.88	83.81	22.67	10	0.28	0.13	2.19	0.11	10.49	0.15	31.56	53.00	47.56	7.26	65.74
SW480106m	NB138/04	40	0.40	0.22	1.85	0.88	83.60	22.73	10	0.42	0.23	1.81	0.17	15.85	0.18	25.50	40.00	20.77	9.88	59.23
Kato 106c	NB184/04	9	0.58	0.26	2.28	1.28	121.85	15.59	10	0.39	0.21	1.85	0.16	14.82	0.29	43.89	9.00	25.90	12.43	79.65
Kato 106m	NB184/04	10	0.37	0.19	1.98	0.81	76.91	24.70	10	0.16	0.08	2.19	0.07	6.23	0.14	51.64	10.00	68.84	6.23	95.00
SW480106c	NB138/04	15	0.65	0.36	1.80	1.43	135.85	13.99	10	0.40	0.19	2.05	0.16	15.12	0.18	27.17	15.00	24.38	12.43	78.05
SW480106m	NB138/04	16	0.66	0.33	2.01	1.45	137.94	13.77	10	0.22	0.10	2.22	0.09	8.28	0.11	30.03	16.00	58.58	8.28	95.00
HT29106c	NB186/04	21	0.59	0.29	2.01	1.30	123.10	15.43	10	0.29	0.15	1.95	0.12	10.98	0.18	36.79	21.00	45.09	10.98	95.00
HT29106m	NB186/04	22	0.50	0.25	1.98	1.11	105.13	18.07	10	0.40	0.20	2.00	0.16	15.31	0.31	46.21	22.00	23.43	12.43	77.08
TMK106c	NB185/04	27	0.68	0.32	2.11	1.49	141.08	13.47	10	0.30	0.14	2.08	0.12	11.32	0.17	35.07	27.00	43.38	11.32	95.00
TMK106m	NB185/04	28	0.31	0.16	1.96	0.68	64.58	29.42	10	0.50	0.23	2.21	0.20	18.92	0.31	37.27	28.00	5.38	12.43	62.38
Kato 106c	NB184/04	33	0.49	0.27	1.86	1.09	103.25	18.40	10	0.22	0.12	1.90	0.09	8.32	0.15	41.14	33.00	58.39	8.32	95.00
Kato 106m	NB184/04	34	0.55	0.28	1.95	1.20	114.32	16.62	10	0.51	0.28	1.86	0.20	19.42	0.34	39.61	34.00	2.91	15.24	74.55
SW480106c	NB138/04	39	0.63	0.29	2.13	1.38	131.04	14.50	10	0.47	0.24	1.92	0.19	17.71	0.34	44.34	39.00	11.46	15.24	81.75
SW480106m	NB138/04	40	0.40	0.22	1.85	0.88	83.60	22.73	10	0.29	0.15	1.91	0.12	10.94	0.19	39.42	40.00	45.28	10.94	95.00
HT29106c	NB186/04	45	0.26	0.13	2.04	0.56	53.30	35.65	10	0.11	0.06	1.85	0.04	4.22	0.09	46.54	45.00	78.91	4.22	95.00
HT29106m	NB186/04	46	0.56	0.23	2.45	1.23	117.04	16.23	10	0.17	0.08	2.16	0.07	6.57	0.11	38.19	46.00	67.13	6.57	95.00
TMK106c	NB185/04	51	0.67	0.35	1.93	1.47	139.82	13.59	10	0.17	0.08	2.14	0.07	6.35	0.10	37.05	51.00	68.27	6.35	95.00
TMK106m	NB185/04	52	0.57	0.30	1.89	1.25	118.50	16.03	10	0.17	0.08	2.29	0.07	6.61	0.17	56.96	52.00	66.94	6.61	95.00
SW480106c	NB138/04	15	0.65	0.36	1.80	1.43	135.85	13.99	10	0.32	0.17	1.89	0.13	12.08	0.11	21.16	15.00	39.58	5.32	41.82
SW480106m	NB138/04	16	0.66	0.33	2.01	1.45	137.94	13.77	10	0.33	0.17	1.91	0.13	12.65	0.10	18.76	16.00	36.73	5.32	39.94
HT29106c	NB186/04	21	0.59	0.29	2.01	1.30	123.10	15.43	10	0.31	0.14	2.19	0.13	11.89	0.10	19.96	21.00	40.53	5.32	42.49
TMK106c	NB185/04	27	0.68	0.32	2.11	1.49	141.08	13.47	10	0.30	0.16	1.89	0.12	11.51	0.10	20.42	27.00	42.43	5.32	43.89
HT29106m	NB186/04	46	0.56	0.23	2.45	1.23	117.04	16.23	10	0.16	0.09	1.80	0.06	6.00	0.04	16.35	46.00	69.98	5.32	84.18
PM1	NB 690	53	0.40	0.22	1.83	0.88	83.81	22.67	10	0.38	0.20	1.90	0.15	14.44	0.10	15.49	53.00	27.80	5.32	35.00
PM2	NB 690	55	0.58	0.29	1.99	1.27	120.59	15.76	10	0.33	0.17	1.90	0.13	12.35	0.06	10.53	55.00	38.25	5.32	40.92
PM2	NB 690	55	0.58	0.29	1.99	1.27	120.59	15.76	10	0.24	0.13	1.91	0.10	9.20	0.10	25.81	55.00	54.02	5.32	54.96
Kato 106c	NB184/04	33	0.49	0.27	1.86	1.09	103.25	18.40	1	0.76	0.37	2.07	0.03	4.42	0.53	41.94	33.00	77.90	4.42	145.00
Kato 106m	NB184/04	34	0.55	0.28	1.95	1.20	114.32	16.62	10	0.17	0.09	1.88	0.07	9.69	0.11	38.49	34.00	51.57	5.81	87.04
SW480106c	NB138/04	39	0.63	0.29	2.13	1.38	131.04	14.50	10	0.49	0.27	1.81	0.20	18.62	0.26	32.36	39.00	6.90	5.81	29.66
Kato 106c	NB184/04	9	0.58	0.26	2.28	1.28	121.85	15.59	10	0.17	0.09	1.82	0.07	9.69	0.11	39.21	9.00	51.57	5.81	87.04
TMK106c	NB185/04	51	0.67	0.35	1.93	1.47	139.82	13.59	10	0.07	0.04	1.66	0.03	2.58	0.03	22.97	51.00	87.08	2.58	95.00
TMK106m	NB185/04	52	0.57	0.30	1.89	1.25	118.50	16.03	10	0.09	0.04	2.16	0.04	3.53	0.07	41.98	52.00	82.33	3.53	95.00
Model	**Code**	**Number**	**A260**	**A280**	**Ratio**	**Start con**	**Start µg**	**20µg vol**	**Dilution**	**A260**	**A280**	**Ratio**	**RNA con**	**Yield**	**A550**	**Dye Incorparation**	**Sample**	**Loss RNA**	**RNA to combine**	**Vol to combine**
MEAN			0.54	0.27	2.01	1.19	112.73	17.99	9.81	0.32	0.16	2.01	0.12	11.63	0.18	33.96		41.85	8.57	76.79
SD			0.12	0.06	0.17	0.26	24.78	5.49	1.30	0.14	0.07	0.17	0.05	4.70	0.10	9.79		23.49	3.53	23.50
RANGE	MIN		0.26	0.13	1.80	0.56	53.30	13.47	1.00	0.07	0.04	1.66	0.03	2.58	0.03	10.53		-1.84	2.58	29.66
	MAX		0.68	0.36	2.45	1.49	141.08	35.65	10.00	0.76	0.37	2.29	0.21	20.37	0.53	56.96		87.08	15.54	145.00

Table 20 Cy 5 Reference label (Columns in blue indicate spectrophotometry readings before label, in red after label procedure)

A260	A280	Dilution	Ratio	Start con	Start µg	20µg vol	Loss RNA	RNA to combine	Vol to combine	A260	A280	Dilution	Ratio	RNA con	Yield	A650	Dye Incorparation
0.36	0.17	55.00	2.14	0.79	74.61	25.46	22.48	15.50	95.00	0.41	0.22	10.00	1.88	0.16	15.50	0.15	12.81
0.36	0.18	55.00	1.98	0.80	75.66	25.11	46.23	10.22	90.30	0.28	0.13	10.00	2.23	0.11	10.75	0.13	17.06
0.36	0.17	55.00	2.14	0.79	74.61	25.46	18.11	13.22	76.71	0.43	0.24	10.00	1.77	0.17	16.38	0.23	18.90
0.36	0.18	55.00	1.98	0.80	75.66	25.11	46.23	10.75	95.00	0.28	0.13	10.00	2.23	0.11	10.75	0.13	17.06
0.36	0.17	55.00	2.14	0.79	74.61	25.46	25.14	14.97	95.00	0.39	0.21	10.00	1.86	0.16	14.97	0.15	13.72
0.36	0.18	55.00	1.98	0.80	75.66	25.11	46.23	10.75	95.00	0.28	0.13	10.00	2.23	0.11	10.75	0.13	17.06
0.36	0.17	55.00	2.14	0.79	74.61	25.46	18.68	15.54	90.78	0.43	0.20	10.00	2.12	0.17	16.26	0.21	17.68
0.36	0.18	55.00	1.98	0.80	75.66	25.11	46.23	10.75	95.00	0.28	0.13	10.00	2.23	0.11	10.75	0.13	17.06
0.39	0.21	55.00	1.88	0.86	81.93	23.19	63.71	7.26	95.00	0.19	0.11	10.00	1.79	0.08	7.26	0.09	16.98
0.58	0.30	55.00	1.94	1.28	121.85	15.59	62.76	7.45	95.00	0.20	0.11	10.00	1.87	0.08	7.45	0.09	15.63
0.30	0.16	55.00	1.84	0.66	62.28	30.51	32.74	10.49	74.07	0.35	0.17	10.00	2.07	0.14	13.45	0.13	12.73
0.39	0.21	55.00	1.88	0.86	81.93	23.19	63.71	7.26	95.00	0.19	0.11	10.00	1.79	0.08	7.26	0.09	16.98
0.39	0.21	55.00	1.88	0.86	81.93	23.19	63.71	7.26	95.00	0.19	0.11	10.00	1.79	0.08	7.26	0.09	16.98
0.39	0.21	55.00	1.88	0.86	81.93	23.19	63.71	7.26	95.00	0.19	0.11	10.00	1.79	0.08	7.26	0.09	16.98
0.36	0.19	55.00	1.92	0.79	74.82	25.39	11.27	7.68	41.09	0.47	0.22	10.00	2.12	0.19	17.75	0.19	14.74
0.39	0.21	55.00	1.88	0.86	81.93	23.19	63.71	7.26	95.00	0.19	0.11	10.00	1.79	0.08	7.26	0.09	16.98
0.39	0.21	55.00	1.88	0.86	81.93	23.19	63.71	7.26	95.00	0.19	0.11	10.00	1.79	0.08	7.26	0.09	16.98
0.37	0.20	55.00	1.88	0.81	76.49	24.84	50.60	9.88	95.00	0.26	0.15	10.00	1.79	0.10	9.88	0.23	31.60
0.26	0.14	55.00	1.89	0.57	54.13	35.10	37.87	12.43	95.00	0.33	0.15	10.00	2.21	0.13	12.43	0.31	33.84
0.26	0.14	55.00	1.89	0.57	54.13	35.10	37.87	6.23	47.65	0.33	0.15	10.00	2.21	0.13	12.43	0.31	33.84
0.26	0.14	55.00	1.89	0.57	54.13	35.10	37.87	12.43	95.00	0.33	0.15	10.00	2.21	0.13	12.43	0.31	33.84
0.26	0.14	55.00	1.89	0.57	54.13	35.10	37.87	8.28	63.33	0.33	0.15	10.00	2.21	0.13	12.43	0.31	33.84
0.26	0.14	55.00	1.89	0.57	54.13	35.10	37.87	10.98	83.96	0.33	0.15	10.00	2.21	0.13	12.43	0.31	33.84
0.26	0.14	55.00	1.89	0.57	54.13	35.10	37.87	12.43	95.00	0.33	0.15	10.00	2.21	0.13	12.43	0.31	33.84
0.26	0.14	55.00	1.89	0.57	54.13	35.10	37.87	11.32	86.57	0.33	0.15	10.00	2.21	0.13	12.43	0.31	33.84
0.26	0.14	55.00	1.89	0.57	54.13	35.10	37.87	12.43	95.00	0.33	0.15	10.00	2.21	0.13	12.43	0.31	33.84
0.26	0.14	55.00	1.80	0.56	53.50	35.51	23.81	8.32	51.88	0.40	0.19	10.00	2.13	0.16	15.24	0.41	36.85
0.26	0.14	55.00	1.80	0.56	53.50	35.51	23.81	15.24	95.00	0.40	0.19	10.00	2.13	0.16	15.24	0.41	36.85
0.26	0.14	55.00	1.80	0.56	53.50	35.51	23.81	15.24	95.00	0.40	0.19	10.00	2.13	0.16	15.24	0.41	36.85
0.26	0.14	55.00	1.80	0.56	53.50	35.51	23.81	10.94	68.23	0.40	0.19	10.00	2.13	0.16	15.24	0.41	36.85
0.26	0.14	55.00	1.80	0.56	53.50	35.51	23.81	4.22	26.30	0.40	0.19	10.00	2.13	0.16	15.24	0.41	36.85
0.26	0.14	55.00	1.80	0.56	53.50	35.51	23.81	6.57	40.99	0.40	0.19	10.00	2.13	0.16	15.24	0.41	36.85
0.26	0.14	55.00	1.80	0.56	53.50	35.51	23.81	6.35	39.56	0.40	0.19	10.00	2.13	0.16	15.24	0.41	36.85
0.26	0.14	55.00	1.80	0.56	53.50	35.51	23.81	6.61	41.22	0.40	0.19	10.00	2.13	0.16	15.24	0.41	36.85
0.37	0.20	55.00	1.85	0.81	77.33	24.57	73.40	5.32	95.00	0.14	0.07	10.00	2.03	0.06	5.32	0.09	24.20
0.37	0.20	55.00	1.85	0.81	77.33	24.57	73.40	5.32	95.00	0.14	0.07	10.00	2.03	0.06	5.32	0.09	24.20
0.37	0.20	55.00	1.85	0.81	77.33	24.57	73.40	5.32	95.00	0.14	0.07	10.00	2.03	0.06	5.32	0.09	24.20
0.37	0.20	55.00	1.85	0.81	77.33	24.57	73.40	5.32	95.00	0.14	0.07	10.00	2.03	0.06	5.32	0.09	24.20
0.37	0.20	55.00	1.85	0.81	77.33	24.57	73.40	5.32	95.00	0.14	0.07	10.00	2.03	0.06	5.32	0.09	24.20
0.37	0.20	55.00	1.85	0.81	77.33	24.57	73.40	5.32	95.00	0.14	0.07	10.00	2.03	0.06	5.32	0.09	24.20
0.37	0.20	55.00	1.85	0.81	77.33	24.57	73.40	5.32	95.00	0.14	0.07	10.00	2.03	0.06	5.32	0.09	24.20
0.37	0.20	55.00	1.85	0.81	77.33	24.57	73.40	5.32	95.00	0.14	0.07	10.00	2.03	0.06	5.32	0.09	24.20
0.34	0.18	55.00	1.92	0.75	71.06	26.74	70.93	4.42	72.22	0.15	0.09	10.00	1.80	0.06	5.81	0.14	33.21
0.34	0.18	55.00	1.92	0.75	71.06	26.74	70.93	5.81	95.00	0.15	0.09	10.00	1.80	0.06	5.81	0.14	33.21
0.34	0.18	55.00	1.92	0.75	71.06	26.74	70.93	5.81	95.00	0.15	0.09	10.00	1.80	0.06	5.81	0.14	33.21
0.34	0.18	55.00	1.92	0.75	71.06	26.74	70.93	5.81	95.00	0.15	0.09	10.00	1.80	0.06	5.81	0.14	33.21
0.34	0.18	55.00	1.92	0.75	71.06	26.74	70.93	2.58	42.22	0.15	0.09	10.00	1.80	0.06	5.81	0.14	33.21
0.34	0.18	55.00	1.92	0.75	71.06	26.74	70.93	3.53	57.75	0.15	0.09	10.00	1.80	0.06	5.81	0.14	33.21

A260	A280	Dilution	Ratio	Start con	Start µg	20µg vol	Loss RNA	RNA to combine	Vol to combine	A260	A280	Dilution	Ratio	RNA con	Yield	A650	Dye Incorporation	
0.33	0.17	55.00	1.90	0.73	69.46	28.33	48.23	8.57	82.18	0.27	0.13	10.00	2.02	0.11	10.35	0.20	26.38	MEAN
0.06	0.03	0.00	0.09	0.14	13.44	5.32	20.65	3.53	20.70	0.11	0.05	0.00	0.17	0.04	4.13	0.12	8.58	SD
0.26	0.14	55.00	1.80	0.56	53.50	15.59	11.27	2.58	26.30	0.14	0.07	10.00	1.77	0.06	5.32	0.09	12.73	RANGE
0.58	0.30	55.00	2.14	1.28	121.85	35.51	73.40	15.54	95.00	0.47	0.24	10.00	2.23	0.19	17.75	0.41	36.85	

13.3 CLASS COMPARISON STUDIES FOR HOST MESOTHELIAL CELLS

GENE NUMBER	GENE ID	DESCRIPTION	PERITONEUM	HT 29	SW 480	TMK	KATO	PARAMETRIC p-VALUE
1	NM_001444	fatty acid binding protein 5 psoriasis-associated; fabp5	16.24	0.39	3.62	3.84	14.61	< 1e-07
2	NM_000249	mutl homolog 1; mlh1	5.60	0.64	1.00	1.14	3.30	< 1e-07
3	NM_007029	superiorcervical ganglia neural specific 10; stmn2	0.55	0.12	4.18	0.61	6.28	< 1e-07
4	NM_080734	wap four-disulfide core domain 2 isoform 4; wfdc2	1.40	3.12	0.78	1.58	0.29	< 1e-07
5	NM_004219	pituitary tumor-transforming protein 1; pttg1	2.74	3.21	0.78	1.18	4.11	< 1e-07
6	NM_003472	dek oncogene dna binding;	0.24	1.21	0.63	2.09	3.51	1.00E-07
7	NM_002354	tumor-associated calcium signal transducer 1; tacstd1	4.59	5.97	0.87	2.28	4.30	1.00E-07
8	NM_002870	rab13 member ras oncogene family;	1.67	0.74	0.31	0.86	0.75	2.00E-07
9	NM_002451	5'-methylthioadenosine phosphorylase; mtap	1.12	0.80	0.38	1.59	1.53	2.00E-07
10	NM_000401	exostoses multiple 2; ext2	1.39	0.40	1.87	1.47	1.93	3.00E-07
11	NM_000611	cd59 antigen p18-20 identified by monoclonal antibodies 16.3a5 ej16 ej30 el32 and g344 cd59.	2.97	0.26	0.45	0.61	2.99	3.00E-07
12	NM_002520	nucleophosmin nucleolar phosphoprotein b23 numatrin; npm1	5.11	1.46	0.80	1.01	4.11	8.00E-07
13	NM_000041	apolipoprotein e; apoe	2.60	2.56	8.36	4.05	3.78	9.00E-07
14	NM_006838	methionyl aminopeptidase 2; metap2	2.26	1.27	0.33	1.23	1.61	1.00E-06
15	NM_003130	sorcin; sri	1.58	0.57	0.54	1.16	2.52	1.20E-06
16	NM_007038	a disintegrin and metalloprotease with thrombospondin motifs-5; adamts5	1.03	0.58	0.29	0.57	1.10	1.30E-06
17	NM_014453	putative breast adenocarcinoma marker 32kd; bc-2	0.56	0.33	0.32	0.63	2.88	1.50E-06
18	NM_000090	alpha type iii collagen; col3a1	0.25	0.67	0.17	2.30	1.59	1.60E-06
19	XM_087218	similar to tropomyosin cytoskeletal type tm30-nm; loc151471	1.84	0.70	2.12	2.81	3.47	2.20E-06

GENE NUMBER	GENE ID	DESCRIPTION	PERITONEUM	HT 29	SW 480	TMK	KATO	PARAMETRIC p-VALUE
20	NM_004486	golgi autoantigen golgin subfamily a 2; golga2	1.03	0.28	4.81	0.57	3.53	2.20E-06
21	NM_001757	carbonyl reductase 1; cbr1	1.36	0.54	1.83	1.79	1.84	2.40E-06
22	NM_006519	t-complex-associated-testis-expressed 1-like 1; tctel1	3.40	0.80	0.91	2.25	8.68	2.50E-06
23	NM_018678	lipopolysaccharide specific response-68 protein; lsr68	2.65	0.96	4.29	5.30	4.11	2.70E-06
24	NM_004585	retinoic acid receptor responder tazarotene induced 3; rarres3	0.53	1.05	1.74	4.79	3.98	3.10E-06
25	NM_012325	microtubule-associated protein rpeb family member 1; mapre1	2.51	0.43	1.87	2.86	2.74	3.20E-06
26	NM_001553	insulin-like growth factor binding protein 7; igfbp7	1.28	0.73	1.72	2.76	0.87	5.70E-06
27	NM_005798	ret finger protein 2; rfp2	0.31	0.87	2.83	1.11	2.81	5.90E-06
28	NM_003732	eukaryotic translation initiation factor 4e binding protein 3; eif4ebp3	0.42	0.68	2.58	1.67	0.77	6.90E-06
29	NM_002592	proliferating cell nuclear antigen; pcna	3.34	1.75	0.56	3.07	4.86	7.20E-06
30	NM_000666	aminoacylase 1; acy1	1.64	3.95	6.66	7.20	5.14	8.40E-06
31	NM_004181	ubiquitin carboxyl-terminal esterase l1 thiolesterase; uchl1	1.17	1.14	2.26	2.10	6.72	8.40E-06
32	NM_000026	adenylosuccinate lyase; adsl	0.30	0.24	0.87	0.27	1.87	9.50E-06
33	NM_080426	guanine nucleotide binding protein g alpha stimulating activity polypeptide isoform alpha-s-1; gnas	3.40	0.88	8.08	2.98	7.97	1.25E-05
34	NM_001321	cysteine and glycine-rich protein 2; csrp2	4.24	1.34	0.84	0.88	6.11	1.37E-05
35	NM_006207	platelet-derived growth factor receptor-like protein; pdgfrl	0.29	0.17	1.62	0.96	2.15	1.37E-05
36	XM_002964	downregulated in ovarian cancer 1; doc1	0.72	0.66	0.23	0.73	0.85	1.43E-05
37	NM_006428	melanoma-associated antigen recognised by t lymphocytes; maat1	1.94	0.59	2.14	1.61	2.28	1.82E-05
38	NM_002291	laminin beta 1; lamb1	0.10	0.23	0.19	0.21	0.84	1.88E-05

GENE NUMBER	GENE ID	DESCRIPTION	PERITONEUM	HT 29	SW 480	TMK	KATO	PARAMETRIC p-VALUE
39	NM_003358	ceramide glucosyltransferase; ugcg	0.62	0.97	2.17	0.67	0.51	2.07E-05
40	NM_006625	tls-associated serine-arginine protein isoform 1; fusip1	1.90	1.88	0.78	1.12	1.11	2.34E-05
41	NM_001299	calponin basic smooth muscle; cnn1	2.46	1.55	5.05	2.57	3.52	2.49E-05
42	NM_033453	inosine triphosphatase nucleoside triphosphate pyrophosphatase; itpa	2.02	0.43	1.47	1.42	1.58	2.54E-05
43	NM_012449	six transmembrane epithelial antigen of the prostate; steap	NA	0.43	0.12	0.33	0.78	2.70E-05
44	NM_004175	small nuclear ribonucleoprotein d3 polypeptide 18kd; snrpd3	1.02	0.48	0.30	1.12	3.41	3.07E-05
45	NM_003072	swisnf related matrix associated actin dependent regulator of chromatin subfamily a member 4; smarca4	0.71	1.49	2.06	1.38	3.47	3.29E-05
46	NM_001150	membrane alanine aminopeptidase; anpep	1.33	1.01	3.66	1.65	3.30	3.56E-05
47	NM_030666	serine or cysteine proteinase inhibitor clade b ovalbumin member 1; serpinb1	3.52	0.30	0.13	0.41	0.84	3.62E-05
48	NM_001803	cdw52 antigen campath-1 antigen;	1.35	2.23	3.30	3.22	2.32	3.68E-05
49	NM_001912	cathepsin l; ctsl	3.73	1.08	3.90	2.87	4.98	4.73E-05
50	NM_002568	polya binding protein cytoplasmic 1; pabpc1	1.22	0.28	1.59	0.44	0.24	6.93E-05
51	NM_002276	keratin 19; krt19	0.33	1.46	0.34	0.66	1.00	8.41E-05
52	NM_002951	ribophorin ii; rpn2	0.97	0.55	0.49	1.20	3.17	9.19E-05
53	NM_006397	ribonuclease hi large subunit; rnasehi	0.18	0.22	0.19	0.53	1.26	0.0001
54	NM_001983	excision repair cross-complementing rodent deficiency complementation group includes overlapping antisense sequence; ercc1	0.93	0.47	0.76	0.60	1.22	0.0001
55	NM_005053	rad23 s. cerevisiae homolog a; rad23a	2.92	0.80	2.47	2.50	3.42	0.0001
56	NM_018412	suppression of tumorigenicity 7 isoform a; st7	1.05	0.82	2.63	1.92	1.59	0.0001

GENE NUMBER	GENE ID	DESCRIPTION	PERITONEUM	HT 29	SW 480	TMK	KATO	PARAMETRIC p-VALUE
57	NM_001792	cadherin type 1; cdh2	1.75	1.29	0.87	2.05	1.66	0.0001
58	NM_004126	guanine nucleotide binding protein 11; gng11	1.11	0.63	0.06	0.96	1.30	0.0001
59	X61498	nf-kb subunit	1.86	2.03	1.91	1.24	0.96	0.0001
60	NM_006087	tubulin beta 5; tubb5	2.24	0.96	1.75	2.80	4.75	0.0001
61	NM_001928	adipsincomplement factor d; df	0.47	1.15	5.48	1.75	4.78	0.0002
62	NM_002228	v-jun avian sarcoma virus 17 oncogene homolog; jun	0.55	3.55	8.85	2.28	5.39	0.0002
63	NM_004294	mitochondrial translational release factor 1; mtrf1	0.85	0.40	0.20	0.63	0.69	0.0002
64	NM_001731	b-cell translocation protein 1; btg1	1.73	1.94	0.68	0.53	0.10	0.0002
65	NM_001527	histone deacetylase 2; hdac2	3.19	3.09	0.59	1.94	1.50	0.0002
66	NM_003348	ubiquitin-conjugating enzyme e2n homologous to yeast ubc13; ube2n	4.32	1.80	2.65	4.55	4.31	0.0002
67	NM_003172	surfeit 1; surf1	0.61	0.30	1.22	1.33	2.20	0.0002
68	NM_017627	hypothetical protein flj20030; flj20030	0.53	0.66	1.10	0.54	3.40	0.0002
69	NM_002975	stem cell growth factor; lymphocyte secreted c-type lectin scgf.	0.37	0.63	0.44	0.51	1.34	0.0002
70	NM_004651	ubiquitin carboxyl-terminal hydrolase x-linked; usp11	1.88	1.53	1.69	1.39	0.41	0.0002
71	NM_001012	ribosomal protein s8; rps8	0.54	0.45	1.12	0.53	0.76	0.0002
72	NM_002643	phosphatidylinositol glycan class f; pigf	5.67	2.53	1.92	2.54	5.51	0.0002
73	NM_006640	mll septin-like fusion; msf	0.93	0.31	1.08	0.80	1.18	0.0003
74	NM_004039	annexin a2; anxa2	1.73	0.50	0.96	1.18	2.70	0.0003
75	NM_012222	muty homolog e. coli; mutyh	1.35	0.31	2.65	1.85	1.66	0.0003
76	NM_018975	trf2-interacting telomeric rap1 protein;	0.24	2.66	0.65	2.77	3.53	0.0003
77	NM_000062	complement component inhibitor; serping1	0.50	1.24	1.67	1.99	1.46	0.0003
78	NM_080648	apex nuclease;	1.64	0.44	2.50	2.50	3.25	0.0003
79	NM_002024	fragile x mental retardation 1; fmr1	1.02	0.31	1.24	0.45	0.25	0.0003

GENE NUMBER	GENE ID	DESCRIPTION	PERITONEUM	HT 29	SW 480	TMK	KATO	PARAMETRIC p-VALUE
80	NM_033011	plasminogen activator tissue type isoform 3; plat	1.18	1.06	0.46	0.90	1.12	0.0003
81	NM_002036	duffy blood group; fy	0.77	2.15	2.81	1.74	2.68	0.0003
82	NM_000729	cholecystokinin 8; cck	2.39	3.52	7.55	5.58	4.94	0.0004
83	NM_006904	protein kinase dna-activated catalytic polypeptide; prkdc	1.48	1.03	0.47	1.26	1.08	0.0004
84	NM_003352	ubiquitin-like sentrin; ubl1	3.80	3.43	0.18	3.37	4.40	0.0004
85	NM_000089	alpha 2 type i collagen; col1a2	0.11	0.23	0.16	0.48	0.45	0.0004
86	NM_052815	immediate early response 3 isoform long; ier3	1.79	1.53	1.31	0.58	0.70	0.0005
87	NM_007110	telomerase-associated protein 1; tep1	0.34	0.64	0.22	NA	0.69	0.0005
88	NM_005954	metallothionein 3 growth inhibitory factor neurotrophic; mt3	1.30	3.33	3.37	1.72	1.03	0.0005
89	NM_004064	cyclin-dependent kinase inhibitor 1b; cdkn1b	0.31	1.25	2.03	2.10	1.28	0.0005
90	NM_000858	guanylate kinase 1; guk1	0.45	0.46	0.86	0.47	0.29	0.0005
91	K00558	Alpha tubulin; replicated spot	3.51	1.50	2.01	2.51	5.73	0.0006
92	K00558	Alpha tubulin_2; replicated spot	4.06	1.72	2.31	3.04	5.69	0.0006
93	NM_000624	protein c inhibitor; serpina5	5.13	6.60	8.04	11.46	0.78	0.0006
94	NM_016252	baculoviral iap repeat-containing apollon; birc6	1.75	0.59	2.23	1.07	1.66	0.0006
95	NM_001769	cd9 antigen p24;	7.48	4.46	2.08	3.46	5.51	0.0006
96	XM_045689	similar to thymosin beta chromosome loc159066.	2.07	0.71	0.82	1.39	1.11	0.0007
97	AF381999_2	haplotype n1b mitochondrion complete genome	2.04	3.70	6.39	4.39	3.17	0.0007
98	NM_014297	protein expressed in thyroid; yf13h12	0.53	1.07	1.32	0.48	2.00	0.0007
99	NM_004939	deadh asp-glu-ala-asphis box polypeptide 1; ddx1	2.16	0.44	0.66	1.85	3.67	0.0007
100	K00558	Alpha tubulin; replicated spot	5.50	1.95	2.28	3.40	7.26	0.0008
101	NM_004318	aspartate beta-hydroxylase isoform a; asph	0.86	1.46	1.05	0.69	0.41	0.0008
102	NM_002443	microseminoprotein beta-; msmb	1.60	3.47	5.08	5.96	5.03	0.0008

GENE NUMBER	GENE ID	DESCRIPTION	PERITONEUM	HT 29	SW 480	TMK	KATO	PARAMETRIC p-VALUE
103	NM_001735	complement component 5; c5	0.41	0.15	0.84	0.57	NA	0.0008
104	NM_002166	inhibitor of dna binding dominant negative helix-loop-helix protein; id2	2.59	0.70	1.12	3.51	3.86	0.0009

13.4 CLASS COMPARISON STUDIES FOR CANCER CELLS

GENE NUMBER	GENE ID	DESCRIPTION	HT 29	SW 480	TMK	KATO	PARAMETRIC p-VALUE
1	NM_000396	cathepsin k pycnodysostosis; ctsk	0.16	0.16	1.90	0.13	< 1e-07
2	NM_006545	homologous to yeast nitrogen permease candidate tumor suppressor; npr2l	0.92	1.33	0.21	2.88	< 1e-07
3	NM_000090	alpha type iii collagen; col3a1	0.90	0.12	3.64	1.75	< 1e-07
4	NM_002167	inhibitor of dna binding 3 dominant negative helix-loop-helix protein; id3	7.66	0.51	8.09	1.28	< 1e-07
5	NM_000700	annexin i; anxa1	0.38	0.15	2.33	1.88	< 1e-07
6	NM_080734	Wap four-disulfide core domain 2 isoform 4; wfdc2	1.25	0.78	0.27	2.17	< 1e-07
7	NM_002276	keratin 19; krt19	0.43	0.24	0.22	1.60	< 1e-07
8	NM_006516	solute carrier family 2 facilitated glucose transporter member 1; slc2a1	0.26	0.67	0.17	1.57	< 1e-07
9	XM_045689	similar to thymosin beta chromosome loc159066.	1.23	0.33	4.16	1.83	< 1e-07
10	NM_004486	golgi autoantigen golgin subfamily a 2; golga2	0.35	2.82	0.96	1.08	< 1e-07
11	NM_003072	swisnf related matrix associated actin dependent regulator of chromatin subfamily a member 4; smarca4	3.45	0.88	2.53	4.37	< 1e-07
12	NM_002412	o-6-methylguanine-dna methyltransferase; mgmt	1.01	0.96	5.51	1.23	< 1e-07
13	NM_004048	beta-2-microglobulin; b2m	6.56	0.86	7.37	13.03	1.00E-07
14	NM_001020	ribosomal protein s16; rps16	0.40	0.30	0.26	1.66	1.00E-07
15	NM_003979	retinoic acid induced 3; rai3	0.23	0.21	1.10	0.19	1.00E-07
16	NM_005077	transducin-like enhancer of split esp1 homolog drosophila; tle1	0.30	2.47	3.95	1.08	1.00E-07
17	NM_001997	ribosomal protein s30; fau	0.46	1.14	0.39	1.44	2.00E-07
18	NM_000089	alpha 2 type i collagen; col1a2	0.30	0.09	1.78	0.31	2.00E-07
19	NM_002376	mapmicrotubule affinity-regulating kinase 3; mark3	0.13	3.16	2.71	2.93	2.00E-07
20	NM_012325	microtubule-associated protein rpeb family member 1; mapre1	0.23	3.02	1.79	1.01	6.00E-07
21	NM_001988	envoplakin; evpl	0.90	0.72	0.38	1.07	6.00E-07
22	NM_000325	paired-like homeodomain transcription factor 2; pitx2	0.57	0.57	0.29	0.93	7.00E-07
23	NM_001321	cysteine and glycine-rich protein 2; csrp2	4.61	0.94	2.78	4.20	1.40E-06
24	NM_006397	ribonuclease hi large subunit; rnasehi	1.36	0.23	0.79	1.03	1.70E-06

GENE NUMBER	GENE ID	DESCRIPTION	HT 29	SW 480	TMK	KATO	PARAMETRIC p-VALUE
25	NM_002871	rab interacting factor; rabif	3.06	1.85	6.81	6.49	2.00E-06
26	BC008442	similar to transmembrane superfamily member clone mgc:14656 image:4101110	1.78	1.20	3.28	3.99	2.10E-06
27	NM_003472	Dek oncogene dna binding;	0.16	0.50	1.55	1.93	2.10E-06
28	NM_080648	apex nuclease;	0.48	2.46	6.13	1.02	2.60E-06
29	NM_000638	vitronectin; vtn	1.76	0.64	1.76	1.10	2.70E-06
30	NM_000969	ribosomal protein l5; rpl5	1.01	0.36	0.74	3.72	2.80E-06
31	NM_001553	insulin-like growth factor binding protein 7; igfbp7	1.24	0.95	12.40	0.87	3.50E-06
32	NM_003793	cathepsin f; ctsf	0.63	1.73	2.12	0.36	4.10E-06
33	NM_032960	mitogen-activated protein kinase-activated kinase isoform 2; mapkapk2	0.71	0.65	0.33	0.94	4.20E-06
34	NM_001175	rho gdp dissociation inhibitor gdi beta; arhgdib	0.58	1.38	0.54	1.72	4.90E-06
35	NM_002848	receptor-type protein tyrosine phosphatase o isoform b; ptpro	0.40	1.07	0.32	1.24	5.40E-06
36	NM_002847	protein tyrosine phosphatase receptor type polypeptide 2; ptprn2	1.06	1.57	0.48	2.00	5.50E-06
37	NM_002178	insulin-like growth factor binding protein 6; igfbp6	0.40	0.43	0.39	3.60	6.90E-06
38	NM_003255	tissue inhibitor of metalloproteinase 2; timp2	1.15	1.13	0.56	1.75	7.00E-06
39	NM_033011	plasminogen activator tissue type isoform 3; plat	1.31	0.46	1.39	1.06	7.10E-06
40	NM_001675	activating transcription factor 4; atf4	0.20	0.12	0.13	0.96	7.30E-06
41	NM_003379	villin 2; vil2	1.00	1.63	0.47	1.24	7.40E-06
42	NM_000190	hydroxymethylbilane synthase; hmbs	0.46	0.88	0.32	1.31	8.30E-06
43	NM_001192	b-cell maturation factor; tnfrsf17	0.17	0.21	0.85	0.14	8.50E-06
44	NM_018487	hepatocellular carcinoma-associated antigen 112; hca112	1.05	2.57	4.16	3.87	9.30E-06
45	NM_002899	retinol-binding protein cellular; rbp1	0.40	0.51	0.18	2.83	9.40E-06
46	NM_000903	nadph menadione oxidoreductase dioxin-inducible; nqo1	0.17	0.46	0.38	1.34	9.80E-06
47	M26880	ubiquitin; replicated spot	1.13	1.32	0.73	2.61	9.90E-06
48	NM_002228	v-jun avian sarcoma virus 17 oncogene homolog; jun	1.21	0.89	1.35	10.87	1.16E-05
49	NM_001363	dyskerin; dkc1	0.69	0.49	1.38	1.88	1.16E-05

GENE NUMBER	GENE ID	DESCRIPTION	HT 29	SW 480	TMK	KATO	PARAMETRIC p-VALUE
50	NM_006986	melanoma antigen family d 1; maged1	0.75	0.52	1.68	1.52	1.29E-05
51	NM_001404	eukaryotic translation elongation factor gamma; eef1g	0.88	0.40	0.58	2.60	1.35E-05
52	NM_000591	cd14 antigen mature peptide;	1.45	0.78	2.06	0.52	1.47E-05
53	NM_000062	complement component inhibitor; serping1	2.29	0.49	4.14	3.99	1.83E-05
54	NM_006902	paired mesoderm homeobox isoform pmx-1a; pmx1	1.42	1.43	2.72	0.88	1.86E-05
55	NM_001640	n-acylaminoacyl-peptide hydrolase; apeh	1.28	0.68	0.53	1.58	1.94E-05
56	NM_003150	signal transducer and activator of transcription acute-phase response factor; stat3	0.84	1.80	2.25	0.86	2.11E-05
57	M26880	ubiquitin; replicated spot	1.01	1.10	0.75	2.35	2.13E-05
58	NM_007218	patched related protein translocated in renal cancer; trc8	0.98	0.57	0.47	1.81	2.16E-05
59	NM_006283	transforming acidic coiled-coil containing protein 1; tacc1	2.84	1.08	3.46	3.22	2.23E-05
60	NM_019102	homeobox protein hox-1.3; hoxa5	0.55	2.46	1.14	1.03	2.44E-05
61	NM_001010	ribosomal protein s6; rps6	0.21	0.15	0.22	0.66	2.59E-05
62	NM_033018	pctaire protein kinase isoform a; pctk1	1.52	1.12	0.52	0.20	3.27E-05
63	NM_003579	rad54-like s. cerevisiae; rad54l	0.74	0.61	0.31	0.97	3.46E-05
64	NM_006149	galectin 4; lgals4	0.41	2.78	1.40	0.66	3.58E-05
65	NM_004905	anti-oxidant protein 2 non-selenium glutathione peroxidase aci; kiaa0106	4.08	1.52	1.47	3.52	3.72E-05
66	NM_005798	ret finger protein 2; rfp2	0.90	0.41	1.38	4.40	4.01E-05
67	NM_001554	cysteine-rich angiogenic inducer 61; cyr61	1.58	2.68	2.74	0.50	4.76E-05
68	NM_002211	integrin beta subunit; itgb1	1.88	1.04	3.88	0.91	4.77E-05
69	NM_003380	vimentin; vim	0.21	0.26	1.01	0.16	5.04E-05
70	NM_012306	lifeguard; kiaa0950	3.40	3.31	3.87	0.82	5.10E-05
71	NM_006087	tubulin beta 5; tubb5	3.26	1.56	3.59	0.84	5.17E-05
72	NM_000610	cd44 antigen homing function and indian blood group system;	0.57	0.99	0.39	1.22	5.26E-05
73	NM_001066	tumor necrosis factor receptor 2 75kd; tnfrsf1b	0.68	1.07	1.32	0.39	5.38E-05
74	NM_003254	tissue inhibitor of metalloproteinase 1; timp1	0.15	0.14	0.39	0.13	5.77E-05
75	NM_000397	cytochrome b-245 beta polypeptide chronic granulomatous disease; cybb	1.38	1.34	0.77	2.27	6.25E-05

GENE NUMBER	GENE ID	DESCRIPTION	HT 29	SW 480	TMK	KATO	PARAMETRIC p-VALUE
76	NM_032945	tumor necrosis factor receptor superfamily member 6b precursor isoform d; tnfrsf6b	0.92	0.68	0.33	0.95	6.37E-05
77	NM_000137	fumarylacetoacetase; fah	1.01	0.95	0.58	1.99	6.85E-05
78	NM_030756	transcription factor 7-like 2 t-cell specific hmg-box; tcf7l2	0.64	0.62	1.04	0.36	8.82E-05
79	NM_000602	plasminogen activator inhibitor-1 mature peptide; serpine1	0.14	0.56	0.17	0.34	9.33E-05
80	NM_006270	related ras viral r-ras oncogene homolog; rras	0.76	2.19	1.22	0.41	9.37E-05
81	NM_004902	rna-binding region rnp1 rrm containing 2; rnpc2	0.41	1.58	0.24	2.95	9.74E-05
82	X01677	glyceraldehyde-3-phosphate dehydrogenase (GAPDH) mRNA; complete cds; glyceraldehyde-3-phosphate dehydrogenase (EC 1.2.1.12); replicated spot	3.76	1.40	1.60	5.98	9.97E-05
83	X01677	glyceraldehyde-3-phosphate dehydrogenase (GAPDH) mRNA; complete cds; glyceraldehyde-3-phosphate dehydrogenase (EC 1.2.1.12)	3.58	1.37	1.50	5.33	0.0001
84	NM_006625	tls-associated serine-arginine protein isoform 1; fusip1	1.19	0.63	0.84	1.58	0.0001
85	NM_014297	protein expressed in thyroid; yf13h12	0.79	0.33	0.41	2.75	0.0001
86	NM_002226	jagged 2; jag2	0.37	0.12	0.86	0.41	0.0001
87	NM_004102	fatty acid binding protein 3; fabp3	1.28	1.16	2.92	0.80	0.0001
88	M26880	ubiquitin; replicated spot	1.18	1.25	0.78	2.52	0.0001
89	NM_006850	suppression of tumorigenicity 16 melanoma differentiation; il24	0.51	1.09	1.31	0.27	0.0001
90	NM_052815	immediate early response 3 isoform long; ier3	0.76	1.33	0.24	0.79	0.0001
91	NM_001753	caveolin 1; cav1	5.13	0.70	4.94	4.45	0.0001
92	X01677	glyceraldehyde-3-phosphate dehydrogenase (GAPDH) mRNA; complete cds; glyceraldehyde-3-phosphate dehydrogenase (EC 1.2.1.12); replicated spot	3.39	1.29	1.49	5.68	0.0002
93	M26880	ubiquitin; replicated spot	1.13	1.34	0.72	2.43	0.0002
94	NM_005978	s100 calcium-binding protein a2; s100a2	0.63	0.15	0.23	1.97	0.0002
95	NM_000983	ribosomal protein l22; rpl22	0.26	0.45	0.22	2.95	0.0002
96	NM_016155	matrix metalloproteinase 17; mmp17	0.91	0.95	0.48	1.01	0.0002
97	NM_001005	ribosomal protein s3; rps3	1.31	2.05	0.88	3.64	0.0002

GENE NUMBER	GENE ID	DESCRIPTION	HT 29	SW 480	TMK	KATO	PARAMETRIC p-VALUE
98	NM_006519	t-complex-associated-testis-expressed 1-like 1; tctel1	2.00	1.56	3.96	7.12	0.0002
99	NM_002291	laminin beta 1; lamb1	0.74	0.21	1.00	1.17	0.0002
100	NM_004460	fibroblast activation protein alpha subunit; fap	0.47	0.28	1.04	1.29	0.0002
101	NM_005248	gardner-rasheed feline sarcoma viral v-fgr oncogene homolog; fgr	0.24	0.34	1.05	0.48	0.0002
102	NM_002166	inhibitor of dna binding dominant negative helix-loop-helix protein; id2	1.05	2.62	2.35	0.99	0.0002
103	NM_006010	arginine-rich protein; armet	1.24	0.36	0.65	1.36	0.0002
104	NM_004339	pituitary tumor-transforming protein 1-interacting protein; pttg1ip	0.21	0.67	1.08	0.78	0.0002
105	NM_012105	beta-site app-cleaving enzyme 2; bace2	0.71	0.48	0.50	1.30	0.0002
106	NM_014555	transient receptor potential cation channel subfamily member 5; trpm5	0.87	0.35	0.83	0.72	0.0003
107	NM_003118	secreted protein acidic cysteine-rich osteonectin; sparc	2.88	2.23	5.36	1.86	0.0003
108	NM_017627	hypothetical protein flj20030; flj20030	0.73	0.57	0.44	1.71	0.0003
109	NM_004585	retinoic acid receptor responder tazarotene induced 3; rarres3	0.63	2.40	3.63	5.49	0.0003
110	NM_004449	v-ets erythroblastosis virus e26 oncogene like avian; erg	0.69	1.07	0.46	1.51	0.0003
111	NM_022118	cutaneous t-cell lymphoma tumor antigen se70-2; se70-2	0.27	0.27	0.28	0.89	0.0003
112	NM_003358	ceramide glucosyltransferase; ugcg	1.16	1.31	0.48	2.44	0.0004
113	NM_017534	myosin heavy polypeptide 2 skeletal muscle adult; myh2	0.55	0.47	0.30	1.20	0.0004
114	NM_005733	rab6 interacting kinesin-like rabkinesin6; rab6kifl	0.38	1.07	0.70	0.60	0.0004
115	NM_006024	tax1 t-cell leukemia virus type i binding protein 1; tax1bp1	0.53	1.15	0.44	2.21	0.0004
116	NM_004708	programmed cell death 5; pdcd5	0.42	0.33	1.08	0.40	0.0004
117	NM_001145	angiogenin; g00-119-679; ang	0.68	1.81	0.40	0.56	0.0004
118	X01677	glyceraldehyde-3-phosphate dehydrogenase (GAPDH) mRNA; complete cds; glyceraldehyde-3-phosphate dehydrogenase (EC 1.2.1.12); replicated spot	3.97	1.41	1.74	5.72	0.0004
119	NM_001634	s-adenosylmethionine decarboxylase alpha chain; amd1	3.73	0.79	1.24	2.16	0.0005
120	NM_003289	tropomyosin beta; tpm2	0.24	0.82	0.35	0.94	0.0006
121	NM_004618	topoisomerase dna iii alpha; top3a	0.85	0.62	0.47	0.92	0.0006

GENE NUMBER	GENE ID	DESCRIPTION	HT 29	SW 480	TMK	KATO	PARAMETRIC p-VALUE
122	NM_016520	hepatocellular carcinoma-associated antigen 59; loc51759	0.48	0.85	0.75	0.14	0.0006
123	NM_006197	pericentriolar material 1; pcm1	0.80	0.76	0.65	1.63	0.0006
124	NM_000207	proinsulin peptide a; ins	0.92	0.50	0.45	1.21	0.0007
125	NM_005063	stearoyl-coa desaturase delta-9-desaturase; scd	0.32	0.77	0.43	2.34	0.0007
126	NM_007275	lung cancer candidate; fus1	1.34	1.07	0.46	2.29	0.0007
127	NM_000938	dna directed rna polymerase ii polypeptide b; polr2b	0.82	0.08	0.42	4.54	0.0007
128	NM_000990	ribosomal protein l27a; rpl27a	0.32	0.24	0.29	0.88	0.0007
129	XM_087218	similar to tropomyosin cytoskeletal type tm30-nm; loc151471	2.82	3.04	3.47	0.79	0.0007
130	NM_000075	cyclin-dependent kinase 4 isoform 1; cdk4	1.46	0.64	0.80	2.03	0.0007
131	NM_004939	deadh asp-glu-ala-asphis box polypeptide 1; ddx1	1.28	1.50	3.52	0.24	0.0008
132	NM_007115	tumor necrosis factor alpha-induced protein 6; tnfaip6	0.77	0.25	0.74	0.65	0.0008
133	NM_002048	growth arrest-specific 1; gas1	0.92	1.34	0.80	1.72	0.0008
134	NM_030666	serine or cysteine proteinase inhibitor clade b ovalbumin member 1; serpinb1	0.29	0.32	0.29	0.99	0.0008
135	NM_006079	cbpp300-interacting transactivator with gluasp-rich carboxy-terminal domain 2; cited2	0.90	1.40	1.43	0.55	0.0008
136	NM_001948	dutp pyrophosphatase; dut	1.57	2.37	6.47	6.34	0.0009
137	NM_006793	antioxidant protein 1; prdx3	5.01	3.09	7.29	5.23	0.0009
138	NM_004217	serinethreonine kinase 12; stk12	0.62	0.40	0.37	0.80	0.0009
139	NM_001003	ribosomal protein p1; rplp1	1.44	0.99	1.05	5.33	0.0010

13.5 RT PCR DATA

13.5.1 CATHEPSIN K

Tables 23 A,B Ct values and ratios for cathepsin K expression in host mesothelial cells (A, samples; B, reference RNA)

A)

Host mesothelial cells Ct	Cathepsin K	GAPDH	Ratio	Cell group	Statistics	Values
HT 29 22	23.26	22.56	1.03	HT 29	Mean	1.03
HT 29 22	22.57	22.40	1.01		ST	0.02
HT 29 22	23.12	22.26	1.04			
Kato 10	29.14	18.82	1.55			
Kato 10	29.32	18.91	1.55			
Kato 10	28.91	18.82	1.54	KATO	Mean	1.40
Kato 34	28.41	22.42	1.27		ST	0.16
Kato 34	28.18	22.32	1.26			
Kato 34	28.08	22.63	1.24			
peritoneum 55	28.24	24.81	1.14	peritoneum	Mean	1.18
peritoneum 55	28.51	24.84	1.15		ST	0.03
peritoneum 55	28.86	24.66	1.17			
peritoneum53	25.6	21.05	1.22			
peritoneum53	25.52	21.04	1.21			
peritoneum53	25.37	20.97	1.21			
SW480 16	19.58	22.59	0.87	SW 480	Mean	1.07
SW480 40	25.75	22.44	1.15		ST	0.14
SW480 40	25.45	22.34	1.14			
SW480 40	26.12	22.97	1.14			
TMK 28	25.7	23.65	1.09	TMK	Mean	1.27
TMK 28	25.92	23.90	1.08		ST	0.17
TMK 52	27.08	18.94	1.43			
TMK 52	26.82	19.63	1.37			
TMK 52	27.02	19.52	1.38			

B)

Reference RNA	Dilutions	Cathepsin K	GAPDH	Ratio	Statistics	Values
2 D2	0.5	25.06	19.49	1.29		
3 D3	0.2	25.24	20.44	1.23		
4 D4	0.1	25.86	21.95	1.18	Mean	1.21
5 D5	0.05	26.69	22.6	1.18	ST	0.05
6 D6	0.02	27.73	23.57	1.18		
7 D7	0.01	28.27	24.52	1.15		
8 D8	0.005	30.36	26.07	1.16		
10 D2	0.5	23.84	18.3	1.30		
11 D3	0.2	25.77	20.36	1.27		
12 D4	0.1	26.97	21.45	1.26		
13 D5	0.05	27.1	22.19	1.22		
14 D6	0.02	27.62	23.24	1.19		
15 D7	0.01	29.21	24.45	1.19		
16 D8	0.005	30.39	25.58	1.19		
18 D2	0.5	24.21	18.73	1.29		
19 D3	0.2	25.62	20.3	1.26		
20 D4	0.1	26.46	21.47	1.23		
21 D5	0.05	27.03	22.06	1.23		
22 D6	0.02	28.03	23.5	1.19		
23 D7	0.01	28.85	24.62	1.17		
24 D8	0.005	29.91	25.65	1.17		
25 D9	0.002	31.42	27.04	1.16		
26 D9	0.002	31.76	27.52	1.15		
27 D9	0.002	31.41	26.98	1.16		

13.5.2 VIMENTIN

Tables 24 A,B Ct values and ratios for vimentin expression in host mesothelial cells (A, samples; B, reference RNA)

Reference RNA	Dilutions	Vimentin	GAPDH	Ratio	Statistics	Values
2 D2	0.5	19.13	17.83	1.07		
3 D3	0.2	20.62	19.47	1.06		
4 D4	0.1	21.05	19.46	1.08		
5 D5	0.05	22.24	20.98	1.06	Mean	1.07
6 D6	0.02	22.52	21.31	1.06	ST	0.01
7 D7	0.01	23.95	22.26	1.08		
8 D8	0.005	24.45	23.3	1.05		
10 D2	0.5	18.77	17.48	1.07		
11 D3	0.2	19.72	18.52	1.06		
12 D4	0.1	20.69	19.53	1.06		
13 D5	0.05	21.76	20.51	1.06		
14 D6	0.02	22.65	21.29	1.06		
15 D7	0.01	23.65	22.3	1.06		
16 D8	0.005	25.57	23.29	1.10		
Negative control			39.43	0		

Host mesothelial cells	Vimentin	GAPDH	Ratio	Cell group	Statistics	Values
HT 29 22	20.77	20.52	1.01	HT 29	Mean	1.02
HT 29 22	20.92	20.19	1.04		ST (*)	
Kato 10	21.28	17.17	1.24	Kato	Mean	1.21
Kato 10	20.64	16.97	1.22		ST	0.02
Kato 34	22.91	19.16	1.20			
Kato 34	24.04	20.11	1.20			
SW480 16	21.55	19.73	1.09	SW480	Mean	1.10
SW480 16	21.2	19.94	1.06		ST	0.03
SW480 40	22.93	20.29	1.13			
SW480 40	22.8	20.63	1.11			
TMK 28	22.54	21.38	1.05	TMK	Mean	1.05
TMK 28	22.16	21.03	1.05		ST	0.02
TMK 52	18.48	17.23	1.07			
TMK 52	18.12	17.54	1.03			

14 REFERENCE LIST

Reference List

1. R.M.H.McMinn. Last's Anatomy. 312-315. 1994.
   Ref Type: Generic

2. Stylianou, E., Jenner, L. A., Davies, M., Coles, G. A., Williams, J. D., 1990. Isolation, culture and characterization of human peritoneal mesothelial cells. Kidney Int. 37, 1563-1570.

3. Jayne, D. G., 2003. The molecular biology of peritoneal carcinomatosis from gastrointestinal cancer. Ann.Acad.Med.Singapore 32, 219-225.

4. Yoshikawa, T., Kanari, M., Tsuburaya, A., Kobayashi, O., Sairenji, M., Motohashi, H., Noguchi, Y., 2003a. Should gastric cancer with peritoneal metastasis be treated surgically? Hepatogastroenterology 50, 1712-1715.

5. Yoshikawa, T., Kanari, M., Tsuburaya, A., Kobayashi, O., Sairenji, M., Motohashi, H., Noguchi, Y., 2003b. Should gastric cancer with peritoneal metastasis be treated surgically? Hepatogastroenterology 50, 1712-1715.

6. Kobayashi, O., Tsuburaya, A., Yoshikawa, T., Osaragi, T., Murakami, H., Yoshida, T., Sairenji, M., 2006. The efficacy of gastrectomy for large gastric cancer. Int.J.Clin.Oncol. 11, 44-50.

7. Culliford, A. T., Brooks, A. D., Sharma, S., Saltz, L. B., Schwartz, G. K., O'Reilly, E. M., Ilson, D. H., Kemeny, N. E., Kelsen, D. P., Guillem, J. G., Wong, W. D., Cohen, A. M., Paty, P. B., 2001. Surgical debulking and intraperitoneal chemotherapy for established peritoneal metastases from colon and appendix cancer. Ann.Surg.Oncol. 8, 787-795.

8. Nakao, A., Fujii, T., Sugimoto, H., Kanazumi, N., Nomoto, S., Kodera, Y., Inoue, S., Takeda, S., 2006. Oncological problems in pancreatic cancer surgery. World J.Gastroenterol. 12, 4466-4472.

9. Chau, I., Norman, A. R., Cunningham, D., Waters, J. S., Oates, J., Ross, P. J., 2004. Multivariate Prognostic Factor Analysis in Locally Advanced and Metastatic Esophago-Gastric Cancer--Pooled Analysis From Three Multicenter, Randomized, Controlled Trials Using Individual Patient Data. J Clin Oncol 22, 2395-2403.

10. Shiraishi, N., Sato, K., Yasuda, K., Inomata, M., Kitano, S., 2007. Multivariate prognostic study on large gastric cancer. J Surg.Oncol 96, 14-18.

11. Assersohn, L., Norman, A., Cunningham, D., Benepal, T., Ross, P. J., Oates, J., 1999. Influence of metastatic site as an additional predictor for response and outcome in advanced colorectal carcinoma. Br.J Cancer 79, 1800-1805.

12. Mahteme, H., Hansson, J., Berglund, A., Pahlman, L., Glimelius, B., Nygren, P., Graf, W., 2004. Improved survival in patients with peritoneal metastases from colorectal cancer: a preliminary study. Br.J Cancer 90, 403-407.

13. Yonemori, K., Okusaka, T., Ueno, H., Morizane, C., Takesako, Y., Ikeda, M., 2007. FP therapy for controlling malignant ascites in advanced pancreatic cancer patients. Hepatogastroenterology 54, 2383-2386.

14. Dorudi, S., Steele, R. J., McArdle, C. S., 2002. Surgery for colorectal cancer. Br.Med.Bull. 64, 101-118.

15. Dicken, B. J., Bigam, D. L., Cass, C., Mackey, J. R., Joy, A. A., Hamilton, S. M., 2005. Gastric adenocarcinoma: review and considerations for future directions. Ann.Surg. 241, 27-39.

16. Fitzgerald, R. C., 2004. Review article: Barrett's oesophagus and associated adenocarcinoma--a UK perspective. Aliment.Pharmacol.Ther. 20 Suppl 8, 45-49.

17. Ilson, D. H., 2003. Oesophageal cancer: new developments in systemic therapy. Cancer Treat.Rev. 29, 525-532.

18. Alexakis, N., Halloran, C., Raraty, M., Ghaneh, P., Sutton, R., Neoptolemos, J. P., 2004. Current standards of surgery for pancreatic cancer. Br.J Surg. 91, 1410-1427.

19. Bray, F., Loos, A. H., Tognazzo, S., La, V. C., 2005. Ovarian cancer in Europe: Cross-sectional trends in incidence and mortality in 28 countries, 1953-2000. Int.J Cancer 113, 977-990.

20. Bertone-Johnson, E. R., 2005. Epidemiology of ovarian cancer: a status report. Lancet 365, 101-102.

21. Parkin, D. M., Bray, F., Ferlay, J., Pisani, P., 2005. Global cancer statistics, 2002. CA Cancer J Clin. 55, 74-108.

22. Ozols, R. F., 2005. Treatment goals in ovarian cancer. Int.J Gynecol.Cancer 15 Suppl 1, 3-11.

23. Sasaki, T., 2003. Current topics of S-1 at the 74th Japanese Gastric Cancer Congress. Gastric.Cancer 6 Suppl 1, 9-12.

24. Kitamura, Y., Hayashi, K., Sasagawa, T., Oguma, H., Takasaki, K., 2003. Pilot study of S-1 in patients with disseminated gastric cancer. Drugs Exp.Clin.Res. 29, 125-130.

25. Tamura, S., Miki, H., Nakata, K., Kim, C., Takiuchi, D., Okada, K., Okamura, S., Aihara, T., Sugimoto, K., Ohzato, H., Tomita, N., Takatsuka, Y., 2006. [A case of recurrent gastric cancer with peritoneal dissemination successfully treated over 1 year 8 months with combined chemotherapy of paclitaxel and TS-1]. Gan To Kagaku Ryoho 33, 255-257.

26. Kobayashi, O., Konishi, K., Kanari, M., Cho, H., Yoshikawa, T., Tsuburaya, A., Sairenji, M., Motohashi, H., 2002. Unusual survival for more than 2 years with peritoneal metastases of gastric cancer. Gastric.Cancer 5, 47-50.

27. Ishizone, S., Maruta, F., Saito, H., Koide, N., Sugiyama, A., Nakayama, J., Miyagawa, S., 2006. Efficacy of S-1 for patients with peritoneal metastasis of gastric cancer. Chemotherapy 52, 301-307.

28. Saikawa, Y., Kubota, T., Kumagai, K., Nakamura, R., Kumai, K., Shigematsu, N., Kubo, A., Kitajima, M., Kitagawa, Y., 2008. Phase II study of chemoradiotherapy with S-1 and low-dose cisplatin for inoperable advanced gastric cancer. Int.J Radiat.Oncol Biol.Phys. 71, 173-179.

29. Fukasawa, T., Shoji, T., Gotoh, H., Taniwaka, K., 2006. [A long-term survivor with stage IV gastric cancer due to postoperative weekly paclitaxel and 5'-DFUR combination therapy]. Gan To Kagaku Ryoho 33, 235-238.

30. Yokoyama, K., Tazawa, Y., Suzuki, I., Aoki, Y., Shiramatsu, K., Kobayashi, J., Morishima, Y., Kobayashi, N., Toyoda, Y., Fukada, T., Horiguchi, K., Yamamoto, K., Nakano, M., Miyazaki, M., 2005. [A case of non-curatively resected scirrhous gastric cancer successfully treated over 2 years with weekly administration of paclitaxel]. Gan To Kagaku Ryoho 32, 385-387.

31. Takiuchi, H., Goto, M., Imamura, H., Furukawa, H., Imano, M., Imamoto, H., Kimura, Y., Ishida, H., Fujitani, K., Narahara, H., Shimokawa, T., 2008. Multi-center phase II study for combination therapy with paclitaxel/doxifluridine to treat advanced/recurrent gastric cancer showing resistance to S-1 (OGSG 0302). Jpn.J Clin Oncol 38, 176-181.

32. Kim, J. Y., Bae, H. S., 2001. A controlled clinical study of serosa-invasive gastric carcinoma patients who underwent surgery plus intraperitoneal hyperthermo-chemo-perfusion (IHCP). Gastric.Cancer 4, 27-33.

33. Yonemura, Y., Kawamura, T., Bando, E., Takahashi, S., Sawa, T., Yoshimitsu, Y., Obata, T., Endo, Y., Sasaki, T., Sugarbaker, P. H., 2004.

[Treatment results of peritoneal dissemination from gastric cancer by neoadjuvant intraperitoneal-systemic chemotherapy]. Gan To Kagaku Ryoho 31, 1723-1726.

34. Meyer, T., Hart, I. R., 1998. Mechanisms of tumour metastasis. Eur.J.Cancer 34, 214-221.

35. Ahmad, A., Hart, I. R., 1997. Mechanisms of metastasis. Crit Rev.Oncol.Hematol. 26, 163-173.

36. Souter, R. G., Wells, C., Tarin, D., Kettlewell, M. G., 1985. Surgical and pathologic complications associated with peritoneovenous shunts in management of malignant ascites. Cancer 55, 1973-1978.

37. Frost, P., Levin, B., 1992. Clinical implications of metastatic process. Lancet 339, 1458-1461.

38. van den Tol, P. M., van Rossen, E. E., van Eijck, C. H., Bonthuis, F., Marquet, R. L., Jeekel, H., 1998. Reduction of peritoneal trauma by using nonsurgical gauze leads to less implantation metastasis of spilled tumor cells. Ann.Surg 227, 242-248.

39. van den, T. P., ten, R. S., van, G. H., Marquet, R., van, E. C., Jeekel, H., 2005. Icodextrin reduces postoperative adhesion formation in rats without affecting peritoneal metastasis. Surgery 137, 348-354.

40. Liotta, L. A., Tryggvason, K., Garbisa, S., Hart, I., Foltz, C. M., Shafie, S., 1980. Metastatic potential correlates with enzymatic degradation of basement membrane collagen. Nature 284, 67-68.

41. Ye, S., 2000. Polymorphism in matrix metalloproteinase gene promoters: implication in regulation of gene expression and susceptibility of various diseases. Matrix Biol. 19, 623-629.

42. Curran, S., Murray, G. I., 2000. Matrix metalloproteinases: molecular aspects of their roles in tumour invasion and metastasis. Eur.J.Cancer 36, 1621-1630.

43. Otani, Y., Okazaki, I., Arai, M., Kameyama, K., Wada, N., Maruyama, K., Yoshino, K., Kitajima, M., Hosoda, Y., Tsuchiya, M., 1994. Gene expression of interstitial collagenase (matrix metalloproteinase 1) in gastrointestinal tract cancers. J.Gastroenterol. 29, 391-397.

44. Inoue, T., Yashiro, M., Nishimura, S., Maeda, K., Sawada, T., Ogawa, Y., Sowa, M., Chung, K. H., 1999. Matrix metalloproteinase-1 expression is a prognostic factor for patients with advanced gastric cancer. Int.J.Mol.Med. 4, 73-77.

45. Mizutani, K., Kofuji, K., Shirouzu, K., 2000a. The significance of MMP-1 and MMP-2 in peritoneal disseminated metastasis of gastric cancer. Surg.Today 30, 614-621.

46. Yoshikawa, T., Tsuburaya, A., Kobayashi, O., Sairenji, M., Motohashi, H., Yanoma, S., Noguchi, Y., 2000. Prognostic value of tissue inhibitor of matrix metalloproteinase-1 in plasma of patients with gastric cancer. Cancer Lett. 151, 81-86.

47. Yonemura, Y., Endo, Y., Fujita, H., Kimura, K., Sugiyama, K., Momiyama, N., Shimada, H., Sasaki, T., 2001. Inhibition of peritoneal dissemination in human gastric cancer by MMP-7- specific antisense oligonucleotide. J.Exp.Clin.Cancer Res. 20, 205-212.

48. Hoekstra, R., Eskens, F. A., Verweij, J., 2001. Matrix metalloproteinase inhibitors: current developments and future perspectives. Oncologist. 6, 415-427.

49. Aparicio, T., Kermorgant, S., Dessirier, V., Lewin, M. J., Lehy, T., 1999. Matrix metalloproteinase inhibition prevents colon cancer peritoneal carcinomatosis development and prolongs survival in rats. Carcinogenesis 20, 1445-1451.

50. Giavazzi, R., Garofalo, A., Ferri, C., Lucchini, V., Bone, E. A., Chiari, S., Brown, P. D., Nicoletti, M. I., Taraboletti, G., 1998. Batimastat, a synthetic inhibitor of matrix metalloproteinases, potentiates the antitumor

activity of cisplatin in ovarian carcinoma xenografts. Clin.Cancer Res. 4, 985-992.

51. Aslam, N., Marino, C. R., 2001. Malignant ascites: new concepts in pathophysiology, diagnosis, and management. Arch.Intern.Med. 161, 2733-2737.

52. Tempia-Caliera, A. A., Horvath, L. Z., Zimmermann, A., Tihanyi, T. T., Korc, M., Friess, H., Buchler, M. W., 2002. Adhesion molecules in human pancreatic cancer. J.Surg.Oncol. 79, 93-100.

53. Ihanus, E., Uotila, L., Toivanen, A., Stefanidakis, M., Bailly, P., Cartron, J. P., Gahmberg, C. G., 2003. Characterization of ICAM-4 binding to the I domains of the CD11a/CD18 and CD11b/CD18 leukocyte integrins. Eur J Biochem 270, 1710-1723.

54. Kaihara, A., Iwagaki, H., Gouchi, A., Hizuta, A., Isozaki, H., Takakura, N., Tanaka, N., 1998. Soluble intercellular adhesion molecule-1 and natural killer cell activity in gastric cancer patients. Res.Commun.Mol.Pathol.Pharmacol. 100, 283-300.

55. Alexiou, D., Karayiannakis, A. J., Syrigos, K. N., Zbar, A., Kremmyda, A., Bramis, I., Tsigris, C., 2001. Serum levels of E-selectin, ICAM-1 and VCAM-1 in colorectal cancer patients: correlations with clinicopathological features, patient survival and tumour surgery. Eur.J.Cancer 37, 2392-2397.

56. Yasuda, M., Tanaka, Y., Tamura, M., Fujii, K., Sugaya, M., So, T., Takenoyama, M., Yasumoto, K., 2001. Stimulation of beta1 integrin down-regulates ICAM-1 expression and ICAM-1-dependent adhesion of lung cancer cells through focal adhesion kinase. Cancer Res. 61, 2022-2030.

57. Oka, H., Shiozaki, H., Kobayashi, K., Tahara, H., Tamura, S., Miyata, M., Doki, Y., Iihara, K., Matsuyoshi, N., Hirano, S., ., 1992. Immunohistochemical evaluation of E-cadherin adhesion molecule

expression in human gastric cancer. Virchows Arch.A Pathol.Anat.Histopathol. 421, 149-156.

58. Yonemura, Y., Endou, Y., Kimura, K., Fushida, S., Bandou, E., Taniguchi, K., Kinoshita, K., Ninomiya, I., Sugiyama, K., Heizmann, C. W., Schafer, B. W., Sasaki, T., 2000. Inverse expression of S100A4 and E-cadherin is associated with metastatic potential in gastric cancer. Clin.Cancer Res. 6, 4234-4242.

59. Hegde, P., Qi, R., Gaspard, R., Abernathy, K., Dharap, S., Earle-Hughes, J., Gay, C., Nwokekeh, N. U., Chen, T., Saeed, A. I., Sharov, V., Lee, N. H., Yeatman, T. J., Quackenbush, J., 2001. Identification of tumor markers in models of human colorectal cancer using a 19,200-element complementary DNA microarray. Cancer Res. 61, 7792-7797.

60. Toyoda, E., Doi, R., Koizumi, M., Kami, K., Ito, D., Mori, T., Fujimoto, K., Nakajima, S., Wada, M., Imamura, M., 2005. Analysis of E-, N-cadherin, alpha-, beta-, and gamma-catenin expression in human pancreatic carcinoma cell lines. Pancreas 30, 168-173.

61. Hynes, R. O., 1992. Integrins: versatility, modulation, and signaling in cell adhesion. Cell 69, 11-25.

62. Ura, H., Denno, R., Hirata, K., Yamaguchi, K., Yasoshima, T., 1998. Separate functions of alpha2beta1 and alpha3beta1 integrins in the metastatic process of human gastric carcinoma. Surg.Today 28, 1001-1006.

63. Davidson, B., Goldberg, I., Reich, R., Tell, L., Dong, H. P., Trope', C. G., Risberg, B., Kopolovic, J., 2003. AlphaV- and beta1-integrin subunits are commonly expressed in malignant effusions from ovarian carcinoma patients. Gynecol.Oncol. 90, 248-257.

64. Ishii, Y., Ochiai, A., Yamada, T., Akimoto, S., Yanagihara, K., Kitajima, M., Hirohashi, S., 2000. Integrin alpha6beta4 as a suppressor and a

predictive marker for peritoneal dissemination in human gastric cancer. Gastroenterology 118, 497-506.

65. Nakashio, T., Narita, T., Akiyama, S., Kasai, Y., Kondo, K., Ito, K., Takagi, H., Kannagi, R., 1997a. Adhesion molecules and TGF-beta1 are involved in the peritoneal dissemination of NUGC-4 human gastric cancer cells. Int.J.Cancer 70, 612-618.

66. Yoshie, O., Imai, T., Nomiyama, H., 2001. Chemokines in immunity. Adv.Immunol. 78, 57-110.

67. Szlosarek, P., Charles, K. A., Balkwill, F. R., 2006. Tumour necrosis factor-alpha as a tumour promoter. Eur.J Cancer 42, 745-750.

68. Dinarello, C. A., 2006. The paradox of pro-inflammatory cytokines in cancer. Cancer Metastasis Rev. 25, 307-313.

69. El-Omar, E. M., Rabkin, C. S., Gammon, M. D., Vaughan, T. L., Risch, H. A., Schoenberg, J. B., Stanford, J. L., Mayne, S. T., Goedert, J., Blot, W. J., Fraumeni, J. F., Jr., Chow, W. H., 2003. Increased risk of noncardia gastric cancer associated with proinflammatory cytokine gene polymorphisms. Gastroenterology 124, 1193-1201.

70. Tahara, E., 2004. Genetic pathways of two types of gastric cancer. IARC Sci.Publ. 327-349.

71. Cayeux, S., Richter, G., Becker, C., Beck, C., Aicher, A., Pezzutto, A., Dorken, B., Blankenstein, T., 1997. Lack of correlation between rejection of tumor cells co-expressing interleukin-2 and B7.1 and vaccine efficiency. Eur.J Immunol. 27, 1657-1662.

72. Schneider, M. R., Hoeflich, A., Fischer, J. R., Wolf, E., Sordat, B., Lahm, H., 2000. Interleukin-6 stimulates clonogenic growth of primary and metastatic human colon carcinoma cells. Cancer Lett. 151, 31-38.

73. Ikeguchi, M., Matsumoto, S., Murakami, D., Kanaji, S., Ohro, S., Maeta, Y., Tatebe, S., Kondo, A., Tsujitani, S., Kaibara, N., 2004. Gene

expression levels of cytokines in peritoneal washings from patients with gastric cancer. Tumour.Biol. 25, 117-121.

74. Gately, M. K., Renzetti, L. M., Magram, J., Stern, A. S., Adorini, L., Gubler, U., Presky, D. H., 1998. The interleukin-12/interleukin-12-receptor system: role in normal and pathologic immune responses. Annu.Rev.Immunol. 16, 495-521.

75. Murakami, S., Okubo, K., Tsuji, Y., Sakata, H., Hamada, S., Hirayama, R., 2004. Serum interleukin-12 levels in patients with gastric cancer. Surg.Today 34, 1014-1019.

76. Murakami, S., Satomi, A., Ishida, K., Murai, H., Matsuki, M., Hashimoto, T., 1994. Serum-soluble interleukin-2 receptor concentrations in patients with gastric cancer. Cancer 74, 2745-2748.

77. Yasumoto, K., Koizumi, K., Kawashima, A., Saitoh, Y., Arita, Y., Shinohara, K., Minami, T., Nakayama, T., Sakurai, H., Takahashi, Y., Yoshie, O., Saiki, I., 2006. Role of the CXCL12/CXCR4 axis in peritoneal carcinomatosis of gastric cancer. Cancer Res 66, 2181-2187.

78. Alkhamesi, N. A., Ziprin, P., Pfistermuller, K., Peck, D. H., Darzi, A. W., 2005. ICAM-1 mediated peritoneal carcinomatosis, a target for therapeutic intervention. Clin.Exp.Metastasis 22, 449-459.

79. Mochizuki, Y., Nakanishi, H., Kodera, Y., Ito, S., Yamamura, Y., Kato, T., Hibi, K., Akiyama, S., Nakao, A., Tatematsu, M., 2004. TNF-alpha promotes progression of peritoneal metastasis as demonstrated using a green fluorescence protein (GFP)-tagged human gastric cancer cell line. Clin.Exp.Metastasis 21, 39-47.

80. van Rossen, M. E., Hofland, L. J., van den Tol, M. P., van Koetsveld, P. M., Jeekel, J., Marquet, R. L., van Eijck, C. H., 2001. Effect of inflammatory cytokines and growth factors on tumour cell adhesion to the peritoneum. J Pathol 193, 530-537.

81. Glass, C. A., Harper, S. J., Bates, D. O., 2006. The anti-angiogenic VEGF isoform VEGF165b transiently increases hydraulic conductivity, probably through VEGF receptor 1 in vivo. J Physiol 572, 243-257.

82. Sooriakumaran, P., Kaba, R., 2005. Angiogenesis and the tumour hypoxia response in prostate cancer: a review. Int.J Surg. 3, 61-67.

83. Fang, J., Zhou, Q., Liu, L. Z., Xia, C., Hu, X., Shi, X., Jiang, B. H., 2007. Apigenin inhibits tumor angiogenesis through decreasing HIF-1alpha and VEGF expression. Carcinogenesis 28, 858-864.

84. Rasila, K. K., Burger, R. A., Smith, H., Lee, F. C., Verschraegen, C., 2005. Angiogenesis in gynecological oncology-mechanism of tumor progression and therapeutic targets. Int.J Gynecol.Cancer 15, 710-726.

85. Aoyagi, K., Kouhuji, K., Yano, S., Miyagi, M., Imaizumi, T., Takeda, J., Shirouzu, K., 2005. VEGF significance in peritoneal recurrence from gastric cancer. Gastric.Cancer 8, 155-163.

86. Sako, A., Kitayama, J., Yamaguchi, H., Kaisaki, S., Suzuki, H., Fukatsu, K., Fujii, S., Nagawa, H., 2003. Vascular endothelial growth factor synthesis by human omental mesothelial cells is augmented by fibroblast growth factor-2: possible role of mesothelial cell on the development of peritoneal metastasis. J.Surg.Res. 115, 113-120.

87. Gerber, S. A., Rybalko, V. Y., Bigelow, C. E., Lugade, A. A., Foster, T. H., Frelinger, J. G., Lord, E. M., 2006. Preferential attachment of peritoneal tumor metastases to omental immune aggregates and possible role of a unique vascular microenvironment in metastatic survival and growth. Am.J Pathol. 169, 1739-1752.

88. Garcia-Gomez, I., Goldsmith, H. S., Angulo, J., Prados, A., Lopez-Hervas, P., Cuevas, B., Dujovny, M., Cuevas, P., 2005. Angiogenic capacity of human omental stem cells. Neurol.Res. 27, 807-811.

89. Ignotz, R. A., Massague, J., 1986. Transforming growth factor-beta stimulates the expression of fibronectin and collagen and their incorporation into the extracellular matrix. J Biol.Chem. 261, 4337-4345.

90. Nakashio, T., Narita, T., Akiyama, S., Kasai, Y., Kondo, K., Ito, K., Takagi, H., Kannagi, R., 1997b. Adhesion molecules and TGF-beta1 are involved in the peritoneal dissemination of NUGC-4 human gastric cancer cells. Int.J Cancer 70, 612-618.

91. Zarnegar, R., Michalopoulos, G. K., 1995. The many faces of hepatocyte growth factor: from hepatopoiesis to hematopoiesis. J Cell Biol. 129, 1177-1180.

92. Ueda, K., Iwahashi, M., Matsuura, I., Nakamori, M., Nakamura, M., Ojima, T., Naka, T., Ishida, K., Matsumoto, K., Nakamura, T., Yamaue, H., 2004. Adenoviral-mediated gene transduction of the hepatocyte growth factor (HGF) antagonist, NK4, suppresses peritoneal metastases of gastric cancer in nude mice. Eur.J.Cancer 40, 2135-2142.

93. Tanaka, T., Shimura, H., Sasaki, T., Narumi, K., Maemondo, M., Nukiwa, T., Matsumoto, K., Nakamura, T., Ikeda, S., 2004. Gallbladder cancer treatment using adenovirus expressing the HGF/NK4 gene in a peritoneal implantation model. Cancer Gene Ther. 11, 431-440.

94. Schena, M., Shalon, D., Davis, R. W., Brown, P. O., 1995. Quantitative monitoring of gene expression patterns with a complementary DNA microarray. Science 270, 467-470.

95. Bull, J. H., Ellison, G., Patel, A., Muir, G., Walker, M., Underwood, M., Khan, F., Paskins, L., 2001. Identification of potential diagnostic markers of prostate cancer and prostatic intraepithelial neoplasia using cDNA microarray. Br.J.Cancer 84, 1512-1519.

96. Dhanasekaran, S. M., Barrette, T. R., Ghosh, D., Shah, R., Varambally, S., Kurachi, K., Pienta, K. J., Rubin, M. A., Chinnaiyan, A. M., 2001.

Delineation of prognostic biomarkers in prostate cancer. Nature 412, 822-826.

97. Hedenfalk, I., Duggan, D., Chen, Y., Radmacher, M., Bittner, M., Simon, R., Meltzer, P., Gusterson, B., Esteller, M., Kallioniemi, O. P., Wilfond, B., Borg, A., Trent, J., Raffeld, M., Yakhini, Z., Ben-Dor, A., Dougherty, E., Kononen, J., Bubendorf, L., Fehrle, W., Pittaluga, S., Gruvberger, S., Loman, N., Johannsson, O., Olsson, H., Sauter, G., 2001. Gene-expression profiles in hereditary breast cancer. N.Engl.J.Med. 344, 539-548.

98. Fukuda, K., Sakakura, C., Miyagawa, K., Kuriu, Y., Kin, S., Nakase, Y., Hagiwara, A., Mitsufuji, S., Okazaki, Y., Hayashizaki, Y., Yamagishi, H., 2004. Differential gene expression profiles of radioresistant oesophageal cancer cell lines established by continuous fractionated irradiation. Br.J.Cancer 91, 1543-1550.

99. Yoshida, S., Furukawa, N., Haruta, S., Tanase, Y., Kanayama, S., Noguchi, T., Sakata, M., Yamada, Y., Oi, H., Kobayashi, H., 2009. Expression profiles of genes involved in poor prognosis of epithelial ovarian carcinoma: a review. Int.J.Gynecol.Cancer 19, 992-997.

100. Witkowska, A., Gumprecht, J., Glogowska-Ligus, J., Wystrychowski, G., Owczarek, A., Stachowicz, M., Bocianowska, A., Nowakowska-Zajdel, E., Mazurek, U., 2010. Expression profile of significant immortalization genes in colon cancer. Int.J.Mol.Med. 25, 321-329.

101. Yang, X., Sun, X., 2010. Meta-analysis of cancer gene-profiling data. Methods Mol.Biol. 576, 409-426.

102. Wang, L., Zhu, J. S., Song, M. Q., Chen, G. Q., Chen, J. L., 2006. Comparison of gene expression profiles between primary tumor and metastatic lesions in gastric cancer patients using laser microdissection and cDNA microarray. World J Gastroenterol. 12, 6949-6954.

103. Mimori, K., Fukagawa, T., Kosaka, Y., Ishikawa, K., Iwatsuki, M., Yokobori, T., Hirasaki, S., Takatsuno, Y., Sakashita, H., Ishii, H., Sasako, M., Mori, M., 2008. A large-scale study of MT1-MMP as a marker for isolated tumor cells in peripheral blood and bone marrow in gastric cancer cases. Ann.Surg.Oncol 15, 2934-2942.

104. Galamb, O., Sipos, F., Fischer, K., Tulassay, Z., Molnar, B., 2005. The results of the expression array studies correlate and enhance the known genetic basis of gastric and colorectal cancer. Cytometry B Clin Cytom. 68, 1-17.

105. Chen, W. C., Lin, M. S., Zhang, B. F., Fang, J., Zhou, Q., Hu, Y., Gao, H. J., 2007. Survey of molecular profiling during human colon cancer development and progression by immunohistochemical staining on tissue microarray. World J Gastroenterol. 13, 699-708.

106. Sakakura, C., Hagiwara, A., Nakanishi, M., Shimomura, K., Takagi, T., Yasuoka, R., Fujita, Y., Abe, T., Ichikawa, Y., Takahashi, S., Ishikawa, T., Nishizuka, I., Morita, T., Shimada, H., Okazaki, Y., Hayashizaki, Y., Yamagishi, H., 2002a. Differential gene expression profiles of gastric cancer cells established from primary tumour and malignant ascites. Br.J.Cancer 87, 1153-1161.

107. Fukui, R., Nishimori, H., Hata, F., Yasoshima, T., Ohno, K., Nomura, H., Yanai, Y., Tanaka, H., Kamiguchi, K., Denno, R., Sato, N., Hirata, K., 2005. Metastases-related genes in the classification of liver and peritoneal metastasis in human gastric cancer. J Surg Res 129, 94-100.

108. Yanagihara, K., Takigahira, M., Tanaka, H., Komatsu, T., Fukumoto, H., Koizumi, F., Nishio, K., Ochiya, T., Ino, Y., Hirohashi, S., 2005. Development and biological analysis of peritoneal metastasis mouse models for human scirrhous stomach cancer. Cancer Sci. 96, 323-332.

109. Yang, Z., Cox, J. L., 2007. Cathepsin L increases invasion and migration of B16 melanoma. Cancer Cell Int. 7, 8.

110. Ioachim, E., Michael, M. C., Salmas, M., Damala, K., Tsanou, E., Michael, M. M., Malamou-Mitsi, V., Stavropoulos, N. E., 2006. Thrombospondin-1 expression in urothelial carcinoma: prognostic significance and association with p53 alterations, tumour angiogenesis and extracellular matrix components. BMC.Cancer 6, 140.

111. Varghese, S., Burness, M., Xu, H., Beresnev, T., Pingpank, J., Alexander, H. R., 2007. Site-specific gene expression profiles and novel molecular prognostic factors in patients with lower gastrointestinal adenocarcinoma diffusely metastatic to liver or peritoneum. Ann.Surg.Oncol 14, 3460-3471.

112. Nishimori, H., Yasoshima, T., Denno, R., Shishido, T., Hata, F., Okada, Y., Ura, H., Yamaguchi, K., Isomura, H., Sato, N., Hirata, K., 2000. A novel experimental mouse model of peritoneal dissemination of human gastric cancer cells: different mechanisms in peritoneal dissemination and hematogenous metastasis. Jpn.J.Cancer Res. 91, 715-722.

113. Jayne, D. G., O'Leary, R., Gill, A., Hick, A., Guillou, P. J., 1999a. A three-dimensional in-vitro model for the study of peritoneal tumour metastasis. Clin.Exp.Metastasis 17, 515-523.

114. Allen, H. J., Porter, C., Gamarra, M., Piver, M. S., Johnson, E. A., 1987. Isolation and morphologic characterization of human ovarian carcinoma cell clusters present in effusions. Exp.Cell Biol. 55, 194-208.

115. Jap, P. H., Mungyer, G. M., Ramaekers, F. C., Poels, L. G., van de Molengraft, F. J., Vooijs, G. P., 1984. Identification of human mesothelial cells in culture by electron microscopy and antibodies. Cell Biol.Int.Rep. 8, 274.

116. Sakakura, C., Hagiwara, A., Nakanishi, M., Shimomura, K., Takagi, T., Yasuoka, R., Fujita, Y., Abe, T., Ichikawa, Y., Takahashi, S., Ishikawa, T., Nishizuka, I., Morita, T., Shimada, H., Okazaki, Y., Hayashizaki, Y., Yamagishi, H., 2002b. Differential gene expression profiles of gastric

cancer cells established from primary tumour and malignant ascites. Br.J.Cancer 87, 1153-1161.

117. Zhang, X. Y., Pettengell, R., Nasiri, N., Kalia, V., Dalgleish, A. G., Barton, D. P., 1999. Characteristics and growth patterns of human peritoneal mesothelial cells: comparison between advanced epithelial ovarian cancer and non- ovarian cancer sources. J.Soc.Gynecol.Investig. 6, 333-340.

118. Jayne, D. G., O'Leary, R., Gill, A., Hick, A., Guillou, P. J., 1999b. A three-dimensional in-vitro model for the study of peritoneal tumour metastasis. Clin.Exp.Metastasis 17, 515-523.

119. Luzzi, V., Mahadevappa, M., Raja, R., Warrington, J. A., Watson, M. A., 2003. Accurate and reproducible gene expression profiles from laser capture microdissection, transcript amplification, and high density oligonucleotide microarray analysis. J Mol.Diagn. 5, 9-14.

120. Kamme, F., Zhu, J., Luo, L., Yu, J., Tran, D. T., Meurers, B., Bittner, A., Westlund, K., Carlton, S., Wan, J., 2004. Single-cell laser-capture microdissection and RNA amplification. Methods Mol.Med. 99, 215-223.

121. Stirewalt, D. L., Pogosova-Agadjanyan, E. L., Khalid, N., Hare, D. R., Ladne, P. A., Sala-Torra, O., Zhao, L. P., Radich, J. P., 2004. Single-stranded linear amplification protocol results in reproducible and reliable microarray data from nanogram amounts of starting RNA. Genomics 83, 321-331.

122. 't Hoen, P. A., de, K. F., van Ommen, G. J., den Dunnen, J. T., 2003. Fluorescent labelling of cRNA for microarray applications. Nucleic Acids Res. 31, e20.

123. McKusick, V. A., 2007. Mendelian Inheritance in Man and its online version, OMIM. Am.J Hum.Genet. 80, 588-604.

124. Dobbin, K., Simon, R., 2002a. Comparison of microarray designs for class comparison and class discovery. Bioinformatics. 18, 1438-1445.

125. Dobbin, K., Simon, R., 2002b. Comparison of microarray designs for class comparison and class discovery. Bioinformatics. 18, 1438-1445.

126. Kerr, K. F., Serikawa, K. A., Wei, C., Peters, M. A., Bumgarner, R. E., 2007. What is the best reference RNA? And other questions regarding the design and analysis of two-color microarray experiments. OMICS. 11, 152-165.

127. Park, P. J., Cao, Y. A., Lee, S. Y., Kim, J. W., Chang, M. S., Hart, R., Choi, S., 2004. Current issues for DNA microarrays: platform comparison, double linear amplification, and universal RNA reference. J.Biotechnol. 112, 225-245.

128. Seo, J., Bakay, M., Chen, Y. W., Hilmer, S., Shneiderman, B., Hoffman, E. P., 2004. Interactively optimizing signal-to-noise ratios in expression profiling: project-specific algorithm selection and detection p-value weighting in Affymetrix microarrays. Bioinformatics 20, 2534-2544.

129. Jain, A. N., Tokuyasu, T. A., Snijders, A. M., Segraves, R., Albertson, D. G., Pinkel, D., 2002. Fully Automatic Quantification of Microarray Image Data. Genome Research 12, 325-332.

130. Simon, R., Lam, A., Li, M. C., Ngan, M., Menenzes, S., Zhao, Y., 2007. Analysis of Gene Expression Data Using BRB-Array Tools. Cancer Inform. 3, 11-17.

131. Eisen, M. B., Spellman, P. T., Brown, P. O., Botstein, D., 1998. Cluster analysis and display of genome-wide expression patterns. PNAS 95, 14863-14868.

132. Hochberg, Y., Benjamini, Y., 1990. More powerful procedures for multiple significance testing. Stat.Med. 9, 811-818.

133. Li, Z., Yasuda, Y., Li, W., Bogyo, M., Katz, N., Gordon, R. E., Fields, G. B., Bromme, D., 2004. Regulation of Collagenase Activities of Human Cathepsins by Glycosaminoglycans. J.Biol.Chem. 279, 5470-5479.

134. Rose, A. A., Siegel, P. M., 2010. Emerging therapeutic targets in breast cancer bone metastasis. Future Oncology 6, 55-74.

135. Rapa, I., Volante, M., Cappia, S., Rosas, R., Scagliotti, G. V., Papotti, M., 2006. Cathepsin K is selectively expressed in the stroma of lung adenocarcinoma but not in bronchioloalveolar carcinoma. A useful marker of invasive growth. Am J Clin.Pathol 125, 847-854.

136. Brubaker, K. D., Vessella, R. L., True, L. D., Thomas, R., Corey, E., 2003. Cathepsin K mRNA and protein expression in prostate cancer progression. J Bone Miner.Res 18, 222-230.

137. Hajra, K. M., Liu, J. R., 2004. Apoptosome dysfunction in human cancer. Apoptosis. 9, 691-704.

138. Chen, J. Y., Chi, C. W., Chen, H. L., Wan, C. P., Yang, W. C., Yang, A. H., 2003. TNF-{alpha} renders human peritoneal mesothelial cells sensitive to anti-Fas antibody-induced apoptosis. Nephrol.Dial.Transplant. 18, 1741-1747.

139. Bibi, R., Pranesh, N., Saunders, M. P., Wilson, M. S., O'dwyer, S. T., Stern, P. L., Renehan, A. G., 2006. A specific cadherin phenotype may characterise the disseminating yet non-metastatic behaviour of pseudomyxoma peritonei. Br.J Cancer 95, 1258-1264.

140. Pfaffl, M. W., 2001. A new mathematical model for relative quantification in real-time RT-PCR. Nucleic Acids Res 29, e45.

141. Wang, Y., Cheong, D., Chan, S., Hooi, S. C., 1999. Heparin/heparan sulfate interacting protein gene expression is up-regulated in human colorectal carcinoma and correlated with differentiation status and metastasis. Cancer Res. 59, 2989-2994.

142. Chen, T. R., Drabkowski, D., Hay, R. J., Macy, M., Peterson, W., 1987. WiDr is a derivative of another colon adenocarcinoma cell line, HT-29. Cancer Genetics and Cytogenetics 27, 125-134.

143. Sekiguchi, M., Sakakibara, K., Fujii, G., 1978. Establishment of cultured cell lines derived from a human gastric carcinoma. Jpn.J.Exp.Med. 48, 61-68.

144. Ochiai, A., Tahara, E., 1986. [Monoclonal antibody 9A3 raised against a human poorly differentiated gastric adenocarcinoma cell line]. Gan To Kagaku Ryoho 13, 1416-1422.

145. Hewitt, R. E., McMarlin, A., Kleiner, D., Wersto, R., Martin, P., Tsokos, M., Stamp, G. W., Stetler-Stevenson, W. G., 2000. Validation of a model of colon cancer progression. J.Pathol. 192, 446-454.

146. Riles, W. L., Erickson, J., Nayyar, S., Atten, M. J., Attar, B. M., Holian, O., 2006. Resveratrol engages selective apoptotic signals in gastric adenocarcinoma cells. World J.Gastroenterol. 12, 5628-5634.

147. Kasuga, T., Tabuchi, T., Shirato, K., Imaizumi, K., Tomoda, A., 2007. Caspase-independent cell death revealed in human gastric cancer cell lines, MKN45 and KATO III treated with phenoxazine derivatives. Oncol.Rep. 17, 409-415.

148. Kemperman, H., Wijnands, Y. M., Roos, E., 1997. alphaV Integrins on HT-29 colon carcinoma cells: adhesion to fibronectin is mediated solely by small amounts of alphaVbeta6, and alphaVbeta5 is codistributed with actin fibers. Exp.Cell Res. 234, 156-164.

149. Ruo, L., Gougoutas, C., Paty, P. B., Guillem, J. G., Cohen, A. M., Wong, W. D., 2003. Elective bowel resection for incurable stage IV colorectal cancer: prognostic variables for asymptomatic patients. J Am Coll.Surg. 196, 722-728.

150. Emmert-Buck, M. R., Bonner, R. F., Smith, P. D., Chuaqui, R. F., Zhuang, Z., Goldstein, S. R., Weiss, R. A., Liotta, L. A., 1996. Laser capture microdissection. Science 274, 998-1001.

151. Bonner, R. F., Emmert-Buck, M., Cole, K., Pohida, T., Chuaqui, R., Goldstein, S., Liotta, L. A., 1997. Laser capture microdissection: molecular analysis of tissue. Science 278, 1481,1483.

152. Simone, N. L., Bonner, R. F., Gillespie, J. W., Emmert-Buck, M. R., Liotta, L. A., 1998. Laser-capture microdissection: opening the microscopic frontier to molecular analysis. Trends Genet. 14, 272-276.

153. Bonferroni CE, 1936. Teoria statistica delle classi e calcolo delle probabilità. Pubblicazioni del R Istituto Superiore di Scienze Economiche e Commerciali di Firenze 8, 3-62.

154. Holm, S. A simple sequentially rejective multiple test procedure. Scandinavian Journal of Statistics 6, 65-70. 1979.

Ref Type: Generic

155. Benjamini Y, Hochberg Y. Controlling the false discovery rate: a practical and powerful approach to multiple testing. Journal of the Royal Statistical Society Series B 57, 289-300. 1995.

Ref Type: Generic

156. Radmacher, M. D., McShane, L. M., Simon, R., 2002. A paradigm for class prediction using gene expression profiles. J.Comput.Biol. 9, 505-511.

157. Korn EL, Troendle JF, McShane LM, Simon R. Controlling the number of false discoveries: Application to high-dimensional genomic data. Journal of the Royal Statistical Planning and Inference 124, 379-398. 2004.

Ref Type: Generic

158. Wise-Draper, T. M., Allen, H. V., Thobe, M. N., Jones, E. E., Habash, K. B., Munger, K., Wells, S. I., 2005. The Human DEK Proto-Oncogene Is a Senescence Inhibitor and an Upregulated Target of High-Risk Human Papillomavirus E7. J.Virol. 79, 14309-14317.

159. DiSepio, D., Ghosn, C., Eckert, R. L., Deucher, A., Robinson, N., Duvic, M., Chandraratna, R. A., Nagpal, S., 1998. Identification and characterization of a retinoid-induced class II tumor suppressor/growth regulatory gene. Proc.Natl.Acad.Sci.U.S.A 95, 14811-14815.

160. So, K., Tamura, G., Honda, T., Homma, N., Waki, T., Togawa, N., Nishizuka, S., Motoyama, T., 2006. Multiple tumor suppressor genes are increasingly methylated with age in non-neoplastic gastric epithelia. Cancer Sci. 97, 1155-1158.

161. Hoekstra, M., Stitzinger, M., van Wanrooij, E. J. A., Michon, I. N., Kruijt, J. K., Kamphorst, J., Van Eck, M., Vreugdenhil, E., Van Berkel, T. J. C., Kuiper, J., 2006. Microarray analysis indicates an important role for FABP5 and putative novel FABPs on a Western-type diet. Journal of Lipid Research 47, 2198-2207.

162. Sidelnikov, E., Bostick, R. M., Flanders, W. D., Long, Q., Cohen, V. L., Dash, C., Seabrook, M. E., Fedirko, V., 2009. MutL-Homolog 1 Expression and Risk of Incident, Sporadic Colorectal Adenoma: Search for Prospective Biomarkers of Risk for Colorectal Cancer. Cancer Epidemiology Biomarkers & Prevention 18, 1599-1609.

163. Kaur, M., Pop, M., Shi, D., Brignone, C., Grossman, S. R., 2006. hHR23B is required for genotoxic-specific activation of p53 and apoptosis. Oncogene 26, 1231-1237.

164. Lee, K. M., Shen, M., Chapman, R. S., Yeager, M., Welch, R., He, X., Zheng, T., Hosgood, H. D., Yang, D., Berndt, S. I., Chanock, S., Lan, Q., 2007. Polymorphisms in immunoregulatory genes, smoky coal exposure and lung cancer risk in Xuan Wei, China. Carcinogenesis 28, 1437-1441.

165. Steinberg, M. L., Hubbard, K., Utti, C., Clas, B., Hwang, B. J., Hill, H. Z., Orlow, I., 2009. Patterns of persistent DNA damage associated with sun exposure and the glutathione S-transferase M1 genotype in melanoma patients. Photochem.Photobiol. 85, 379-386.

166. Shao, C., Zhang, F., Kemp, M. M., Linhardt, R. J., Waisman, D. M., Head, J. F., Seaton, B. A., 2006. Crystallographic analysis of calcium-dependent heparin binding to annexin A2. J Biol.Chem. 281, 31689-31695.

167. Lehnigk, U., Zimmermann, U., Woenckhaus, C., Giebel, J., 2005. Localization of annexins I, II, IV and VII in whole prostate sections from radical prostatectomy patients. Histol.Histopathol. 20, 673-680.

168. Sharma, M. R., Koltowski, L., Ownbey, R. T., Tuszynski, G. P., Sharma, M. C., 2006. Angiogenesis-associated protein annexin II in breast cancer: selective expression in invasive breast cancer and contribution to tumor invasion and progression. Exp.Mol.Pathol 81, 146-156.

169. Madoiwa, S., Someya, T., Hironaka, M., Kobayashi, H., Ohmori, T., Mimuro, J., Sugiyama, Y., Morita, T., Nishimura, Y., Tarumoto, T., Ozawa, K., Saito, K., Sakata, Y., 2007. Annexin 2 and hemorrhagic disorder in vascular intimal carcinomatosis. Thromb.Res 119, 229-240.

170. Emoto, K., Sawada, H., Yamada, Y., Fujimoto, H., Takahama, Y., Ueno, M., Takayama, T., Uchida, H., Kamada, K., Naito, A., Hirao, S., Nakajima, Y., 2001. Annexin II overexpression is correlated with poor prognosis in human gastric carcinoma. Anticancer Res 21, 1339-1345.

171. Iwai, K., Hirata, K., Ishida, T., Takeuchi, S., Hirase, T., Rikitake, Y., Kojima, Y., Inoue, N., Kawashima, S., Yokoyama, M., 2004. An anti-proliferative gene BTG1 regulates angiogenesis in vitro. Biochem Biophys.Res Commun. 316, 628-635.

172. Feldmann, G., Nattermann, J., Nischalke, H. D., Gorschl++ter, M., Kuntzen, T., Ahlenstiel, G., Gerhardt, T., Wolff, M., Sauerbruch, T., Spengler, U., Dumoulin, F. L., 2006. Detection of Human Aspartyl (Asparaginyl) Beta-Hydroxylase and Homeobox B7 mRNA in Brush Cytology Specimens from Patients with Bile Duct Cancer. Endoscopy 38, 604-609.

173. Sawada, M., Shii, J., Akedo, H., Tanizawa, O., 1994. An experimental model for ovarian tumor invasion of cultured mesothelial cell monolayer. Lab Invest 70, 333-338.

174. Jayne, D. G., Perry, S. L., Morrison, E., Farmery, S. M., Guillou, P. J., 2000. Activated mesothelial cells produce heparin-binding growth factors: implications for tumour metastases. Br.J.Cancer 82, 1233-1238.

175. Casey, R. C., Koch, K. A., Oegema, T. R., Jr., Skubitz, K. M., Pambuccian, S. E., Grindle, S. M., Skubitz, A. P., 2003. Establishment of an in vitro assay to measure the invasion of ovarian carcinoma cells through mesothelial cell monolayers. Clin.Exp.Metastasis 20, 343-356.

176. Rieppi, M., Vergani, V., Gatto, C., Zanetta, G., Allavena, P., Taraboletti, G., Giavazzi, R., 1999. Mesothelial cells induce the motility of human ovarian carcinoma cells. Int.J.Cancer 80, 303-307.

177. Sakata, K., Shigemasa, K., Uebaba, Y., Nagai, N., Ohama, K., 2002. Expression of matrix metalloproteinases-2 and -9 by cells isolated from the peritoneal fluid of women with ovarian carcinoma. Acta Cytol. 46, 697-703.

178. Mizutani, K., Kofuji, K., Shirouzu, K., 2000b. The significance of MMP-1 and MMP-2 in peritoneal disseminated metastasis of gastric cancer. Surg.Today 30, 614-621.

179. Bittinger, F., Brochhausen, C., Skarke, C., Kohler, H., Kirkpatrick, C. J., 1997. Reconstruction of peritoneal-like structure in three-dimensional collagen gel matrix culture. Exp.Cell Res. 236, 155-160.

180. Maruo, Y., Gochi, A., Kaihara, A., Shimamura, H., Yamada, T., Tanaka, N., Orita, K., 2002. ICAM-1 expression and the soluble ICAM-1 level for evaluating the metastatic potential of gastric cancer. Int.J.Cancer 100, 486-490.

181. Tanaka, H., Yashiro, M., Sunami, T., Sakate, Y., Kosaka, K., Hirakawa, K., 2004. ICAM-2 gene therapy for peritoneal dissemination of scirrhous gastric carcinoma. Clin.Cancer Res. 10, 4885-4892.

182. Parums, D. V., Cordell, J. L., Micklem, K., Heryet, A. R., Gatter, K. C., Mason, D. Y., 1990. JC70: a new monoclonal antibody that detects vascular endothelium associated antigen on routinely processed tissue sections. J Clin.Pathol 43, 752-757.

183. Wilkinson, L. S., Edwards, J. C., Poston, R. N., Haskard, D. O., 1993. Expression of vascular cell adhesion molecule-1 in normal and inflamed synovium. Lab Invest 68, 82-88.

184. Li, J., Adams, L., Schwartz, S. M., Bumgarner, R. E., 2003. RNA amplification, fidelity and reproducibility of expression profiling. Comptes Rendus Biologies 326, 1021-1030.

185. Van Gelder, R. N., von Zastrow, M. E., Yool, A., Dement, W. C., Barchas, J. D., Eberwine, J. H., 1990. Amplified RNA synthesized from limited quantities of heterogeneous cDNA. Proc.Natl.Acad.Sci.U.S.A 87, 1663-1667.

186. Eberwine, J., 1996. Amplification of mRNA populations using aRNA generated from immobilized oligo(dT)-T7 primed cDNA. Biotechniques 20, 584-591.

187. Seth, D., Gorrell, M. D., McGuinness, P. H., Leo, M. A., Lieber, C. S., McCaughan, G. W., Haber, P. S., 2003a. SMART amplification maintains representation of relative gene expression: quantitative validation by real time PCR and application to studies of alcoholic liver disease in primates. Journal of Biochemical and Biophysical Methods 55, 53-66.

188. Seth, D., Gorrell, M. D., McGuinness, P. H., Leo, M. A., Lieber, C. S., McCaughan, G. W., Haber, P. S., 2003b. SMART amplification maintains representation of relative gene expression: quantitative

validation by real time PCR and application to studies of alcoholic liver disease in primates. Journal of Biochemical and Biophysical Methods 55, 53-66.

189. Kenzelmann, M., Klaren, R., Hergenhahn, M., Bonrouhi, M., Grone, H. J., Schmid, W., Schutz, G., 2004. High-accuracy amplification of nanogram total RNA amounts for gene profiling. Genomics 83, 550-558.

190. Ji, W., Zhou, W., Gregg, K., Lindpaintner, K., Davis, S., Davis, S., 2004. A method for gene expression analysis by oligonucleotide arrays from minute biological materials. Analytical Biochemistry 331, 329-339.

191. Kelz, M. B., Dent, G. W., Therianos, S., Marciano, P. G., McIntosh, T. K., Coleman, P. D., Eberwine, J. H., 2002. Single-cell antisense RNA amplification and microarray analysis as a tool for studying neurological degeneration and restoration. Sci.Aging Knowledge.Environ. 2002, re1.

192. Pfaffl, M. W., Tichopad, A., Prgomet, C., Neuvians, T. P., 2004. Determination of stable housekeeping genes, differentially regulated target genes and sample integrity: BestKeeper--Excel-based tool using pair-wise correlations. Biotechnol.Lett. 26, 509-515.